UNIVERSIDAD DE LAS AMÉRICAS PUEBLA

ENGINEERING FACULTY

INDUSTRIAL, MECHANICAL AND LOGISTIC ENGINEERING DEPARTMENT

Comparison of two sheet metal forming processes from a geometric analysis of the pieces and their similarity to an ideal piece.

Thesis that the student present to complete the requirements of the honors program.

LAURA SOFÍA FERNÁNDEZ RODRÍGUEZ

ID: 151384

BACHELOR´S IN INDUSTRIAL ENGINEERING

Dr. Rafael Carrera Espinoza

Co-Director: Dr. Rogelio Pérez Santiago

o

San Andrés Cholula, Puebla. **Spring 2019**

SIGNATURE SHEET

Thesis that the student present to complete the requirements of the honors program Laura Sofía Fernández Rodríguez with ID 151384.

Thesis Director

_____

Dr. Rafael Carrera Espinoza

Thesis Co-Director

_____

Dr. Rogelio Pérez Santiago

Thesis President

_____

Dr. Pablo Moreno Garibaldi

Thesis Secretary

_____

Mtra. Paola Torres Madrid

ACKNOWLEDGEMENT

La culminación de esta investigación, significa mucho para mí, ya que me hace pensar que no defraudé a todos aquellos que creyeron en mi capacidad de lograr esto y es justamente a ellos a los que tengo todo para agradecer.

Empezando por el apoyo de mis directores para la tesis, el Dr. Rafael Carrera y el Dr. Rogelio Pérez, a los sinodales, la Mtra. Paola Torres y el Dr. Pablo Moreno; a todos ustedes gracias por apoyarme aun teniendo todo el tiempo encima.

Agradezco grandemente a todo el equipo de investigación, el Dr. Rogelio Pérez, Arturo Belmont, Carlos Caballero, Ernesto Quiroz y Rodrigo Cruz, disfrute mucho aprender con ustedes y espero que su futuro siempre sea brillante y lleno de posibilidades.

Me gustaría también agradecer a mi familia, los cuales me alegraron y se empeñaron en respaldarme cuando estaba a punto de dejar todo; Especialmente a mi mami por estar ahí siempre, por consentirme y apoyarme aun sin entender el tema, tú eres el calor que derrite mi corazón y lo ha moldeado en lo que soy, a José por hacerme reír y ser eternamente mi complemento, tú me fortaleces para desafiarme y no tener miedo, a mi tía Lupita por acogerme en los momentos de desesperación y ayudarme grandemente, sinceramente esto no lo hubiera completado sin tu ayuda.

También gracias a mis amigos por entender mis tiempos, disculparme por faltar a todo y ayudarme aunque los explote como esclavos, sé que en algún momento se los compensaré.

Y por último pero jamás menos importante, gracias Emanita por creer en que siempre puedo ser mejor, en mostrarme la magia que esconde la lectura y el conocimiento, esto es el resultado de todo lo que dejaste sembrado en mí. Este es el primer gran logro que cumplo por nosotras, pero no te preocupes, que habrán muchos más.

INDEX

LIST OF FIGURES

LIST OF TABLES

ABSTRACT

After the industrial revolution, the goal of the majority of industries was to produce as much products as they could, without taking in count the excess, but nowadays it has been studied the impact of the leftover material, pieces, warehouses space, extra resources, manpower, financial imbalance, etc.; so many studies have searched for the optimum needed production, the best routes to take a certain material from one point to another, the most effective way to increment the utilities, among other improvements that have been researched.

The manufacturing improvements have not been left behind, that is why not only the existing manufacturing processes have been analyzed, but new processes have been created. It is known that the *deep drawing* process is one of the favorite methods to deform a metal sheet into a certain shape, but since the customization expanding requirements new alternatives have been researched among these the incremental sheet forming process arouse and have been refining.

That is why, this investigation aims to help other researches to get interested in the topic and to have the basis to improve this relatively new manufacturing process, giving a geometrical analysis. This research is not only intended to stay between academics, but to reach interested rookies.

The following investigation presents a descriptive analysis of a comparison achieved through the resulting pieces created by a group of bachelor students in the Mexican university UDLAP.

CHAPTER I

1.1 Approach to the problem

The main objective of this research is the evaluation of the Single Point Incremental Forming (SPIF) as an alternative of the deep draw forming process. Although the SPIF process is not as fast as the stamping process in production cycle, SPIF is an extremely flexible process that enables the possibility of customization. This is a tendency in the market, and not only by the fact of buying unique things, but also to create your own products and develop prototypes that other people can get interested in. This phenomenon can be seen in other relative new technologies such as 3D printing and programming, where communities of people interested in creating, get involved and start to learn with their own means. Later, these people discoveries are shared for others to try, even people without much knowledge in the topic can get immersed easily and enjoy the product of their ideas. From my own perspective, this is the path to the future of this technology, since is quite easy to apply and more people are paying attention to it.

SPIF is also a process that tries to reduce very common problems in the industry such as turn-around time and costs related to the manufacturing and setup of tooling, so more fluent manufacturing could be achieved, and less time and money would be wasted.

Three main aspects will be the focus for this investigation: Geometry accuracy, resulting thickness, and the surface finishing. These are the principal aspects in sheet metal forming to evaluate if two processes are capable to reproduce the same piece.

This study is also intended to give an easy-to-understand description on the procedure to create and analyze a sheet metal piece made either with SPIF or stamping process, so more enthusiasts can be attracted to develop their own investigations and improve the knowledge of this forming process. And finally, this work is the third of a sequence of investigations performed by the student´s team guided by the Dr. Rogelio Perez Santiago at the UDLAP

under the project “Numerical characterization and validation for sheet metal forming processes”.

1.2 General objective

The general objective is to compare the SPIF and traditional deep drawing method with the purpose of concluding whether their outcomes make them an alternative between each other.

1.3 Specific objectives

1.3.1 The process to be compared are:

- Conventional Stamping
- Single Point Incremental Forming (SPIF)

1.3.2 The characteristics to be compared are:

- Thickness
- Geometry precision
- Superficial Finish

1.3.3 The following software were used:

- Creo parametric 4.0
- Autodesk Inventor Enzo 2017
- Ls-Dyna (Ls-PrePost 4.1)
- Gom Scan 2016
- Gom Inspect 2016
- Minitab 18
- Microsoft Office 2016
- Ultimaker Cura 2.5.0

1.3.4 Material definition

- SPIF clamping framework

The framework base and clamping plates are made of Aluminum 6061.

The supporting columns are made of AISI A2 tool steel.

- Stamping set

  The dies, drawbeads plates and the framework bases are made of Aluminum 6061.

  The supporting columns and the pins are made of AISI A2 tool steel

- The material used in the metal sheets to create the pyramids is a stainless steel AISI 304, which is a chrome-nickel austenitic steel.

1.4 Study aims

Giving the following information, this investigation looks for the opening to a different technology. Even though deep drawing is one of the most used processes in the forming area, this thesis is intended to demonstrate the useful tool that the SPIF process can become, by setting the most vital and important parameters to show a little demonstration of their effects and a basis of the geometrical results for further investigation, increasing the use and research on this topic.

CHAPTER II

2.1 Introduction

There are several alternatives to give a certain shape to a metal sheet. Among them, we can find well known processes that have been studied and standardized for a long time, and there are new processes that are still in the process of developing industrial maturity. This is the reason the current research aims to identify the parameters affecting the resulting product. Before getting there, this chapter briefly explains those critical aspects related to our own research work.

2.2 Stamping

Defined by Mikell Groover [18] [19], stamping, deep draw forming, or pressing, is one of the more common processes to give a certain shape to a metal sheet, this process allows to give the final product a great variety of geometries. The process requires a press machine, a set of dies (a punch and a matrix), a blank holder, and a metal flat sheet (called blank). This process relies on pressing forces, applied by tools with specific shape and orientation, applied in the metal sheet. The blank takes the form of the cavity between punch and die and gets permanently deformed. When the final piece is taken out, some recuperation of the original shape, called springback, may be present in the sheet. Sometimes, extra material is required to form a certain part, this material is called addendum and serves to improve the formability of the material during the drawing phase. Additionally, thin veins are formed on the addendum, these are called drawbeads, and their main function is to control the material flow to the cavity.

Surface finishing is one of the main advantages of this process since it leaves a smooth finish. Geometry of the formed part has a great similarity to the dies, but to achieve this result, some calculations need to be made, since the springback might change the form and tolerances of the pieces.

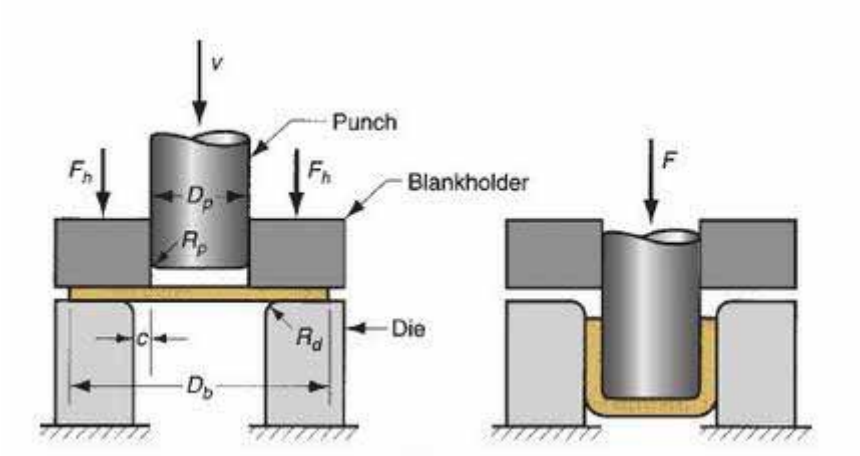

Figure 1: Groover's deep drawing explanation [18].

One of the more important factors of the process is the material that will be deformed, in this case we are talking about metals, and for this it is preferable a metal with a low yield strength and high ductility.

There are four main defects than Mikell Groover [18] [19] tell us that can be presented in a stamping process, these are wrinkling in the flange or in the wall, tearing, earing, and surface scratches.

In the exceeding material, two of these problems (wrinkling in the flange and earing) can be eliminated with a second process, but it is highly undesirable to have wasted material, time and tooling and equipment resources oriented to this. To mitigate these problems there are some resources that can be used:

For wrinkling in flange, the force in the blankholder could be increased, also the addition of drawbeads can decrease or eliminate this problem. For wrinkling in the walls, the rise of the blankholder force, the blank thickness, and a right space between the punch and the matrix could be good parameters to find a solution. In the tearing case, the opposite could be happening so the blankholder force should be reduced or eliminated, or in case of having drawbeads, they could be eliminated, also increasing the radius in the dies, so the cracks in the deep drawing can disappear. In case of earing, this defect is usually caused by the anisotropy in the material, so an isotropic metal is recommended to eliminate this flaw. And

finally, for surface scratches dies may be checked to find imperfections, also the application of lubricants to reduce the friction in the parts could solve this problem.

Another important consideration would be the dies design, since they are the basis for this operation, some important aspects to consider is the space between them, the geometry in these ones (the angles of every surface, the radius in every intersection, and surface finish), material and thermal treatments (depending on the usage of these, the forces used, the speed, friction, and temperatures involved in the drawing).

There can always be cases where other aspects are important, for example, the temperature. Usually stamping and the sheet forming related processes are done at room temperature, but sometimes higher temperatures are needed to deform the material and obtain certain characteristics. The closer to the "cold" forming conditions, the better precision in the tolerances, better surface finish, higher strength, and stiffness will result. However, at ambient conditions, the material´s ductility and toughness are limited.

Another inconvenience are the forces needed to deform the material and therefore the machine´s power. In the case of warm forming, material is heated below recrystallization temperature, there is less stiffness and strength and more ductility due to the softening effect of temperature in most metals. In turn, less force is needed as well as power, also more complex shapes are possible to create. Hot stamping is the deep drawing process in which the blank´s temperature is over its recrystallization point. The advantages of this variant are the complex geometries achieved, less pressing power is used, and fragile materials can be drawn easier, but some disadvantages are presented, more energy is required to warm the blank, both surface finish and precision are affected, and the dies´ life is shorter.

A final aspect to take into count is the friction generated between the dies and the blank, which is helpful, but also harmful. The friction is helpful if there is enough to produce a certain heat beneficial for the drawing, but in counterpart, it can produce fractures in the blank, reduce the dies´ life, and also in some cases, it creates a critical condition where adhesion between the dies and the blank happens. To avoid the bad friction effects, lubrication is used to reduce this coefficient, usually some water, oils or greases are applied.

2.3 Incremental Sheet Metal Forming (ISMF)

Incremental Sheet Forming (ISF) is a sheet metalworking method where a metal sheet is clamped to a blankholder; then a spinning tool (flat or spherical) push the sheet downward while moving simultaneously in the x and y directions, following the path programmed with a CAM software, producing a local plastic deformation. There are two types of ISF techniques also subdivided in two:

2.3.1 Two Point Incremental Forming (TPIF).

Method developed by Powell and Andrew [26] and later called backward bulge method thanks to Matsubara. In this configuration for ISF there is a fixed die that guides the path for the piece, this feature improves the precision in the geometry; Also, the blankholder is moving downward as the tool go through the sheet deforming it and creating the final piece, therefore, forces are applied in two directions, the first one is the forming tool going downward creating the shape, and simultaneously the second one is the partial/full die that exerts a force upward, and these two points applying forces are the reason it is called two point incremental forming. The differences between the two types of TPIF is the die used since it can be a complete or full die, or just a partial die, both in both cases dies do not need to have to be very accurate or flawless.

2.3.2 Single Point Incremental Forming (SPIF).

For this technique as its name says, there is only one point providing a force to deform the blank. This method has the big benefit that is completely dieless, therefore time, material and costs involved in the dies production is avoided. In both SPIF cases, a fixed blankholder is used, but the differences between the two types of SPIF lies in the usage of a counter tool that helps to the creation of the final piece.

In both cases, a small tool is used, this can have a tip either flat or a spherical, tool´s material and even treatment can change, because it will give different results in the final shape, tool´s lifetime, and surface finish, so this is a factor to take in count. A great advantage in this process is that symmetry is not restricted, so asymmetric shapes can be accomplished.

Change between geometries is not a problem in this sheet forming process since the same tool can be used, or its change is very easy, also the setup for the new piece is simple, because only the new path needs to be set in the machine.

Even though it is a great process, factors have an important effect in the final piece characteristics, like roughness, formability, final shape. Friction is one of these factors that SPIF faces, since high speed spinning increases heat, this can be useful because this improves formability, but also this friction between the tool and the sheet can affect the surface finish, so lubrication is a great instrument to avoid this defect and control heat though out the deformation process. To support and hold the metal sheet to be deformed, a platform is used so the piece can grow downward without the fear of the tool colliding with the table. This platform has a simple structure, since it is composed by a blankholder, four pillars, and a base.

There are some limits that this process faces: (a) maximum drawing angle, a parameter delimited by the sheet material, because it is the maximum point to deform the blank before it breaks. There is a special machine designed for this work, but also a 3 axis CNC milling machine is useful to accomplish this process, so it is a very accessible process.

Talking about thickness Jeswiet and Hagan in 2002 [27] made an analysis of the accuracy of the sheet thickness against the sine law, and concluded that having only one pass to create the shape, the thickness in the shape follows the sine law

$$T_f = T_i * sin\,(90 - \theta)$$

Where θ is the angle at which the piece will be deformed.

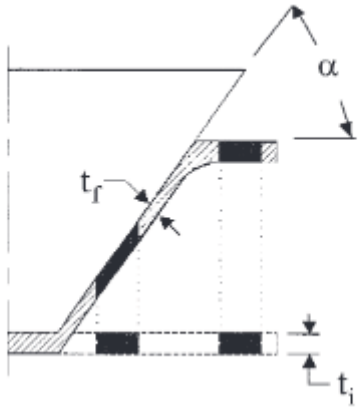

Figure 2: Jeswiet's SPIF thickness explanation [27].

2.4 Surface finishing

According to D.K. Singh [40], surface texture is defined as the resulting irregularities arising from the plastic flow of metal during a machining operation. These irregularities are peaks or valleys seen from a micro or nanoscopic view, these are usually called asperities. Even though materials have a natural texture the method used to produce a certain piece directly affects the final texture though the workpiece. There are three main components in the surface texture:

2.4.1 Roughness

Roughness is also known as primary texture, is the smallest irregularities in the surface texture, and is inherent in the production process. It shows the deviation of the surface of a component from a perfect} and smooth plane.

- Roughness measurement Ra

  The Ra value method is frequently used and has been recommends by ISO for expressing surface roughness. The deviation of surface irregularities from the centerline is the measure of roughness and it is measured in micrometers.

$$Ra = \frac{1}{N}\sum_{1}^{N}|Zi - \mu|$$

This measurement does not give a clear indication of the shape of the physical surface. The surface profile for Ra can be obtained through measuring with a stylus instrument.

2.4.2 Waviness

Waviness, also known as the secondary texture, is a slow undulation in the component surface resulting from the machine or work deflection, sideway wear, vibrations and chatter. It is the larger irregularities upon which roughness irregularities are superimposed, but there is not a distinguishable bound between roughness and waviness

2.4.3 Lay

Lay is the direction of the surface pattern generated by the machining method.

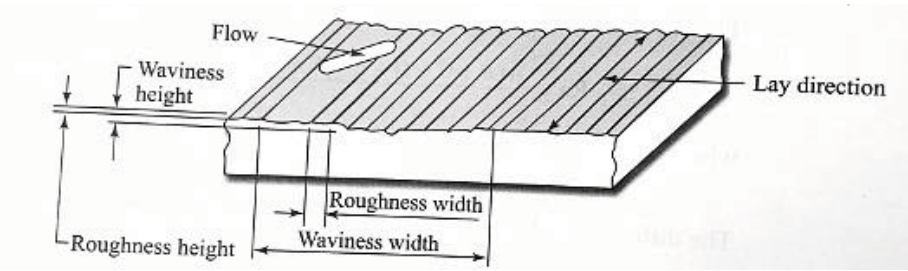

Figure 3: Singh´s surface finishing description [40].

The interaction in motion between two surfaces results in rubbing, in which power loss, friction and surface wear occurs.

Friction occurs when an object is moving, sliding or rolling on the surface of another and is related to the real area of contact.

Wear is defined as the progressive loss or removal of material at surfaces due to rubbing. Loss in materials presented by wear may alter designed surfaces and change their performance. Excessive wear can increase friction and induce surface failures.

Lubrication is an effective way to reduce friction and wear. The lubricant must have a certain viscosity, and the two surfaces must be in a relative motion. Both pressure and temperature affect lubricant viscosity.

Surface topography is very important to machine component lubrication because the two mating surfaces are the boundaries of the lubrication flow in between, and the real contact of surface occurs at asperities, not the nominal area of contact.

Tolerances on surface finish should not be greater than required as acceptable functional operation of the part and the finished product, since more strict tolerances and finish requirements would represent more precise machining operations which would drive up cost.

2.5 Optical measurement

There are several methods for three-dimensional measurement [9] [31] [38], the most common is 3D Scanning. This is a measurement system which uses optical triangulation, photogrammetry and fringe projection method, which creates a digital model that later can be inspected, modified or tested though different software. One of the main advantages of this technology is that the physical piece is only involved at the beginning, when it is scanned, so later there is no need for more pieces to be produced or affected, resulting in a saving of time, material and money. Within 3D scanning there are two main methods in which it can be divided, contact and non-contact scanning. Contact scanning is characterized by the fact that has the best precision between both thanks to its tip with a sensor, but this type is limited to the complexity of the piece. Both scanning types are distinguished by the short production time compared to the time implicated in a CAD modeling of a piece with a complex shape from scratch, but it is known that the contact 3D scanning takes more time than the non-contact one. We´ll be concentrating in de non-contact one.

Non-contact 3D scanning equipment works though two cameras and a light beam, the cameras capture several pictures of the piece with several reference points on the surface, these points are registered in the system as well as the distance between each other. The software makes many operations to determine the shape and size of the scanned piece. The first step is when the picture is taken, in this moment several patterns projected with the light beam are recorded by both cameras locating the position of the reference points, here the time the light beam takes to go to the piece and come back determine the distance to which

the part is placed and the distance to each reference point visible in the shoot. To locate the position of the next picture, the software uses triangulation though the position of at least 3 reference point in order to decide the plane the picture is showing, in that way the next photo can be aligned with the previous one. To establish the part´s shape the cameras have a chip that turn the intensity of the light returned to a grey scale and assign a number of the scale (0-255) to each pixel, when the difference of number (color) between a pixel and its neighbor is a lot, the software interprets this color gap as an edge, if several edge points are found, a border line is created.

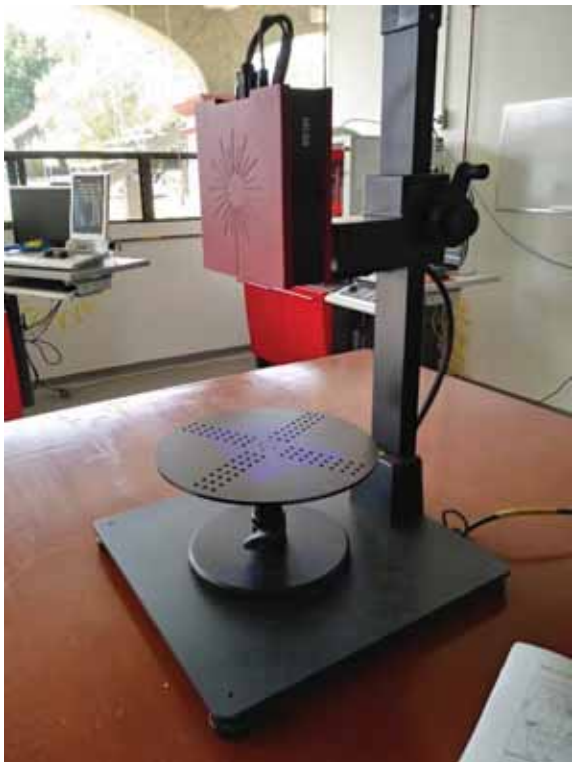

Figure 4: 3D Scanner, GOM, Atos Core 200 (source: own creation).

3D scanning technology has a great application area since it can be effectively applied to replication and restoration, reverse engineering, and obviously to metrology. Also, the factor that precision is improving and costs for this technology is decreasing are aspects that expands its use.

2.6 Three-Dimensional Printing

3D printing is a process of the family of the additive manufacturing, it is usually used in prototyping, but according to Garechana et al. [20] already 9.1% of the real world 3DP machines are for actual production, which would represent the capacity of this process to keep expanding and improving as fast as it has done so far. Some of these advantages improving in 3d printing are the short process time cycle, the low cost not only in the material, but also in the machinery, the precision in the printed pieces, and the level of customization maintained by the flexibility to change this process has, making it a process able to fit for different situations.

There are several processes regarding 3d printing, but we´ll be focusing in the material extrusion one, since it's the most common between the 3d printers. For this process the most common materials are the thermoplastics Acrylonitrile Butadiene Styrene (ABS) and Polylactide Acid (PLA). So the plastic wire goes though the machine, where it is heated up to a point where the melted material can be extruded though the machine´s tip and a leave a thin layer applied on the machine´s table following the path previously created in G code. The software used to create the toolpath slice the piece in the needed layers to create the piece considering the thickness parameter.

CHAPTER III

3.1 Introduction

In this section, the preparation that was needed to achieve the results of this investigation will be explained. It is important to mention that several activities were developed with the help of the research group comprised by Dr. Rogelio Pérez, who assisted us as our tutor and the students Arturo Belmont, Ernesto Quiroz and Rodrigo Cruz, besides myself.

3.1.1 Investigation and literature

The idea to start with this project came from the enthusiasm of our professor Dr. Rogelio in the present topic and his belief that Single Point Incremental Forming is a process with a vast working area and several applications for the future. Taking this in count, he succeeded to get the rest of the team as myself interested in this process and the investigation project he was proposing. He wanted us to understand the topic, so we started to check exiting documentation about Incremental Sheet Forming beginning with his doctoral thesis going through Jeswiet et al ´s state of art [21] and many other articles [3] [22] [25] [26] [30] and books talking about the previous described matters.

The next information is a brief introduction to the sequence of activities that were followed by our team. If there´s a greater interest to know the details of the processes of our investigation and costs analysis, please head to the work of Arturo Belmont [8]. If the interest is directed to the simulation area and the formability limits of the SPIF process, please refer to the research performed by Ernesto Quiroz [45].

3.1.2 Process theoretical comparison

The following table summarizes the theoretical information known about each process. Some of these points are the ones that this investigation is trying to prove or solve.

Table 1: Theoretical comparison between SPIF and deep drawing (source: own creation).

	Single Point Incremental Forming	Deep Draw Forming
Used for	Prototyping, small batches	Big batches
Time per piece	Long forming time	Short forming time
Tooling costs	Cheap tooling manufacturing	Expensive tooling manufacturing
Geometrical accuracy	Low geometrical accuracy	High geometrical accuracy
Surface finishing	Bad surface finish	Good surface finish
Flexibility	High customization level	Low customization level
Forming level achievable	High forming limit	Normal forming level
Machinery adaptability	High adaptability to every CNC machine	Low adaptability to every press
Energy consumption per piece	High consumption	Low consumption

3.1.3 Machinery

The following equipment is the one used in the university for educational purposes, also is the one used by us to develop this investigation

- CNC EMCO Concept mill 55

Table 2: CNC EMCO parameters description (source: own creation).

CNC EMCO Concept mill 55							
Dimensions (X/Y)	Possible Z height	Axes	Speed range	Max. power	Feeding pressure	Max. tool diameter	Feed rate
190 x 140mm	190mm	3	150-3500 rpm	0.75 kW	6 bar	40mm	0-2 m/min

- Universal testing machine WDW-300E

Table 3: Universal tensile machine parameters description (source: own creation).

Tensile Test Universal Machine WDW-300E								
Max. Load capacity	Accuracy of load	Deformation measuring range	Deformation measuring accuracy	Dimensions	Speed range	Width test space	Power supply	Feed rate
300 kN	± 0.5%	0.2% ~100%	±0.5%	70 x 770 x 2558 m	005-500 mm/mi	760mm	5 kW	0-2 m/min

- Scanner 3D Atos Core

Table 4: Gom Atos Core 80 parameters

Gom Metrology Scanner ATOS Core 80				
Measuring area	Working distance	Sensor dimensions	Temperature range	Power supply
80 x 60 mm	170 mm	206 x 205 x 64 mm	5 - 40°C	90-230 v

- Kossel mini 3D printer

Table 5: Kossel mini 3D printer parameters description (source: own creation).

Kossel Mini 3D Printer				
Building plate size	Max. Building height	XY resolution	Z resulution	Speed
17cm	27cm	0.035 mm	0.1 mm	320 mm/s

- Emco Mat-17/20 manual lathe

Table 6: EMCO Mat-17/20 parameters (source: own creation).

EMCO MAT-17/20 Manual Lathe				
Distance between points	Power	Spindle speed	Force	working dimension
700 mm	5.0 kW	55-2350 rpm	1600 N	600 x 220 x 110 mm

- Emco FB-3 manual mill

Table 7: EMCO manual mill parameters (source: own creation).

EMCO FB-3 Manual Mill				
Dimensions	Power	Speed range	Force	Required Temperature
300 x 200 350 mm	1.4 kW	80-2200 rpm	1600 N	10-35 °C

- Mitutoyo roughness meter

Table 8: Mitutoyo roughness tester parameters description (source: own creation).

Surface Roughness Measuring Tester SJ-210					
Standard	Cut off lenght λc	Number of sampling	Measuring speed	Measuring range	Measuring force
ISO 1997	0.08 mm	x5	0.5 mm/s	16 mm	4mN

3.1.4 Software

The following are the software used to build this research.

- Creo parametric 4.0.
- Gom scan 2016.
- Gom Inspect 2016.
- Autodesk Inventor Enzo 2017.
- Ultimaker Cura 2.5.
- Microsoft Office 2016.

3.1.5 Geometry design.

On the literature read it is said that a truncated pyramid is a simple geometry that can be created without much effort and that is efficient to evaluate the possibility of creation of more complex parts, since this geometry covers sections with different shapes (straight and round) and can prove the capacity of the process to deform the metal sheet.

On the other hand, the limits of the material and the machinery were taken in count for the geometry. In our tutor´s thesis, a formula for precision was investigated taking in count the needed force to be applied. For further information, please direct to his thesis [ ],

so that is the reason of the 45° angle and the number of steps down calculated for our pyramid. The design was implemented with the use of two software: Creo Parametric and later with Autodesk Inventor.

3.1.6 Toolpath design.

The toolpath is the route to guide the tool through the process, this is an algorithm in G code language, which is the language that Computer numerical control (CNC) machines use to follow the shape of a part mathematically described in a CAD software. In our case, toolpaths were needed for the SPIF process as well as the 3D printing processes.

For the SPIF case, the toolpath was obtained though the software Autodesk Inventor, where the truncated pyramid designed was transformed with the software´s CAM tools into a toolpath for a generic CNC milling machine. Later it was seen that lubrication needed to be applied through the forming process, since friction heat melted the lubricant and surface finish resulted affected, so stops were needed to replace the liquefied lubricant. The pauses in the program were placed every certain quantity of steps down thanks to the code M00, also other details were adjusted to adapt to our process. After all the needed changes, the G code can be imported to the CNC milling machine.

For the 3D printing case, the design was done in the Autodesk inventor software, but to get the toolpath Ultimaker Cura software was used. Some of the parameters employed are the ones specified for the material PLA, while others were specified by us. In the following table these parameters are shown.

Table 9: 3D printing parameters for PLA material (source: own creation).

PLA parameters						
Layer height	Infill density	Print temperature	Plate temperature	Printing speed	Shell thickness	Support
0.25 mm	0.2	210° C	60° C	60 mm/s	0.8 mm	No

So, the software takes the CAD shape and slice it to the layer thickness size, and then what is inside of each layer gets a gridding with the specified density, also all the borders and edges get a thicker filling thanks to the shell thickness parameter. Two printed parts, the middle marker and the sheet support, no printing support was needed, but for the 3D scanning prototype, the support was added on the sides. After all the parameters are selected, the program estimates the time it will take to create the piece, also the quantity of material that will be used. All the selected parameters and the design of the piece is then transformed into a G code format that can be passed to the 3D printer.

3.1.7 Clamping design.

The design of the clamping device was an idea taken from the one used by Dr. Rogelio Pérez in his own doctoral research. Some modifications were needed, like the position of the screws and the little step made in the middle of the lower clamping plate to hold the blank better in its place.

Figure 5: Clamping device design

The clamping device is compound by a base, 4 columns, 2 clamping plates, and 8 screws (Figure 6). The base has de necessary dimensions to grip to the CNC milling machine base, the two clamping plates have the required dimension to create a shape of 70 x 70, and the columns height is the desired to fit in the milling machine. More clamping design information can be found in Appendix B.2.

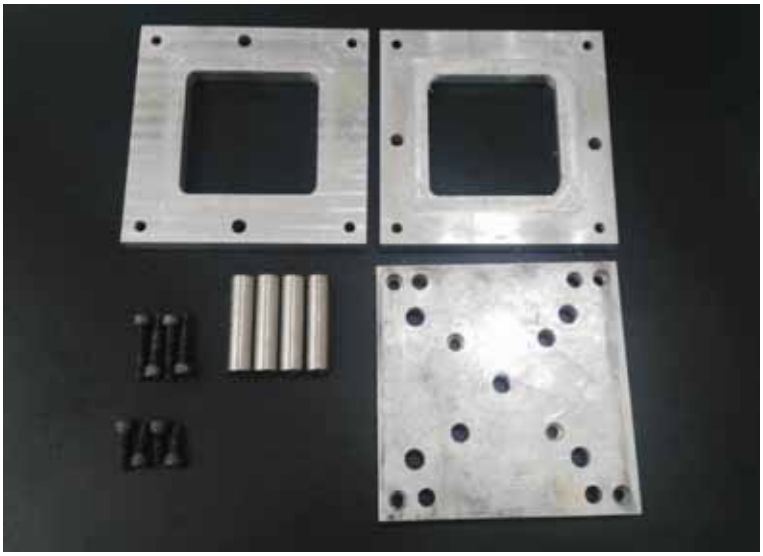

Figure 6: Clamping device components (source: own creation).

3.1.8 Tooling definition.

There are three main documented types of tools: the semispherical ones, the bearing ones and the ones with a flat end, but we decided to stick to the basic one that is the semispherical one. The tools were not machined by us, we bought a kit with several spherical tools of different radius sizes. The tool radius selection depends of the smallest radii in the manufactured part. Jeswiet et al. [21] indicated that a smaller tool radius would improve the surface finishing, but also more steps and time would be required, that is why through the 18 try out SPIF samples three possible tool radius were tested, at the end, the selected radii size for our tool was of 6.5 mm which was also in the range recommended by the article.

Figure 7: Tool used for SPIF process (source: own creation).

3.1.9 Sheet´s material definition.

The material selected for the pyramids is a stainless steel AISI-304 sheet, which is a metal material basically compound by iron, chromium and nickel, this material presents good mechanical properties that enable it to be the most employed stainless steel, having a great working utilization on forming and welding areas. Thanks to the chromium, stainless steel presents a resistance to water and therefore a protection against rust. Nowadays, many products are made of stainless steel so there is a wide application area for the results acquired in our research. Even though the material was purchased with a nominal sheet thickness of 0.50 mm, in reality our metal sheet presents an actual thickness of 0.45 mm.

3.1.10 Clamping device´s material definition.

The materials for the clamping device were thought based on the forces that would be given to the zone. That´s why the base and the clamping plates were made of aluminum 6061, since not much force would be applied on those zones, and the columns were made of tooling steel AISI A2, since no deformation in the height of the piece could be accepted, so a strong material to hold the process forces was selected. Those are the reasons of the material selection for our framework.

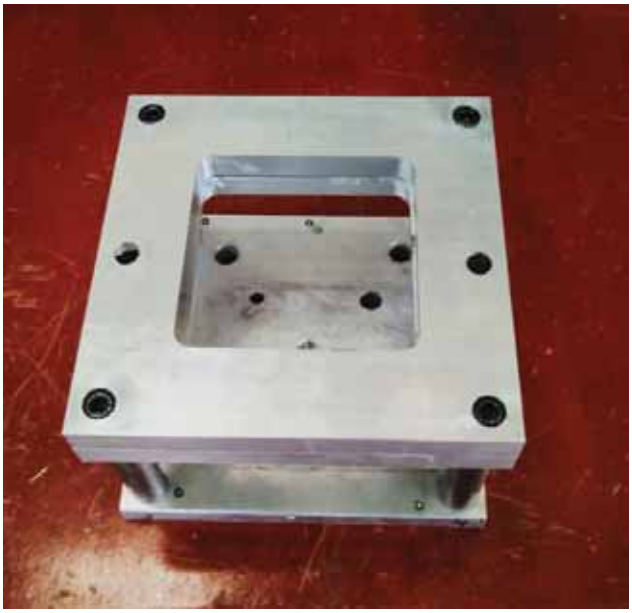

Figure 8: SPIF clamping device (source: own creation).

3.1.11 Creation of SPIF instrumentation.

Compound with a base, four columns, 2 clamping plates and the spherical tool; the base and clamping plates are made of aluminum, while the columns are made of steel. Regarding the tools, a set of spherical tip tools were purchased. From it, three tools, with diameter of 4.29, 6.34 and 7.92 mm, were selected and given a nitriding thermos-chemical treatment. All the parts of the framework were machined by us, the columns were manufactured in the manual lathe, and the base and plates were made in the manual milling.

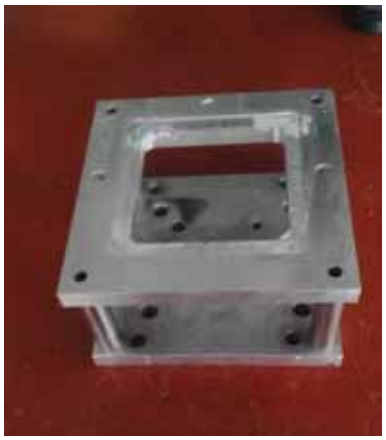

Figure 9: Views of the SPIF clamping device open (source: own creation).

3.1.12 Creation of sheet support for SPIF and middle marker.

On the course of the try outs for the final selection of our SPIF parameters we could notice that the tool path was smaller than the space on the inner part of the clamping plates, so there was a gap that resulted in a deformation in the pyramid, making its measurement more complicated, so the decision of creating a support for the blank was taken. The sheet backing plate is an ABS 3D printed square shape with the center made to the exact measurements of the pyramid, so no deformation would happen to it during the SPIF process. The support design can be found in Appendix B.3.

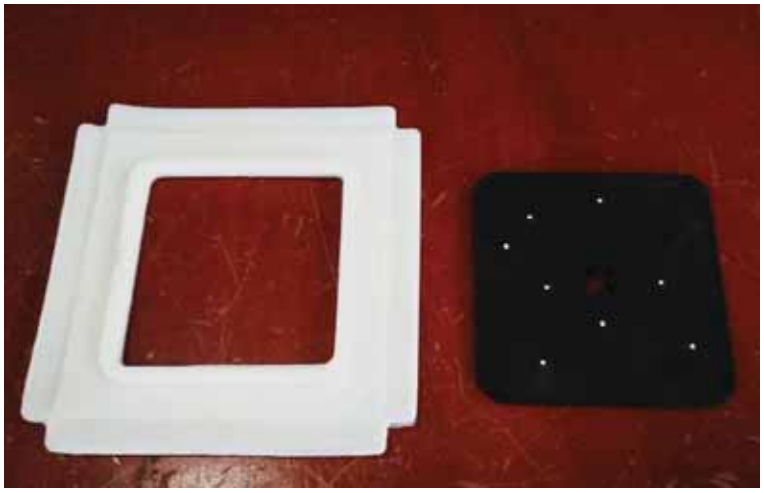

Figure 10: 3D printed supports for SPIF process (source: own creation).

On the other hand, it was seen that placing the tool in the exact middle was difficult and sometimes it wasn´t successful, so the creation of the middle marker allowed to achieve a higher level of repeatability. The middle marker was made of 3D PLA printing. The design can be found in Appendix B.3

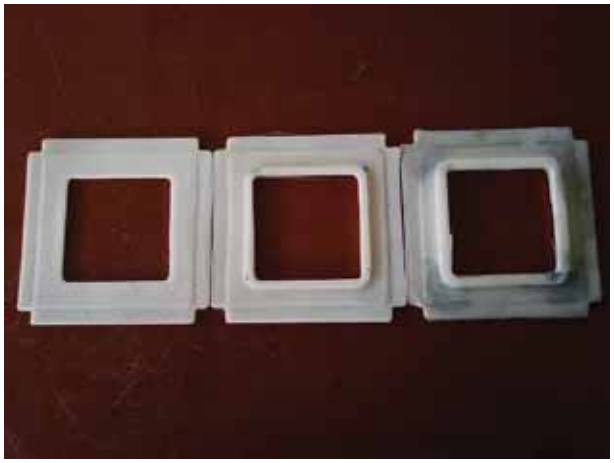

Figure 11: 3D printed SPIF support evolution (source: own creation).

3.1.13 Pyramids creation.

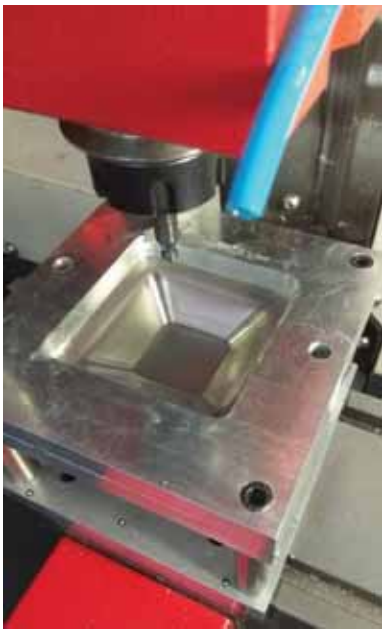

Figure 12: SPIF actual process (source: own creation).

We made 21 SPIF pyramid samples using a toolpath created by Dr. Rogelio and modified by Lic. Ernesto Quiroz. There were some changes made throughout the samples path, but is important to take in count that when the optimum parameters were achieved, only three pyramids more were produced and those were the ones to be considered for the subsequent analysis.

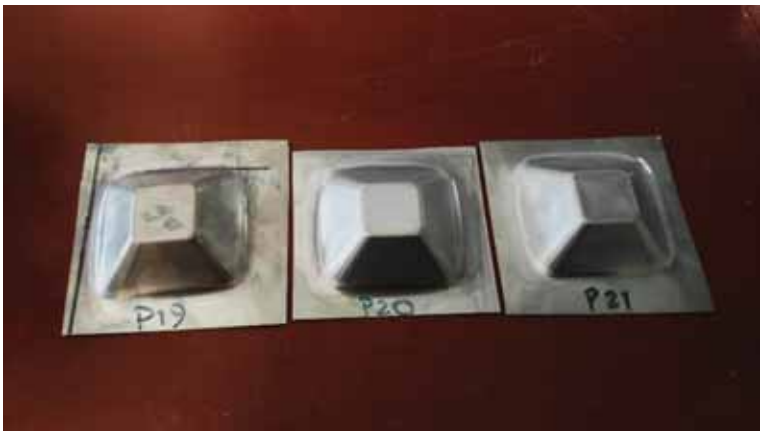

Figure 13: Top view of the resulting pyramids (source: own creation).

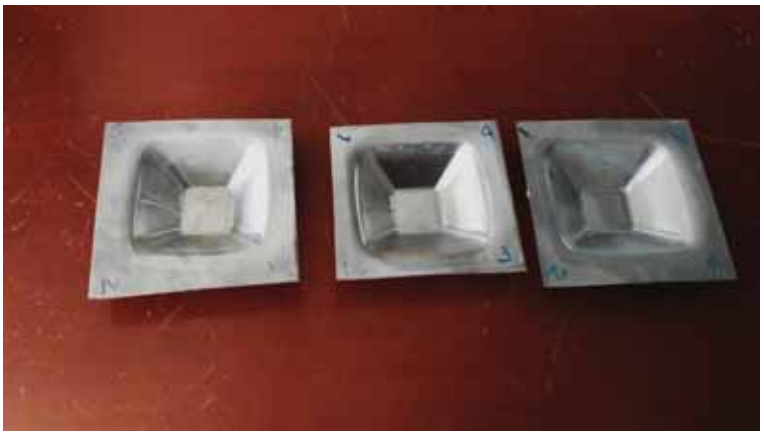

Figure 14: Bottom view of the resulting pyramids (source: own creation).

The first three pyramids were the samples where a lot of adjustments were discovered, starting with the lubricant needing, problem that was seen from the initial samples presenting a grave wear situation on the surface of the pyramids, also the pieces presented burnt marks, so modifications in the tool feed were made.

Table 10: Pyramids 1-3 parameters (source: own creation).

Angle	Number of steps	Step height	Tool diameter	Tool feed	Spindle speed	Pyramid dimension
45°	80	0.25 mm	6 mm	1000 mm/min	1000 rpm	70x70x20 mm

Figure 15: Resulting pyramid 1-3 appearance (source: own creation).

The next three produced even better parameters to the process, but even though improvement was seen, it was not enough for the investigation, also these pyramids were

made with the first tool we used, this tool had no thermal treatment, so it got deformed after the third pyramid, so marks were seen when the next pieces got inspected. The problem with the pyramid displacement from the center was also detected on these three samples.

Table 11: Pyramids 4-6 parameters (source: own creation).

Angle	Number of steps	Step height	Tool diameter	Tool feed	Spindle speed	Pyramid dimension
45°	80	0.25 mm	6.09 mm	2000 / 350 / 500 mm/min	1000 rpm	70x70x20 mm

The next three pyramids got an even better appearance thanks to the tests made with other two tool feed factors, but the toolpath was still marking the final piece. The piece was finally centered so no fine-tuning was needed to avoid the collision between the clamping device and the tool. It was at this point were the code M00 was finally added and the problem with the lack of lubrication was solved.

Table 12: Pyramids 7-9 parameters (source: own creation).

Angle	Number of steps	Step height	Tool diameter	Tool feed	Spindle speed	Pyramid dimension
45°	80	0.25 mm	6.09 mm	400 / 800 mm/min	1000 rpm	70x70x20 mm

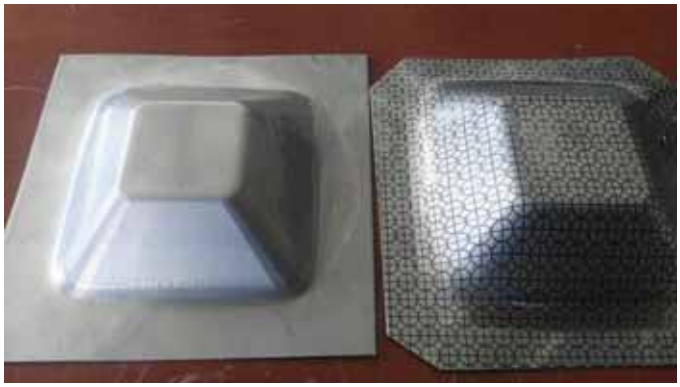

Figure 16: Resulting pyramids 7-9 appearance (source: own creation).

The next three pyramids were done with the new set of tools with the nitriding treatment, the tested tools had the following radius 4.29, 6.35, and 7.92 mm, each was tested with a pyramid and with a visual inspection was proved that the 6.35 radius tool gave the best results. Since on the past three samples a displacement matter was noticed, on this phase

is when the middle marker was introduced, having great results in the location precision, also on the setup time.

Table 13: Pyramids 10-12 parameters (source: own creation).

Angle	Number of steps	Step height	Tool diameter	Tool feed	Spindle speed	Pyramid dimension
45°	80	0.25 mm	4.29 / 6.35 / 7.92 mm	500 mm/min	1500 rpm	70x70x20 mm

After the decision over the tool diameter, considering the visual resulting appearance, was taken choosing the tool with a diameter of 6.35mm; some tests were made over the spindle speed without changing the other parameters. Here it was seen that 1200rpm made the best visual result.

Table 14: Pyramids 13-15 parameters (source: own creation).

Angle	Number of steps	Step height	Tool diameter	Tool feed	Spindle speed	Pyramid dimension
45°	80	0.25 mm	6.35 mm	500 mm/min	1000 / 1200 / 1500 rpm	70x70x20 mm

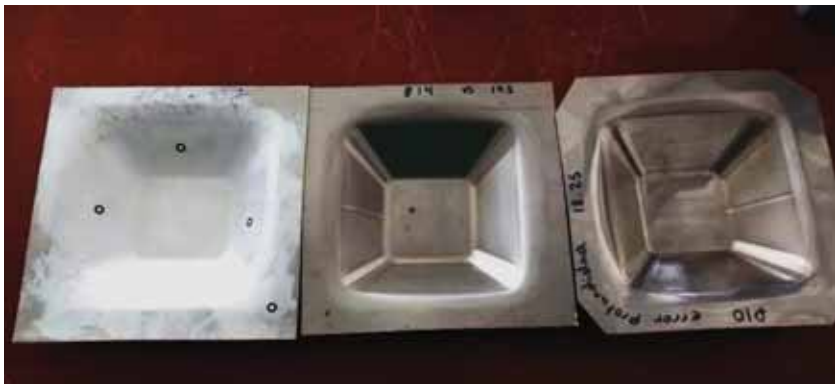

Figure 17: Resulting pyramids 10-15 appearance (source: own creation).

The next were an experiment to perform different shapes, so conical shapes were tried to see the reaches of our process, also different heights and base sizes were applied, the design for these parts was also made in Autodesk Inventor, and later the toolpath was obtained. The parts got good shapes, none of them presented fractures or wear. The parameters were the same used as the previous pyramids with the exception that the spindle speed was 1200rpm in all of them

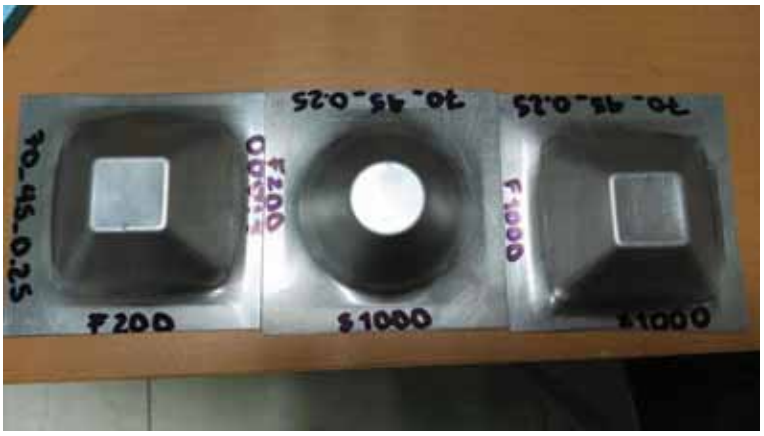

Figure 18: Resulting experimental shapes appearance (source: own creation).

In the next three pyramids are where we discovered the issue with the height difference caused by the sheet deformation at the beginning of the pyramids shape, so here is where the SPIF support was designed and printed. Three prototypes were created, the first one was very thin, and the working area was exactly the size of the pyramid, the second one was 1mm thicker and took in count the space of the tool radii on each side, and the third one, was 2 mm thicker than the first one and had the same inner space as the second one, each of them had a sample, and it was proved that this deformation was drastically reduced, the best results were achieved with the second prototype. Also, on this point of the pyramids production, it was discovered that a relationship between two parameters that gave very good results. This relationship is between the spindle and the feed rate which we saw that needs to be close to 2.5.

Table 15: Pyramids 16-18 parameters (source: own creation).

Angle	Number of steps	Step height	Tool diameter	Tool feed	Spindle speed	Pyramid dimension
45°	80	0.25 mm	6.35 mm	300 mm/min	750 rpm	70x70x20 mm
45°	80	0.25 mm	6.35 mm	500 mm/min	1250 rpm	70x70x20 mm

For the last three pyramids all the collected improvement information was applied so the following parameters were used:

Table 16: Pyramids 19-21 parameters (source: own creation).

Angle	Number of steps	Step height	Tool diameter	Tool feed	Spindle speed	Pyramid dimension
45°	80	0.25 mm	6.35 mm	500 mm/min	1250 rpm	70x70x20 mm

These pyramids (Figure 13 and 14) presented great visual appearance, defined geometry, no fracture was detected on any of them, no displacement was perceived on the sheet, and no deformation was seen on the beginning of the piece forming.

Figure 19: Production of SPIF pyramid seen from below (source: own creation).

3.1.14 Dies creation and framework modification

To develop the comparison between the two processes, the creation of the stamping tooling was necessary, that´s why the punch and the matrix were created, both were made of aluminum blocks and machined in the same university´s machining center adapted for the SPIF process. The stamping set is compound by a matrix, a punch, 2 guides, 2 clamping plates, 4 columns, a bottom base plate, a top base plate, and 8 screws (Figure 20).

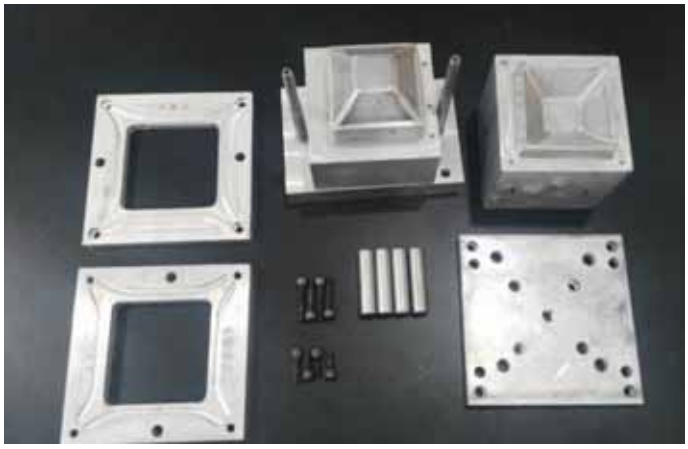

Figure 20: Stamping dies set (source: own creation).

The dies shape was planned to follow the ideal truncated pyramid´s shape, and only a difference in the radii zones were planned, but a problem with the piece alignment arise and at the end the final shape needed to be changed. That is the reason of the limitation of our stamping dies production and the impact seen in the resulting data.

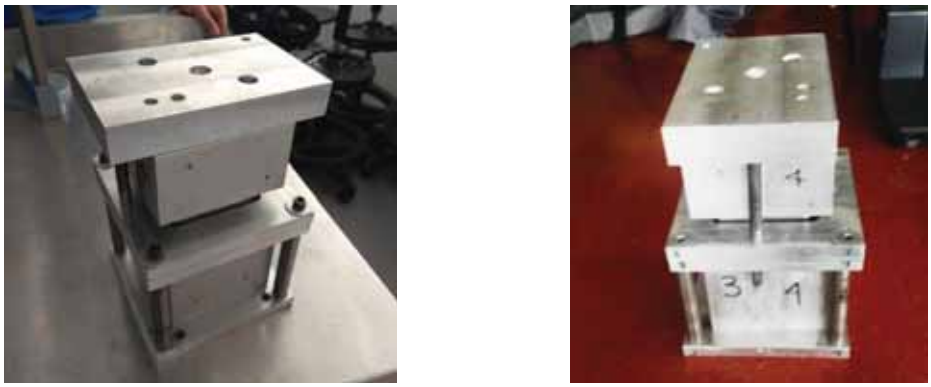

Figure 21: a) Front and b) right view of the stamping assembled dies (source: own creation).

With the intention of use the existing framework and prove that both processes can be achieved with the same basis. Some modifications were applied so this could be used later in the compression side of the universal tensile machine. For this change, new supporting columns were built because the existing ones were short for the die's framework, and the new ones couldn´t be used in SPIF process since the CNC´s lathe machine space is reduced for these columns. Another change improved is the use of drawbeads. This enhancement was done thanks to the support of our team member Lic. Rodrigo Cruz, who made several

stamping simulations with the software Ls Dyna to validate the optimum results affected by the stamping equipment, the outcome of the simulations was that drawbeads must be used to reduce the wrinkle appearance in the pyramids, so this modification was also added to the framework. The blank holding plates were also made of aluminum and the drawbeads design was machined in the CNC milling machine.

At the end, we got a modular clamping frame that could be used in any of the two processes.

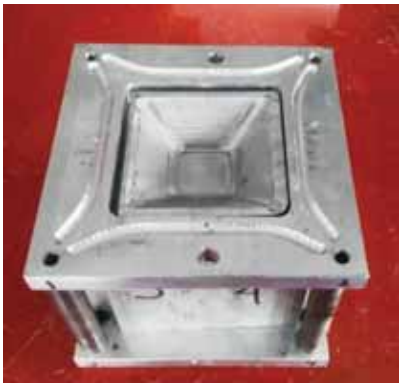

Figure 22: Open pressing dies to show drawbeads and matrix shape (source: own creation).

3.1.15 Stamped pyramids

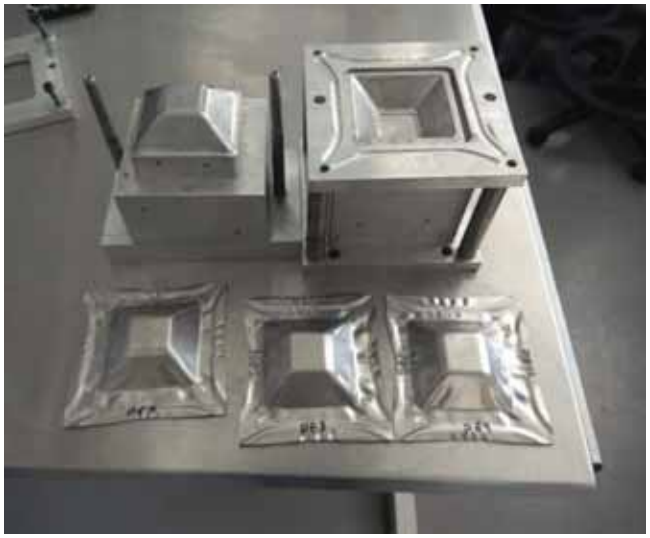

Figure 23: Deep drawing dies and resulting stamped pyramids (source: own creation).

The stamping process was executed in the Tensile Test Universal machine in the compression side. In the following table the parameters used in the machine are displayed.

Table 17: Tensile test universal machine parameters (source: own creation).

Tensile Test Universal machine parameters			
Test type	Maximum load	Extensometer limit	Rate
Compression	60 KN	25mm	5 mm/min

Figure 24: Inner appearance of the stamped pyramids (source: own creation).

The Nine stamped samples were done, but only 3 of them were useful for this research.

Figure 25: Tensile test universal machine running a stamping test (source: own creation).

The first set of 3 pyramids had the problem of been more compressed than necessary and they were stopped when they reached the maximum load, so the problem in the dies machining was strongly printed in the pieces, so they were useless. For the next set of three, the stamping process was stopped much earlier, each sample was stopped when they reached 13 KN. This prevented the sheet to really take the shape of the dies, but the needed height wasn´t reached. And finally, the last set of three pyramids, these are the pyramids that were used for the next analysis, in this case, the pyramids compression tests were stopped once the deformation graph presented a quick increase, this happened when the tests were around 19 KN, so they got the height and shape required for the analysis.

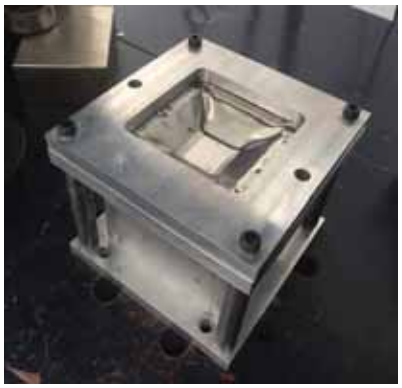

Figure 26: Open dies after a pressing test (source: own creation).

3.1.16 Pyramids 3D scanning

An investigation of accuracy, demands the use of measurement resources to keep track of the results. There are many ways to measure a piece, but the capacity to reproduce the same results depends on the accuracy of the measuring device, the ability of the operator, and the faculty to stablish a standard to execute the measurement.

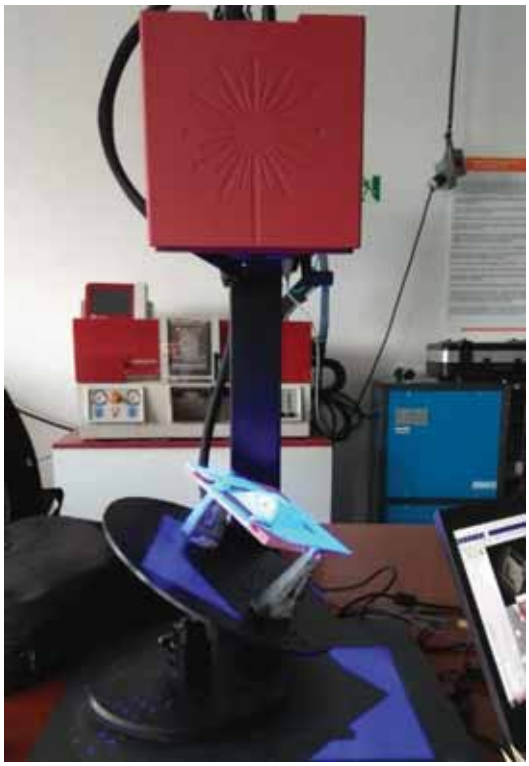

Figure 27: Scanning of a stamped pyramid with the second holding device (source: own creation).

For this investigation, the first tools that were utilized are the common measuring devices like the Vernier and the dial height gauge, but with the deformation at the beginning of the piece and the complication to create a measuring standard, soon it was seen that this weren´t the ideal devices to analyze the measurements in our project, that is why, we started to use the 3D scanner.

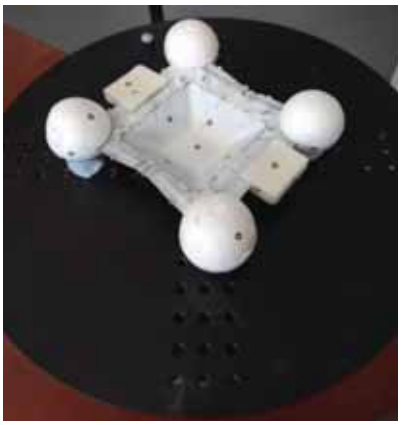

Figure 28: Scanning with the final holding set (source: own creation).

The scanning process is a very simple one, but it can be tedious for the time it may take to get a great measurement. An advantage of this process is that is almost has no process variables. The only ones, are the plate temperature, which is usually between 21 to 23°C and the allowed shooting movement, which was defined as 0.20 pixels for our case.

As it has been said from the beginning of this research, we are looking for the resulting thickness in our pyramids, so a good scanning of the pyramid without movement or variation was important to effectively study the sheet resulting thickness in the pieces.

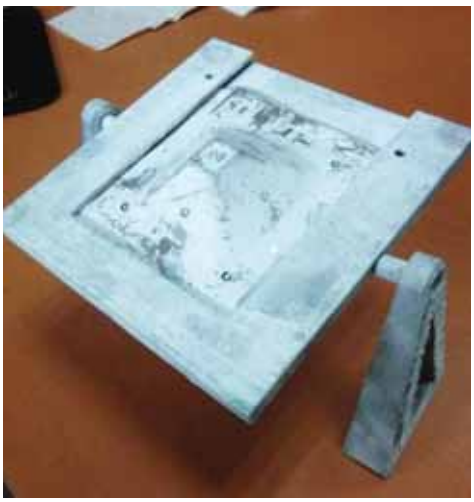

Figure 29: First scanning 3D printed holding set (source: own creation).

When we started to scan the pyramids, we found that with only the pyramid it was impossible to get scanned, since no common reference points could be scanned to later mate both sides of the pyramid to complete the piece, so the first idea was to create a device that could allow us to make the scanning. This frame had a thicker side. But the problem of the movement of the piece arise, so the scanned piece presented a lot of deviation.

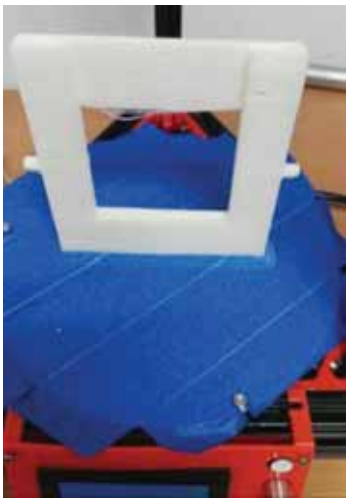

Figure 30: 3D printing of the first holding device (source: own creation).

The second and final option was the use of Styrofoam balls of 10cm of diameter, but the sheet thickness problem stayed, so this problem was solved with a 5cm part of the printed frame side, so the thickness could be identified and jointed at the end of the scanning process.

Figure 31: Final set to aid on the scanning process (source: own creation).

CHAPTER IV

4.1 Introduction

After explaining the main steps to obtain the data from the sample pyramids, in this section the results will be showed and analyzed. For this analysis, the scanned pyramids were transformed into reports and data tables, roughness result were also saved in a table. The following will be focused as a descriptive analysis to know better the behavior of each process.

4.2 Reports

From the acquired reports the following tables will be shown so the perception and understanding of the results will be better.

4.2.1 Initial pyramid alignment

The following are the resulting meshes from the scanned pyramids. For each process there is a certain position stablished, so all of them gave similar results. In the case of the SPIF placement, the string of the step down is heading to the X positive direction as shown in Figure 33. In the case of the stamping location, deformation on the top is aligned with the X axis, the smallest deformation is directed to the positive direction (Figure 34). The ideal pyramid has no need for a specific initial alignment so the automatic one is employed (Figure 32).

- Ideal pyramid

  The ideal pyramid is a CAD model of 20mm height, 45° angle, and has a base of 70 X 70 mm. It was modeled on Autodesk Inventor software and exported with a format IGES.

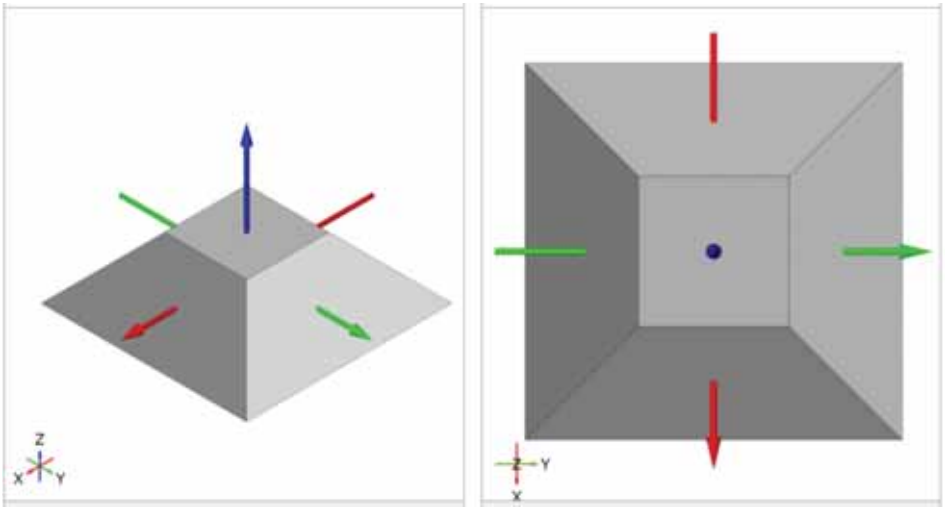

Figure 32: Ideal pyramid used model and alignment (source: own creation).

- SPIF

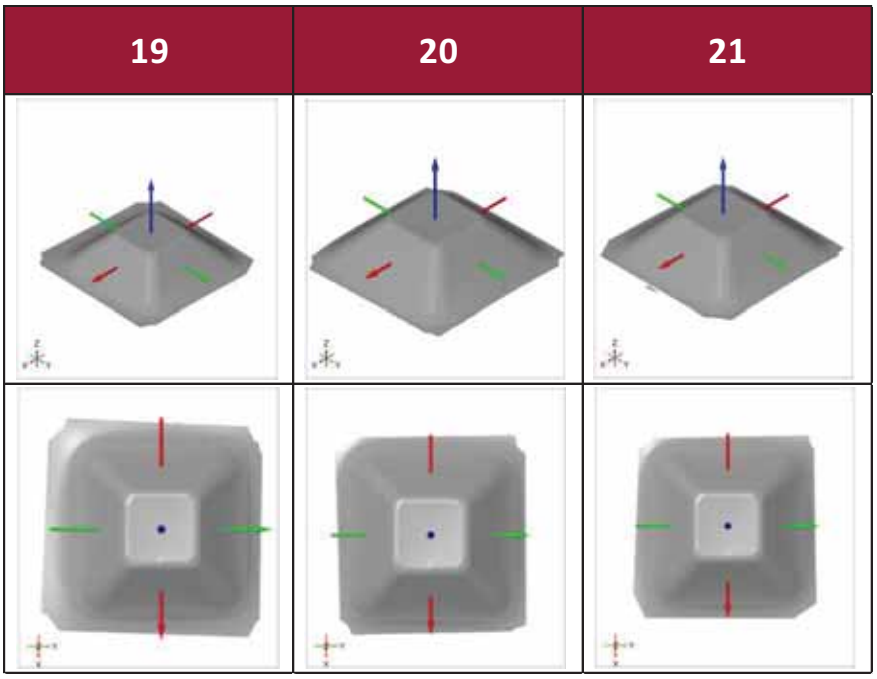

Figure 33: SPIF process pyramids alignment against coordinate system (source: own creation).

- Stamping

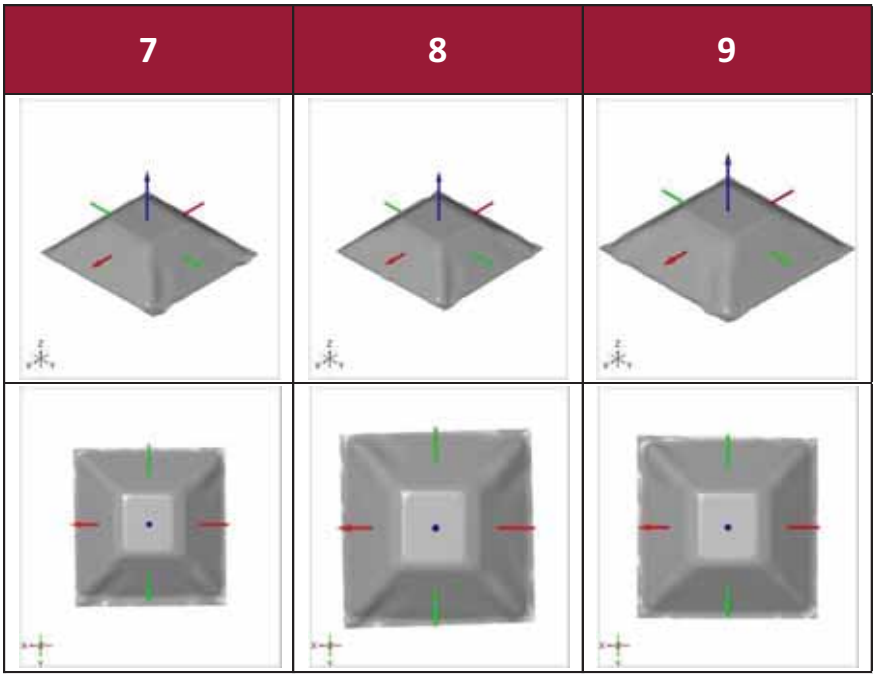

Figure 34: Stamped pyramids alignment against coordinate system (source: own creation).

4.2.2 Alignment between pyramids

An analysis of each pyramid against the others was performed, so the alignment of each possible pair for both processes were made. As mentioned before, the alignment of specific areas was performed, so the area with the special zones with the string could be analyzed without affecting other areas. In the case of SPIF pyramids (Figure 35), the special area was determines by the presence of the toolpath string. For the stamped case (Figure 36), the pyramids were aligned depending on the deformation presence.

- SPIF

SPIF Alignment	19	20	21	Ideal
19	-		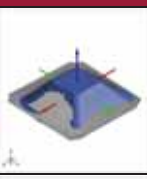	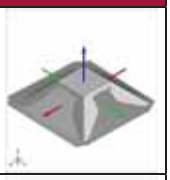
20		-	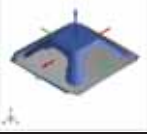	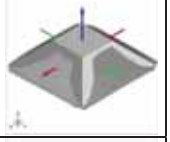
21			-	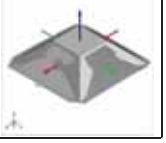

Figure 35: Resulting alignment between each pair of SPIF pyramids (source: own creation).

- Stamping

Stamping Alignment	7	8	9	Ideal
7	-			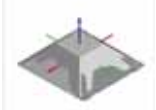
8		-	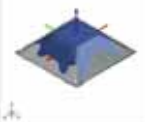	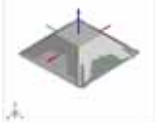
9			-	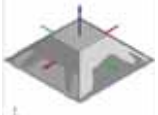

Figure 36: Resulting alignment between each pair of stamped pyramids (source: own creation).

4.2.3 Geometry accuracy.

The tool Surface comparison on the software Gom Inspect, is very helpful to match both shapes and let the user see how similar both pieces are, on this case, the aligned pyramids, already were as close as possible, so the surface comparison let us see how precise the processes are to succeed in reproducing the pyramids as similar to the calculated, and how natural or external causes have an effect in the resulting geometry. To help the understanding of the following images, the meaning of the color scheme is: red is for values over the mean, so the piece is far to the outside; green for the closest values to the mean, so the shapes difference is almost null; blue is for the values lower to the mean, so the piece is far to the inside.

- SPIF

19 vs Ideal

On the case of the comparison between the ideal and 19th pyramids, a smooth change between the pyramids walls can be seen, also it is obvious the difference created by the radius on the 19th pyramid, shown on the edges between the walls.

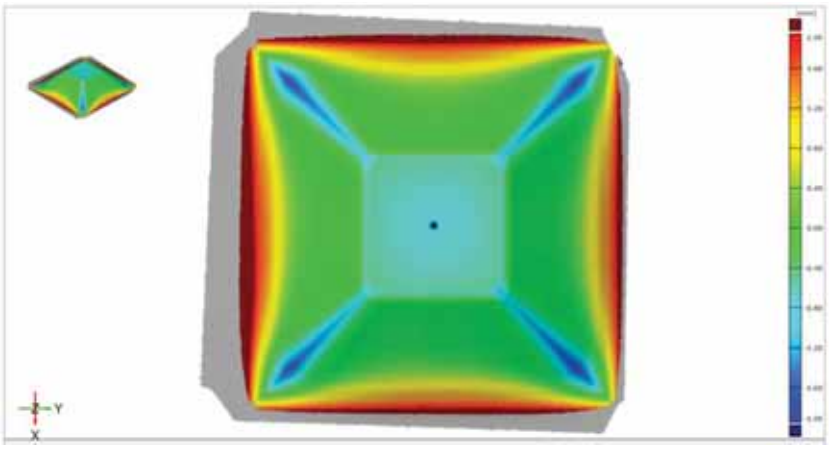

Figure 37: Geometrical comparison 19 vs ideal (source: own creation).

19 vs 20

On the comparison between the 19th and the 20th a bad comparison can be seen, although the persistent color is green, a lot of blue and yellow is visible

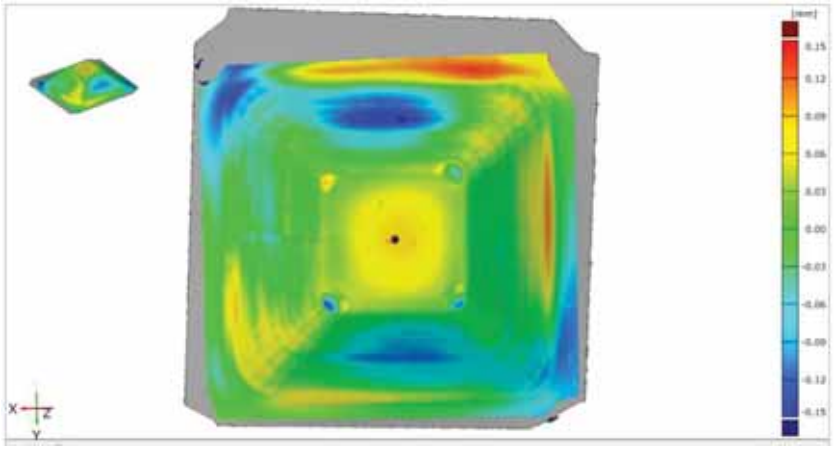

Figure 38: Geometrical comparison 19 vs 20 (source: own creation).

19 vs 21

On the comparison between 19th and the 21st a good precision between both pyramids is perceptible, except for axis x, where the piece might be open on those areas

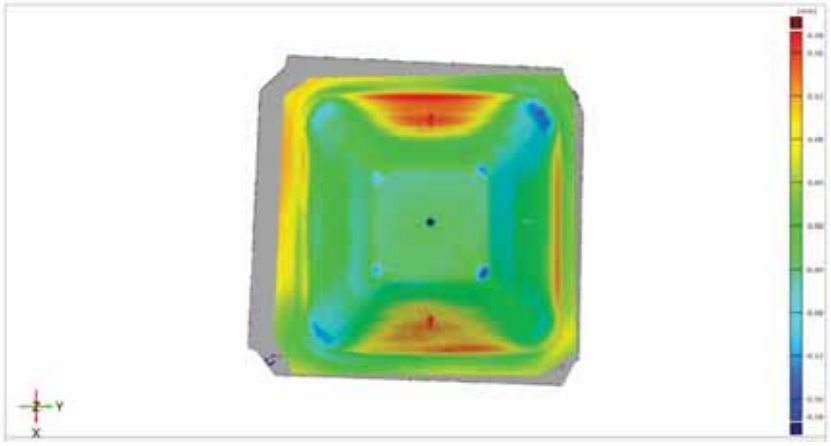

Figure 39: Geometrical comparison 19 vs 21 (source: own creation).

20 vs Ideal

As seen on the 19th piece against ideal, the walls present a constant value of precision between each other, but in this pyramid the top of the pyramid present a lower value to the mean.

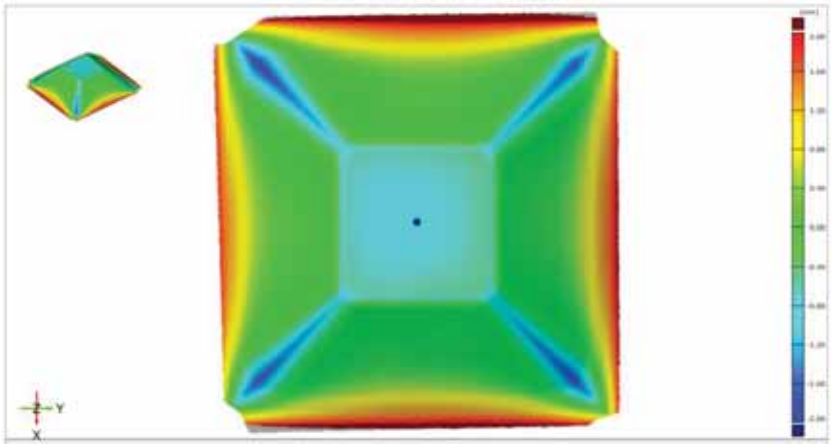

Figure 40: Geometrical comparison 20 vs ideal (source: own creation).

20 vs 21

The comparison between the 20th and 21st present the worst values, this pyramid has a lot of differences to the mean, and that is detectable by all the colors throughout the piece instead of green.

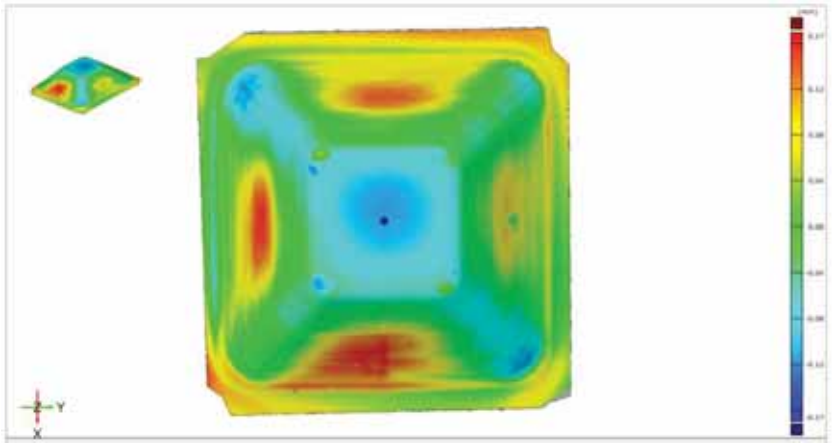

Figure 41: Geometrical comparison 20 vs 21 (source: own creation).

21 vs Ideal

This pyramid presents the best shape, because of the constant color throughout the piece. As well as the other comparisons to the ideal pyramid, the only areas were difference is evident, is on the edges between the walls.

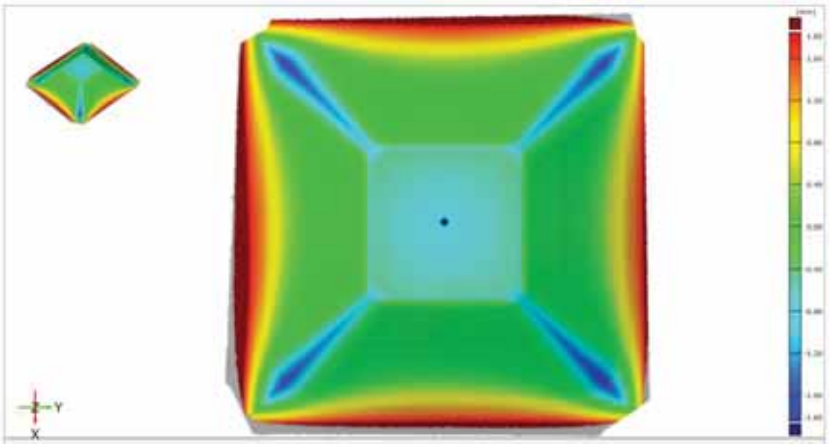

Figure 42: Geometrical comparison 21 vs ideal (source: own creation).

- Stamping

7 vs Ideal

For the case of the stamped pyramids, the differences between the wall edges is unimportant, since the main difference is noticeable on the top area, where the deformation is presented.

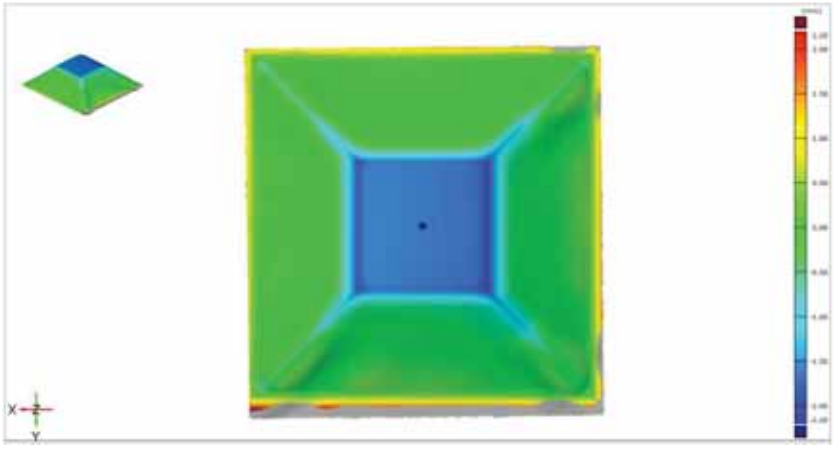

Figure 43: Geometrical comparison 7 vs ideal (source: own creation)

7 vs 8

For the comparison between the 7th and the 8th pyramids, a great difference is located on the top part between the positive “x” and “y” axes. Also on the bottom part differences can be observed caused by the wrinkles.

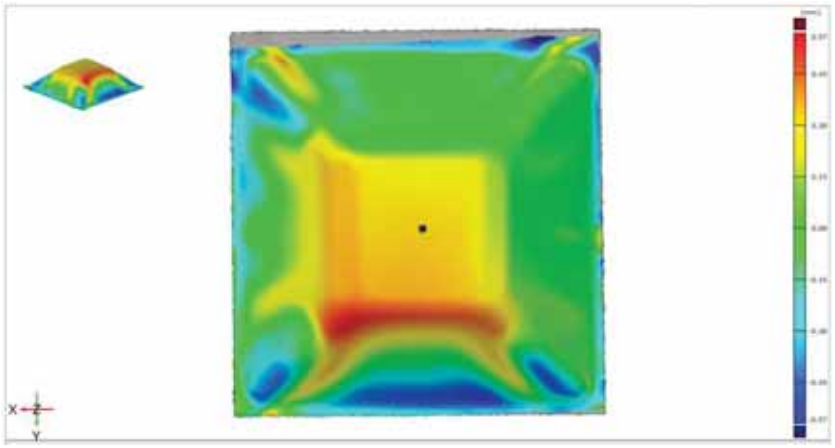

Figure 44: Geometrical comparison 7 vs 8 (source: own creation).

7vs 9

The differences presented between the 7th and the 9th pyramids is almost null, only some spots located in the positive “x” and negative “y” axes are visible.

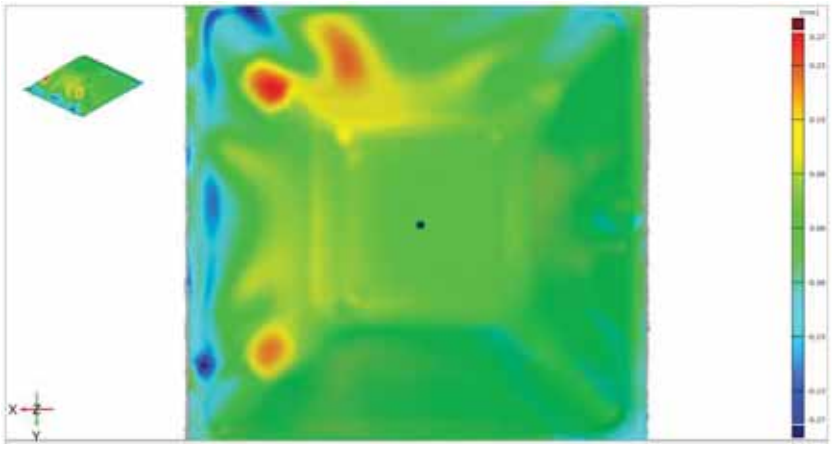

Figure 45: Geometrical comparison 7 vs 9 (source: own creation).

8 vs Ideal

The presented differences are consistent to the ones shown on the 7th vs ideal and the 9th vs ideal.

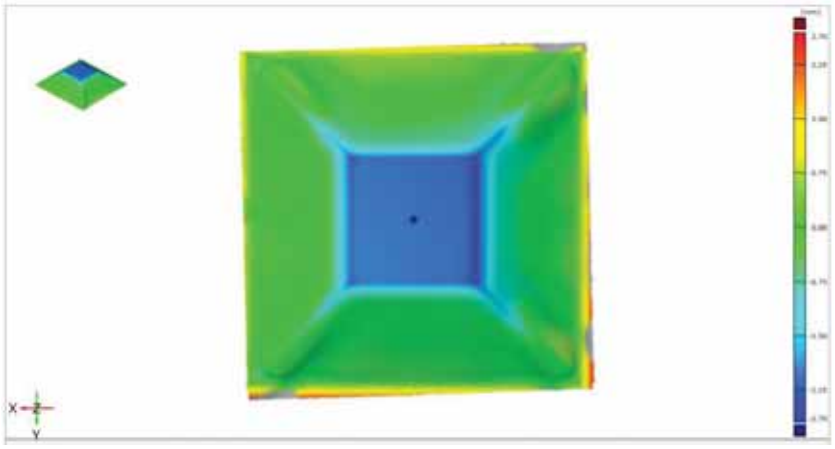

Figure 46: Geometrical comparison 8 vs ideal (source: own creation).

8 vs 9

The differences found between the 8th and 9th are the worst on the stamping set, more than half of the colors on the piece exhibit the shape deficiency located on the positive "x" and "y" axes.

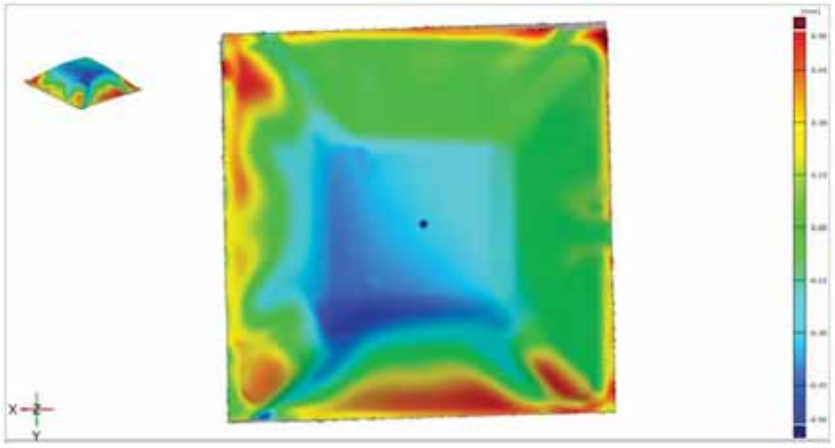

Figure 47: Geometrical comparison 8 vs 9 (source: own creation).

9 vs Ideal

The presented differences are consistent to the ones shown on the 7th vs ideal and the 9th vs ideal.

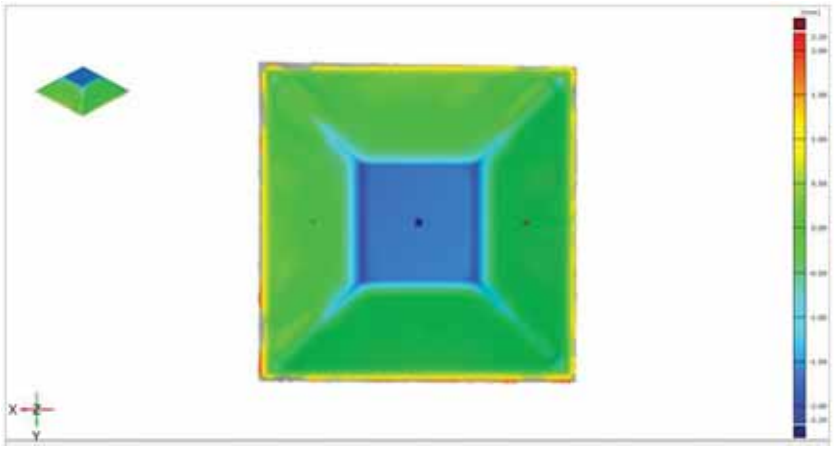

Figure 48: Geometrical comparison 9 vs ideal (source: own creation).

- Geometry analysis over X and Y axes

  A cut was created over the X and the Y axes of each pyramid to show the geometry differences throughout the surface. The resulting variation for the SPIF set is presented on the Figure 49, and the ones for the Stamping set of pyramids are shown on the Figure 50.

  - SPIF

SPIF X / Y Cut	19	20	21	Ideal
19	-	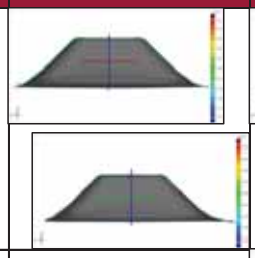	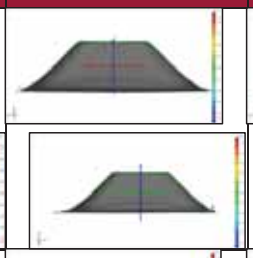	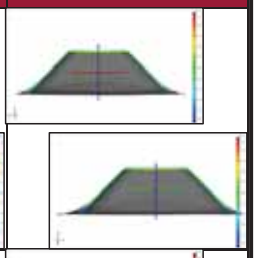
20		-	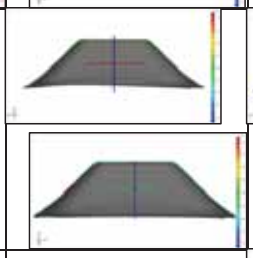	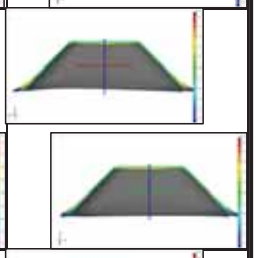
21			-	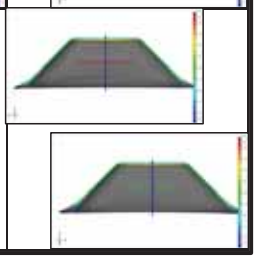

Figure 49: SPIF geometrical differences over de "x" and "y" axes (source: own creation).

- Stamping

Stamping X / Y Cut	7	8	9	Ideal
7	-	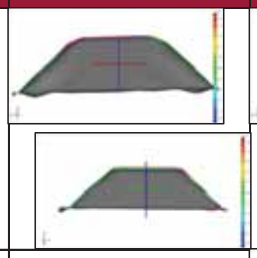	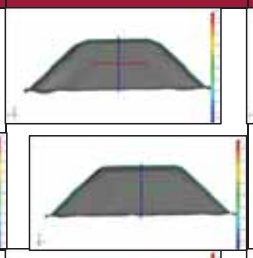	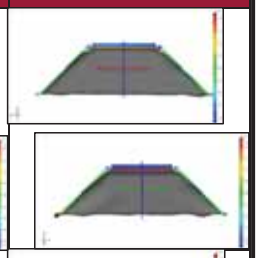
8		-	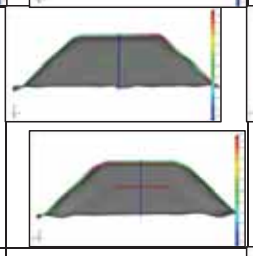	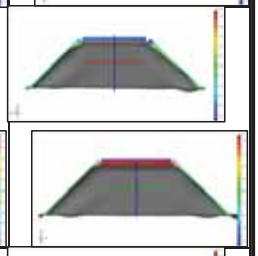
9			-	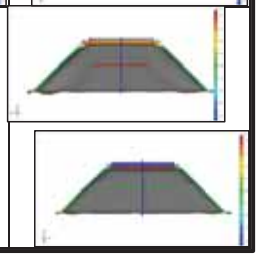

Figure 50: Stamping geometrical differences over de "x" and "y" axes (source: own creation).

4.2.4 Thickness analysis over axes X and Y

To get a good perception of the thickness behavior on the pyramids, it was decided to make the analysis at the middle of the pyramids in each axis, so it could be seen how the thickness changes throughout every pyramid. The following figures (51 and 52) shows the resulting thickness measurement of one of the pyramids (19 vs Ideal).

- X

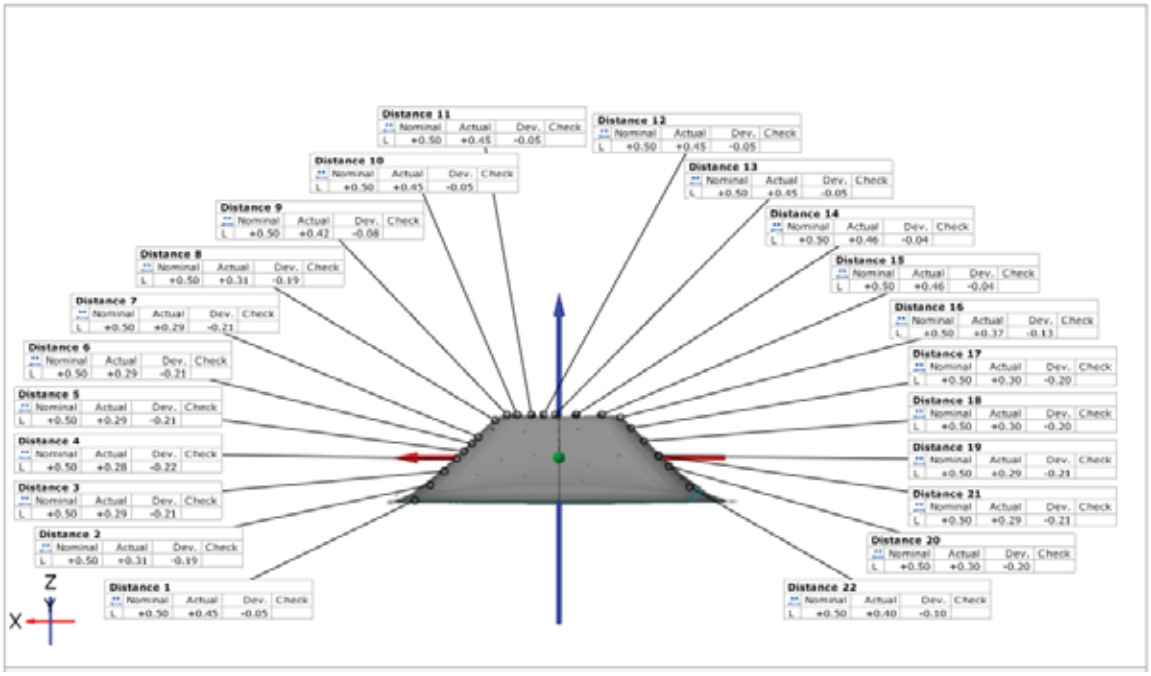

Figure 51: Resulting thickness measurements on the "x" axis (source: own creation).

- Y

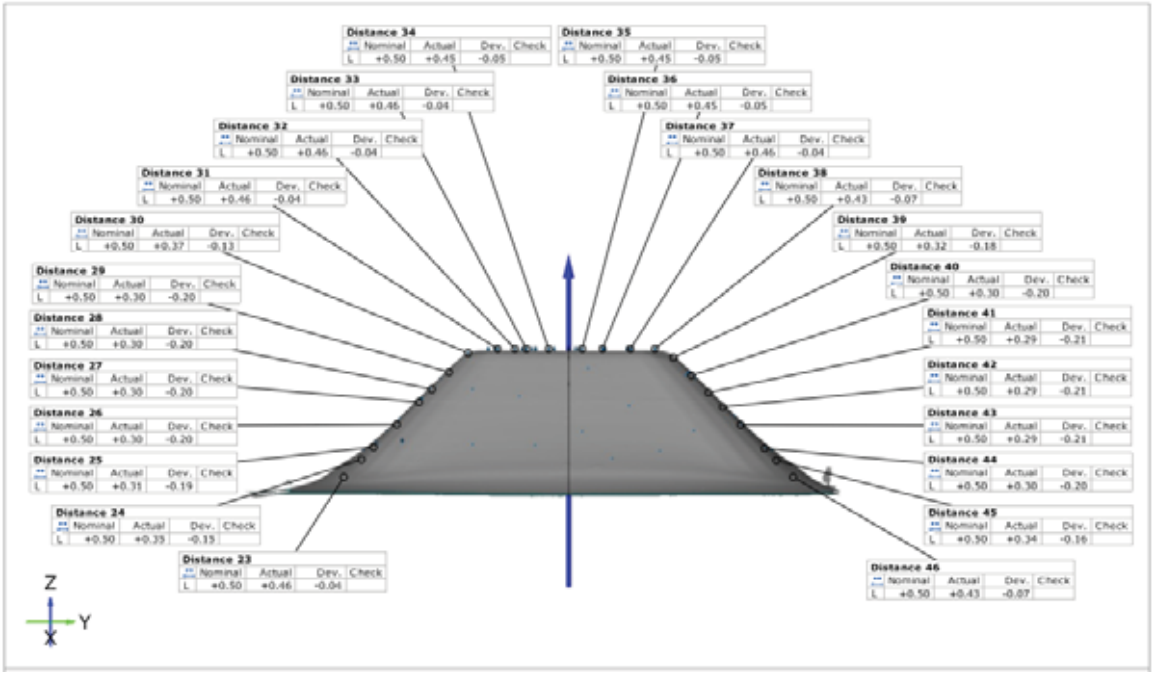

Figure 52: Resulting thickness measurements on the "y" axis (source: own creation).

- SPIF

  The following table shows the thickness data collected from the SPIF pyramids, each column presents the position of the measurement on each axis “X”, “Y”, and “Z” respectively; on the fourth column, the resulting thickness is showed.

Table 18: SPIF thickness measurement over each axis (source: own creation).

SPIF Thickness Measurement (mm)												
Point	19				20				21			
	x	y	z	Thickness	x	y	z	Thickness	x	y	z	Thickness
1	33.87	0	-8.73	0.45	-31.58	0	-6.45	0.43	32.22	0	-7.64	0.41
2	29.9	0	-5.71	0.31	-29.52	0	-5.01	0.35	28.96	0	-5.14	0.29
3	26.42	0	-2.85	0.29	-27.2	0	-3.12	0.31	25.8	0	-2.49	0.28
4	23.43	0	-0.1	0.28	-24.34	0	-0.49	0.3	21.73	0	1.41	0.29
5	21.74	0	1.55	0.29	-21.48	0	2.32	0.3	17.96	0	5.28	0.28
6	19.96	0	3.33	0.29	-18.71	0	5.04	0.3	12.66	0	9.2	0.4
7	18.46	0	4.79	0.29	-14.25	0	9.08	0.36	5.64	0	9	0.45
8	14.59	0	8.55	0.31	-9.87	0	9.44	0.46	-3.53	0	9	0.45
9	11.9	0	9.18	0.42	-6.21	0	9.35	0.46	-12.9	0	9.17	0.39
10	9.62	0	9.05	0.45	-0.76	0	9.31	0.47	-16.87	0	6.38	0.29
11	6.34	0	8.99	0.45	5.5	0	9.36	0.46	-19.11	0	4.18	0.29
12	3.55	0	8.97	0.45	13.98	0	9.19	0.36	-21.76	0	1.47	0.28
13	0.87	0	8.96	0.45	17.74	0	5.87	0.31	-24.51	0	-1.23	0.28
14	-3.9	0	8.97	0.46	20.42	0	3.23	0.31	-27.77	0	-4.09	0.3
15	-9.77	0	9.06	0.46	23.1	0	0.64	0.31	-30.52	0	-6.25	0.38
16	-13.75	0	8.94	0.37	25.96	0	-2.05	0.31	0	32.34	-7.64	0.44
17	-16.43	0	6.81	0.3	29.44	0	-4.96	0.34	0	28.88	-4.97	0.32
18	-19.41	0	3.9	0.3	0	-29.69	-5.57	0.37	0	25.82	-2.36	0.3
19	-22.89	0	0.5	0.29	0	-26.92	-3.25	0.3	0	22.36	0.94	0.31
20	-25.28	0	-1.73	0.3	0	-23.79	-0.33	0.28	0	17.88	5.43	0.29
21	-27.46	0	-3.67	0.29	0	-21.02	2.36	0.29	0	12.48	9.2	0.4
22	-30.45	0	-6.02	0.4	0	-17.36	5.93	0.3	0	4.43	9	0.45
23	0	-31.98	-7.02	0.46	0	-12.09	9.03	0.43	0	-4.02	8.99	0.45
24	0	-29.1	-5.01	0.35	0	-4.85	8.85	0.46	0	-11.87	9.16	0.43
25	0	-27.21	-3.52	0.31	0	5.42	8.91	0.46	0	-16.35	6.94	0.29
26	0	-23.83	-0.51	0.3	0	11.68	9.14	0.45	0	-19.5	3.82	0.28
27	0	-20.75	2.54	0.3	0	15.97	7.24	0.3	0	-23.07	0.22	0.28
28	0	-18.96	4.31	0.3	0	19.45	3.91	0.3	0	-26.23	-2.66	0.28
29	0	-16.58	6.66	0.3	0	22.04	1.38	0.31	0	-29.89	-5.6	0.35
30	0	-13.59	8.99	0.37	0	26.42	-2.75	0.31	0	0	0	0
31	0	-7.43	9.01	0.46	0	29.63	-5.45	0.37	0	0	0	0
32	0	-5.84	8.99	0.46	0	0	0	0	0	0	0	0
33	0	-2.76	8.97	0.45	0	0	0	0	0	0	0	0
34	0	1.92	8.96	0.45	0	0	0	0	0	0	0	0
35	0	4.7	8.98	0.45	0	0	0	0	0	0	0	0
36	0	8.58	9.03	0.46	0	0	0	0	0	0	0	0
37	0	11.96	9.15	0.43	0	0	0	0	0	0	0	0
38	0	14.44	8.59	0.32	0	0	0	0	0	0	0	0
39	0	17.03	6.19	0.3	0	0	0	0	0	0	0	0
40	0	19.41	3.84	0.29	0	0	0	0	0	0	0	0
41	0	21.4	1.86	0.29	0	0	0	0	0	0	0	0
42	0	23.89	-0.57	0.29	0	0	0	0	0	0	0	0
43	0	27.36	-3.71	0.3	0	0	0	0	0	0	0	0
44	0	29.15	-5.17	0.34	0	0	0	0	0	0	0	0
45	0	31.84	-7.15	0.43	0	0	0	0	0	0	0	0

- Pressing

  The following table shows the thickness data collected from the stamped pyramids, each column presents the position of the measurement on each axis “X”, “Y”, and “Z” respectively; on the fourth column, the resulting thickness is showed.

Table 19: Stamped thickness measurement over each axis (source: own creation).

Pressing Thickness Measurement (mm)												
Point	19				20				21			
	x	y	z	7	x	y	z	8	x	y	z	9
1	32.41	0	-8.55	0.46	31.29	0	-7.55	0.45	31.2	0	-7.88	0.43
2	29.54	0	-5.79	0.45	27.98	0	-4.38	0.44	26.69	0	-3.6	0.43
3	27.31	0	-3.58	0.45	24.79	0	-1.2	0.43	21.95	0	0.88	0.42
4	24.32	0	-0.7	0.45	20.91	0	2.59	0.43	16.19	0	6.12	0.4
5	20.67	0	2.81	0.44	16.86	0	6.2	0.41	11.68	0	7.94	0.4
6	17.72	0	5.64	0.44	12.42	0	8.01	0.41	4.65	0	8.1	0.41
7	14.16	0	7.65	0.44	3.01	0	8.11	0.41	-3.78	0	8.11	0.41
8	11.04	0	8.56	0.44	-5.53	0	8.07	0.41	-9.99	0	8.13	0.41
9	7.6	0	8.56	0.44	-13.83	0	6.99	0.41	-14.8	0	6.98	0.42
10	3.88	0	8.54	0.43	-17.87	0	4.57	0.42	-22.41	0	0.57	0.43
11	0.08	0	8.52	0.43	-20.72	0	2.04	0.42	-26.33	0	-3.34	0.43
12	-1.22	0	8.51	0.43	-23.7	0	-0.58	0.43	-30.1	0	-7.08	0.44
13	-6.36	0	8.47	0.43	-29.02	0	-5.23	0.44	0	-32.38	-8.31	0.42
14	-11.5	0	8.34	0.43	-31	0	-7.02	0.44	0	-29.65	-5.74	0.43
15	-14.69	0	7.15	0.43	0	-32.61	-8.2	0.43	0	-25.73	-2.08	0.42
16	-19.02	0	4.09	0.43	0	-29.69	-5.55	0.44	0	-21.58	1.85	0.42
17	-21.41	0	1.87	0.43	0	-26.55	-2.78	0.43	0	-15.52	7.39	0.4
18	-25.6	0	-1.99	0.44	0	-23.69	-0.24	0.43	0	-11.89	8.49	0.41
19	-28.55	0	-4.68	0.45	0	-19.75	3.27	0.42	0	-5.09	8.51	0.41
20	-31.76	0	-7.62	0.44	0	-13.23	7.92	0.41	0	4.23	8.53	0.41
21	0	-33.06	-9.52	0.44	0	-4.26	8.08	0.41	0	10	8.54	0.41
22	0	-31.75	-8.53	0.44	0	6.83	8.12	0.41	0	15.4	7.7	0.4
23	0	-27.59	-4.51	0.44	0	15.09	7.42	0.4	0	20.57	2.96	0.41
24	0	-25.69	-2.66	0.44	0	19.14	3.99	0.41	0	24.12	-0.51	0.41
25	0	-21.32	1.61	0.44	0	23.62	-0.14	0.41	0	28.78	-5.04	0.42
26	0	-17.29	5.55	0.43	0	27.16	-3.43	0.42	0	0	0	0
27	0	-14.2	7.79	0.43	0	28.55	-4.71	0.42	0	0	0	0
28	0	-10.85	8.08	0.43	0	31.33	-7.31	0.41	0	0	0	0
29	0	-5.31	8.09	0.43	0	0	0	0	0	0	0	0
30	0	-0.08	8.09	0.43	0	0	0	0	0	0	0	0
31	0	2.4	8.08	0.44	0	0	0	0	0	0	0	0
32	0	7.15	8.08	0.43	0	0	0	0	0	0	0	0
33	0	9.42	8.06	0.43	0	0	0	0	0	0	0	0
34	0	12.56	8.01	0.43	0	0	0	0	0	0	0	0
35	0	15.27	6.92	0.42	0	0	0	0	0	0	0	0
36	0	17.54	4.88	0.43	0	0	0	0	0	0	0	0
37	0	20.86	1.81	0.44	0	0	0	0	0	0	0	0
38	0	24.23	-1.3	0.44	0	0	0	0	0	0	0	0
39	0	27.25	-4.11	0.45	0	0	0	0	0	0	0	0

4.2.5 Angle Analysis

The resulting angle on the pieces is a vital parameter to guarantee that the geometry shape was achieved. That is why, on the following figures (Figure 53 and Figure 54), the resulting angles on the "x" (left side) and "y" (right side) axes are presented.

- SPIF

SPIF Angle Result	19	20	21	Ideal
19	-	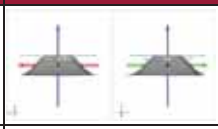	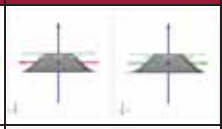	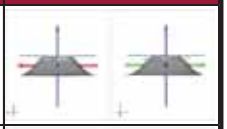
20		-	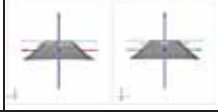	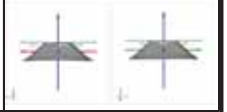
21			-	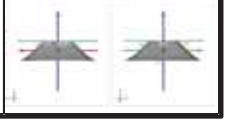

Figure 53: Resulting angles on the SPIF set (source: own creation).

- Stamping

Stamping Angle Result	7	8	9	Ideal
7	-	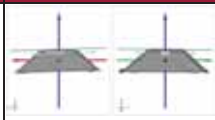	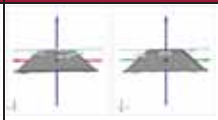	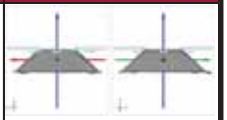
8		-	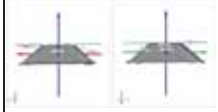	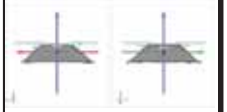
9			-	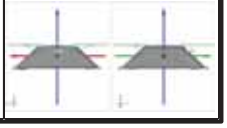

Figure 54: Resulting angles on the pressing set (source: own creation).

4.2.6 Roughness

For the roughness analysis, the use of the Mitutoyo surface roughness measuring testes was needed (Figure 55). This device is user friendly, but it needs to be calibrated, to do so, there is a calibration specimen to proof the results given by the tested (Figure 56).

Figure 55: Mitutoyo surface finishing tester (source: own creation).

Figure 56: Roughness calibration specimen.

Because of the shape of the pyramids it can be a challenge to take the samples of the surface finishing. For that reason, and to keep a consistency in the data, the following were the used parameters.

Table 20: Roughness samples parameters (source: own creation).

iso 1997
0.5mm/s
λc 0.08
x5

For this investigation, 30 measurements were taken of each pyramid to ensure the smoothness of the surface, two sets were taken the internal and external to validate the reliability of the data. This measurements are reported on the table 21

Table 21: Roughness tests (source: own creation).

Rugosímetro (Ra)µm												
N	SPIF						Estampado					
	Externo			Interno			Externo			Interno		
	P19	P20	P21	P19	P20	P21	PE7	PE8	PE9	PE7	PE8	PE9
1	0.481	0.045	0.404	0.697	0.379	0.748	0.129	0.127	0.114	0.093	0.204	0.081
2	0.512	0.045	0.426	0.401	0.565	0.772	0.107	0.118	0.09	0.116	0.164	0.151
3	0.439	0.034	0.363	0.546	0.496	0.334	0.102	0.09	0.114	0.088	0.115	0.082
4	0.453	0.238	0.374	0.721	0.606	0.522	0.229	0.098	0.111	0.012	0.094	0.064
5	0.433	0.169	0.643	0.647	0.399	0.452	0.124	0.106	0.179	0.053	0.107	0.093
6	0.353	0.469	0.507	0.542	0.65	0.46	0.128	0.112	0.116	0.072	0.092	0.102
7	0.347	0.378	0.404	0.718	0.722	0.689	0.113	0.098	0.128	0.088	0.118	0.062
8	0.366	0.562	0.374	0.576	0.644	0.595	0.091	0.15	0.146	0.102	0.101	0.158
9	0.494	0.465	0.326	0.597	0.605	0.339	0.136	0.06	0.096	0.094	0.106	0.11
10	0.42	0.538	0.46	0.634	0.757	0.624	0.121	0.088	0.112	0.118	0.099	0.127
11	0.321	0.442	0.406	0.753	0.555	0.372	0.094	0.118	0.111	0.118	0.076	0.132
12	0.381	0.454	0.416	0.565	0.68	0.578	0.122	0.133	0.05	0.092	0.125	0.109
13	0.443	0.501	0.379	0.876	0.565	0.713	0.144	0.1	0.095	0.115	0.172	0.092
14	0.371	0.454	0.526	0.557	0.785	0.588	0.143	0.088	0.097	0.095	0.14	0.114
15	0.396	0.391	0.489	0.629	0.531	0.46	0.15	0.113	0.114	0.118	0.024	0.082
16	0.431	0.461	0.226	0.404	0.487	0.641	0.124	0.147	0.124	0.118	0.146	0.07
17	0.34	0.435	0.501	0.655	0.546	0.529	0.157	0.123	0.099	0.113	0.018	0.104
18	0.481	0.529	0.454	0.73	0.615	0.585	0.08	0.082	0.118	0.085	0.062	0.042
19	0.318	0.427	0.622	0.483	0.44	0.592	0.074	0.054	0.265	0.086	0.13	0.088
20	0.43	0.442	0.345	0.605	0.604	0.454	0.087	0.101	0.127	0.1	0.185	0.15
21	0.463	0.516	0.587	0.711	0.571	0.703	0.11	0.09	0.103	0.086	0.078	0.068
22	0.412	0.482	0.331	0.529	0.399	0.611	0.097	0.125	0.104	0.145	0.147	0.176
23	0.42	0.537	0.522	0.661	0.529	0.521	0.15	0.1	0.05	0.138	0.091	0.202
24	0.53	0.436	0.394	0.76	0.587	0.486	0.093	0.089	0.079	0.118	0.116	0.17
25	0.333	0.377	0.063	0.559	0.975	0.867	0.096	0.131	0.087	0.186	0.098	0.171
26	0.049	0.484	0.04	0.503	0.549	0.767	0.16	0.149	0.172	0.097	0.134	0.16
27	0.07	0.656	0.653	0.457	0.615	0.584	0.111	0.225	0.089	0.113	0.192	0.131
28	0.069	0.397	0.034	0.663	0.462	0.588	0.414	0.178	0.092	0.099	0.12	0.131
29	0.037	0.614	0.033	0.633	0.58	0.841	0.478	0.138	0.108	0.152	0.151	0.138
30	0.04	0.476	0.034	0.506	0.716	0.597	0.334	0.09	0.213	0.136	0.058	0.161

4.3 Results of the statistical analysis.

In this section all the information analyzed will be presented. The intention here is to explain the analysis and focus on the obtained results of each test.

There is a resulting deviation that affected both of our main topics (geometry accuracy and thickness comparison), and this is the deviation presented in the alignment of the reference points when both scans of each were joint.

Table 22: Resulting deviation of the reference point (source: own creation).

P	Deviation (mm)
18	0.025
19	0.021
20	0.019
21	0.022
E7	0.033
E8	0.021
E9	0.015
Average	0.02229

4.3.1 Geometrical accuracy

The following tables present the resulting average deviation in the alignment between the CAD and the mesh, which could be interpreted as the average deviation in the surface accuracy.

Table 23: Alignment deviation on the SPIF set on mm (source: own creation).

SPIF				
Deviation	19	20	21	Ideal
19	-	0.0415	0.0469	0.3425
20		-	0.0512	0.3631
21			-	0.328

It can be seen that between each other, the pyramids have a really similar geometry alignment, the problem is presented when they are compared to the ideal, but it needs to be remembered that even if the real metal sheet had a 0.45mm thickness measure, the one that was set on the ideal parameters is a 0.50mm, so it can be inferred that this affects the resulting geometry accuracy, since both surfaces of the sheet are taken in count for the alignment. For the stamping process we have the following results.

Table 24: Alignment deviation on the stamping set on mm (source: own creation).

Deep Drawing Forming				
Deviation	7	8	9	Ideal
7	-	0.1915	0.0561	0.2749
8		-	0.2093	0.3436
9			-	0.253

In the case of the deep drawing results we see a bigger difference in the deviation, even between each other. A more detailed inspection of the geometry accuracy behavior was performed, taking in count all the created labels on the inspection between each pyramid and the ideal.

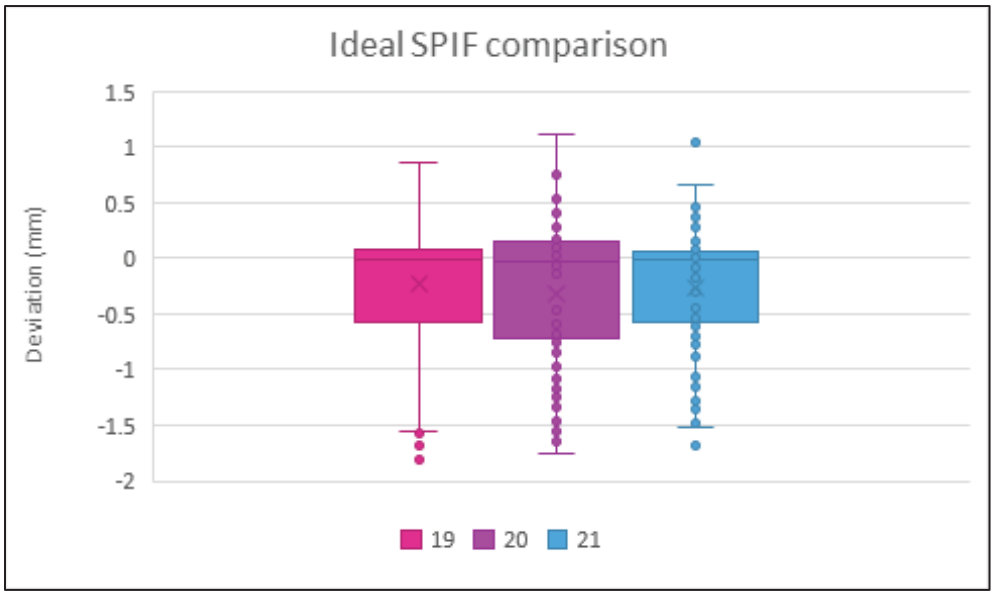

Figure 57: SPIF geometry accuracy graph (source: own creation).

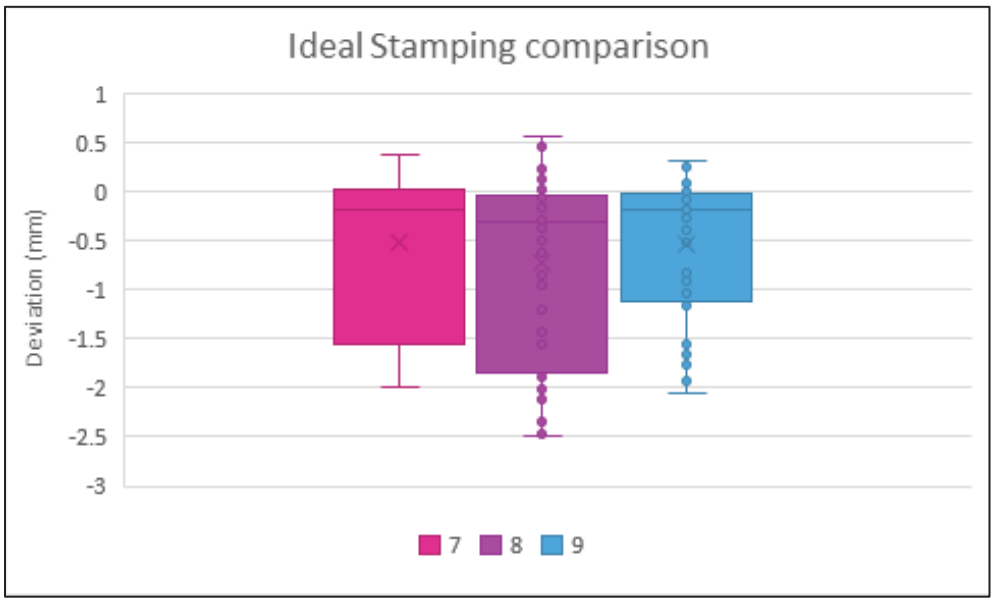

Figure 58: Stamping geometry accuracy graph (source: own creation).

The previous graphs (Figure 57 and 58) show us that the SPIF results present less variation between the achieved shape and the ideal shape, also it can be seen that the variation in the average lines in the SPIF case are more stable than the stamping ones, which would mean that SPIF is a more accurate process that the stamping one.

If the final results are taken as its capacity to be employed in the real industry, taking 0.10mm of deviation as the limit to be used in the medium to high end automotive industry and 0.50mm for the low to medium end automotive industry. The global SPIF average would give 0.19mm, meaning that this process can be applied without any problem in the low to medium end industry, but if the ideal was changed, taking in count the radii in the piece, the average would decrease enabling it to be taken in count for a high-end automotive industry. On the other hand, the global average of the pressing process gave a 0.22mm deviation, and it is already known that this process is applied in all the range of automotive industry.

4.3.2 Thickness comparison

As it was showed earlier, the thickness data collect was done over the X and Y axes, so they would cover all the information. Then point were placed randomly over the line and the exact

position and thickness at that point were obtained. After that, graphs were made so the information was easily to understand.

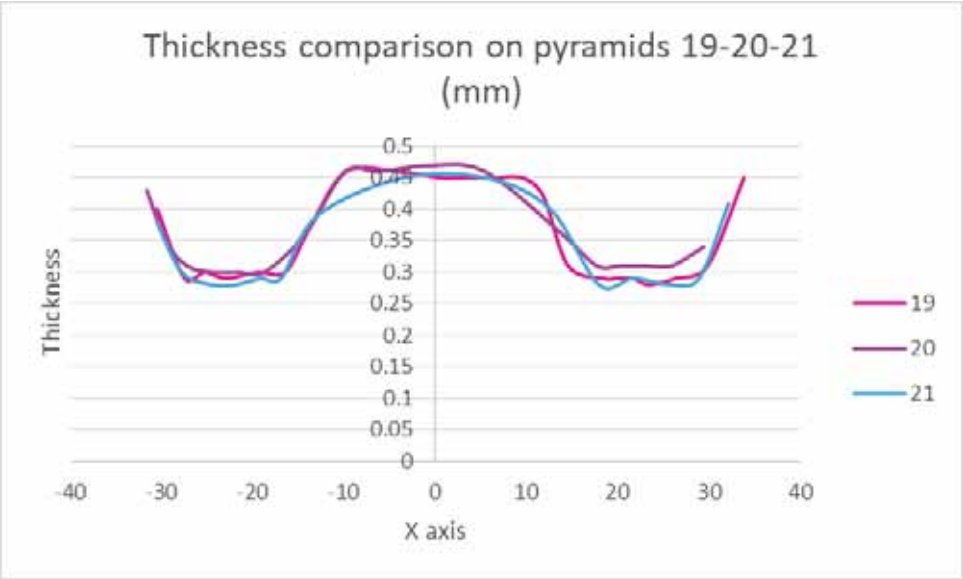

Figure 59: Thickness comparison in "x" axis for SPIF (source: own creation).

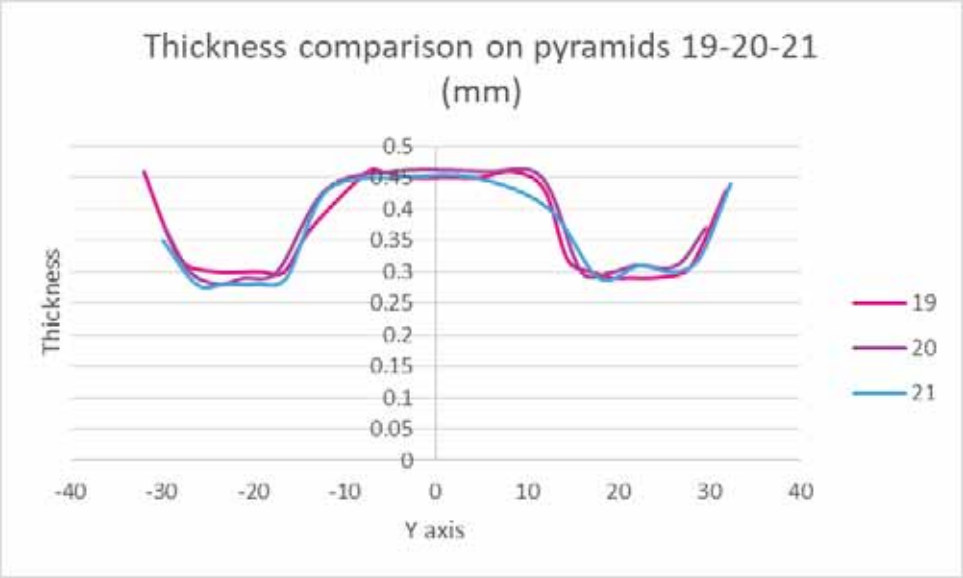

Figure 60: Thickness comparison in "y" axis for SPIF (source: own creation).

The previous are the graphs of the resulting thickness on the SPIF pyramids (19, 20 & 21) over the axis X (Figure 59) and Y (Figure 60). In them, we can see that the difference is very small, and that the thickness on the three pyramids is constant, which would mean

that further pyramids would show the same behavior. Following the sine law to estimate the final thickness $T_f = T_i*(90-\theta)$, having a 45° wall angle and an initial thickness of 0.45mm, the resulting calculated resulting thickness would give an approximate of 0.382mm. Comparing it to the actual thickness result of 0.348mm, giving us only 0.03mm of deviation on the results. On the other hand, we have the resulting thickness graphs for the press process.

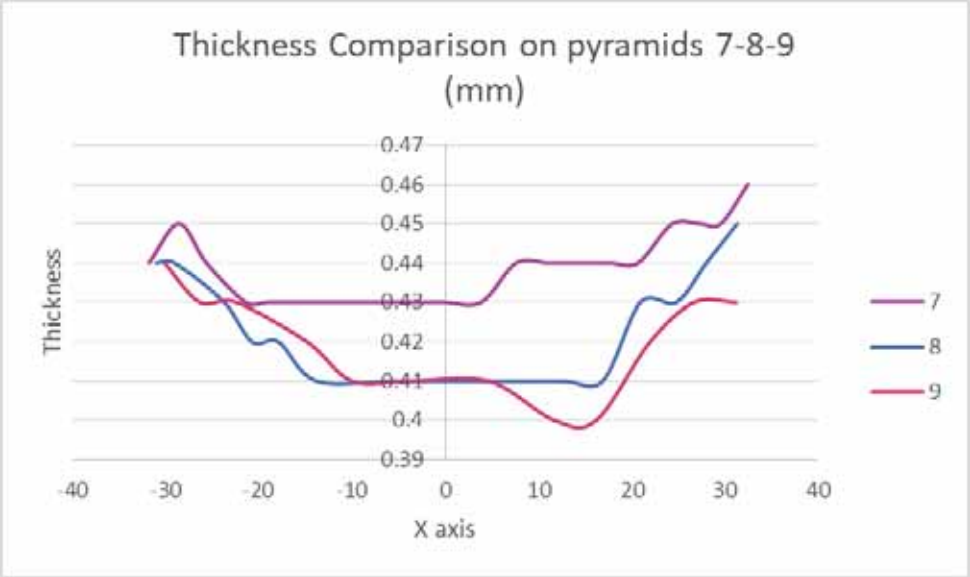

Figure 61: Thickness comparison in "x" axis for pressing (source: own creation).

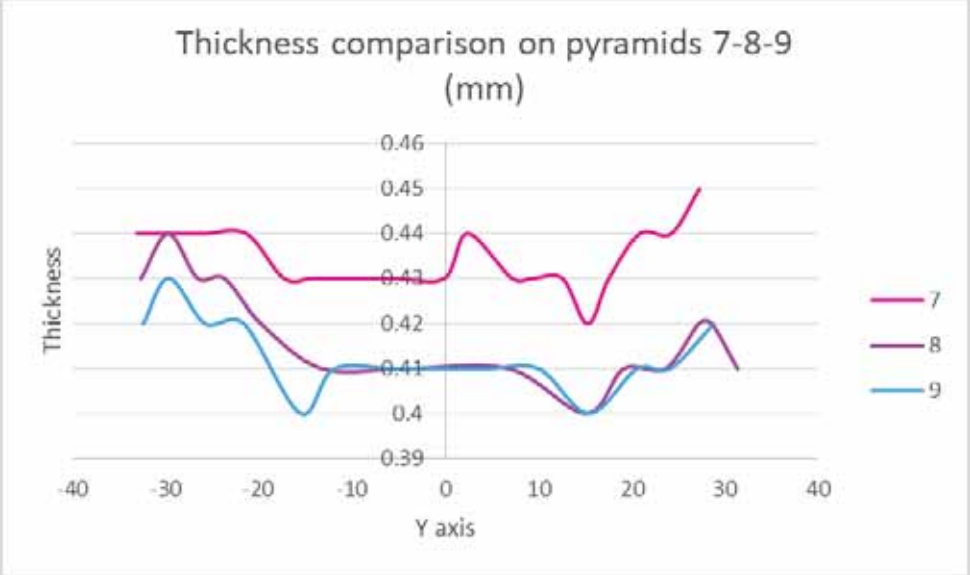

Figure 62: Thickness comparison in "y" axis for pressing (source: own creation).

On the pressing case, there is not an evident path that the thickness follows, but the deviation perceived in SPIF 0.06mm is greater than the one from the stamping process 0.01mm, what would mean that stamping process keep a constant thickness along the deformed pyramids.

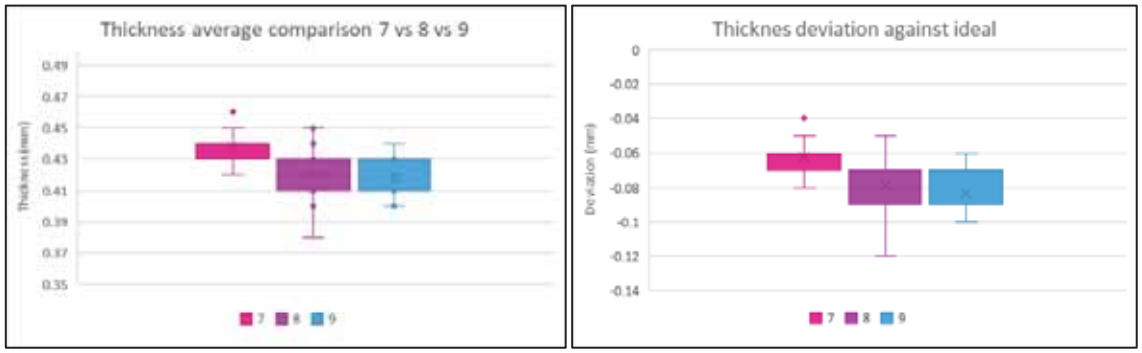

Figure 63: Thickness final results (average {left side} and deviation {right side}) (source: own creation).

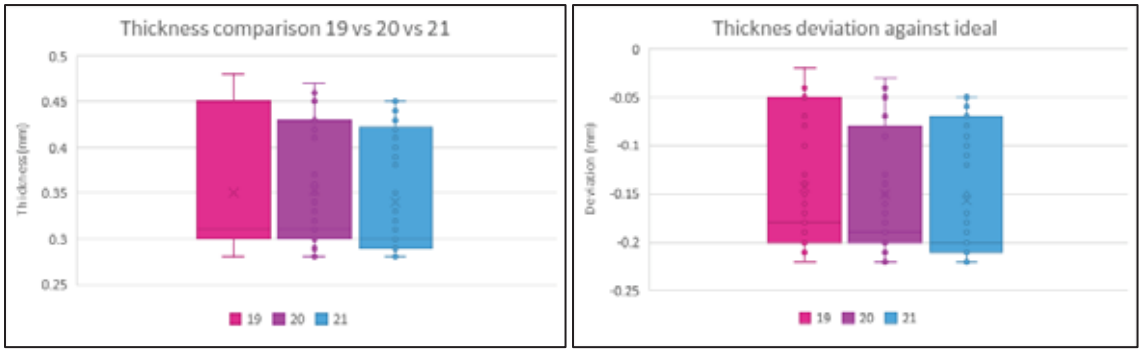

Figure 64: Thickness final results (average {left side} and deviation {right side}) (source: own creation).

4.3.3 Surface Finishing Results

After all the samples were taken, the resulted mean of the inspected area was analyzed. It can be seen that in the stamping case, the results are steady, while in the SPIF case, the inner roughness shows the trace of the tool from its fabrication.

Roughness Average µm												
SPIF						Estampado					
Externo			Interno			Externo			Interno		
P19	P20	P21	P19	P20	P21	PE7	PE8	PE9	PE7	PE8	PE9
0.35443	0.41513	0.37787	0.61060	0.58713	0.58707	0.14993	0.11403	0.11677	0.10487	0.11543	0.11737

Figure 65: Overall roughness average Roughness Average (source: own creation).

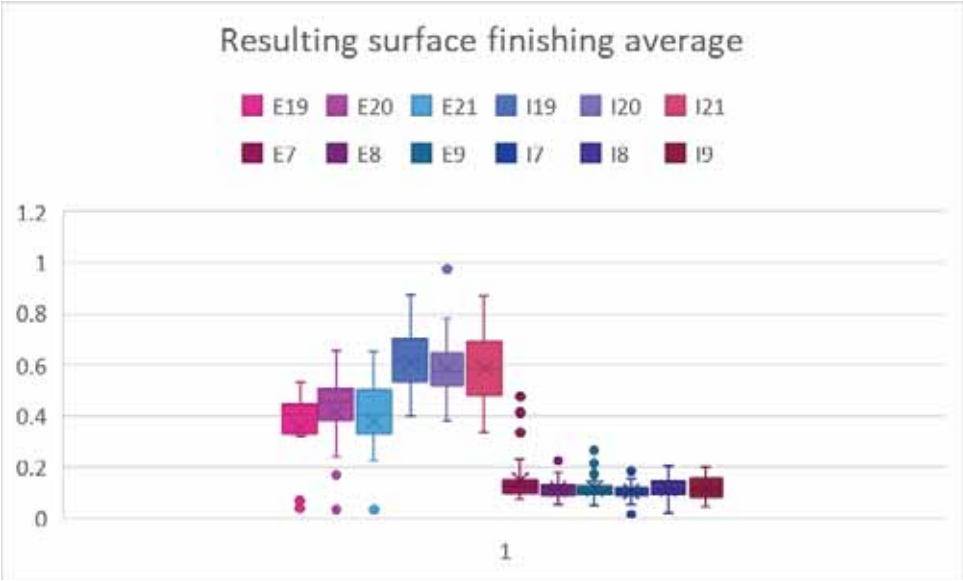

Figure 66: Average roughness pyramid on mm (source: own creation).

On the previews graph the overall roughness per pyramid is presented, in this graph it is easy to observe that the stamping roughness average deviation in almost insignificant, while SPIF process presents a higher deviation almost of 0.11 micrometers. It can be inferred that stamping has a better surface finishing than the SPIF process.

CHAPTER V

5.1 Introduction

This chapter synthetizes the conclusions about specific objectives and general objective. It also mentions the original work done in this project. Limitations for this study are also mentioned in a section. Finally some recommendations are presented.

5.2 Conclusions about specific objectives

The process compared were Conventional Stamping and Single Point Incremental Forming (SPIF), so this objective was achieved.

The characteristics compared were Thickness, Geometry precision and Superficial Finish, so this objective was also attained.

The software used was Creo parametric 4.0, Autodesk Inventor Enzo 2017, Ls-Dyna (Ls-PrePost 4.1), Gom Scan 2016, Gom Inspect 2016, Minitab 18, Microsoft Office 2016, Ultimaker Cura 2.5.0, so the software used objective was also reached.

In regard to the material definition: SPIF clamping framework, the framework base and clamping plates were made of Aluminum 6061; the columns, on the other hand, were made of Steel AISI-304, and it can be states that this objective was also accomplished.

In reference to the Stamping set used, the dies, drawbeads plates and the framework bases were made of Aluminum 6061; the columns and the pins were made of Steel AISI-304; the material used in the metal sheets to create the pyramids was a stainless steel AISI 306, which is a chrome-nickel austenitic steel, so that specific objective was also conquered.

5.3 Conclusions about the general objectives

The general objective to compare the SPIF and traditional deep drawing method with the purpose of determine if they have the same characteristics to make them replaceable between each other, it was attained, because we reached the conclusion that SPIF may replace the traditional deep drawing method if the tolerances of surface finishing aren't very close

because for geometrical precision the SPIF process can achieve a good precision. And for resulting thickness the initial design can include the thinning of the material.

5.4 Original work

The comparison between the SPIF and traditional deep drawing method with the purpose of determine if they have the same characteristics to make them replaceable between each other, is not reported in literature, so that is the original work presented here.

5.5 Limitations to this study

It is important to notice that the stamping dice is far from perfect, so that must be taken into account in future design and comparison projects.

5.6 Recommendations

Future work in this project requires to correct the stamping dies and a design of experiments might be performed to analyze different factors to determinate which ones affects more than the rest of them the resulting surface finishing to optimize the values to improve the quality of the product.

APPENDICES

This section is intended to help understand the information, and to answer some technical questions that may arise from the last chapters. Every image´s and blueprint´s source is of own creation.

APPENDIX A

A.1 Scanning (GOM Scan)

This appendix has the intention to make clearer the procedure taken by our team to make the inspection of the pyramids in case this procedure wants to be replicated.

The 3D scanning was executed with the help of the ATOS Core scanner, and the following is the special software made for this purpose. This is the start page of the software Gom Scan, here it can be seen that four main buttons are presented: New Project, Open Project, Recently Used Project, and Gom Community. The last one is a platform where you can find tutorials and a forum where specialist answer your questions. It can be also seen that on the top left side there is a menu button, here it can be found the link to the start, the set up, and the scanner.

Accessing to the set up section we´ll see the following screen, on the top right side, we find the sensor initialization button, right next to it, the light bulb will show us when the scanner is warm enough to start the scanning (when the color is yellow, the scanner isn´t ready, when the color is white, the scanner is ready to use), next to the menu button on the left side, we can find the calibration parameters button, if we click on it a window will pop up asking

some parameters (plate temperature, main camera, ellipse parameters, maximum movement), after filling all the spaces, the calibration can start.

For the calibration step it is needed to count with the calibration plate, the previous parameter "plate temperature", is obtained taking the temperature on this plate.

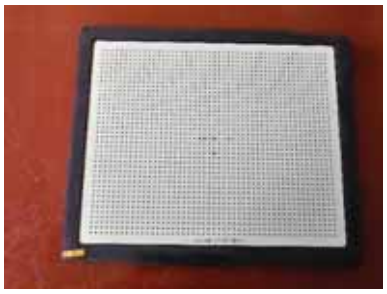

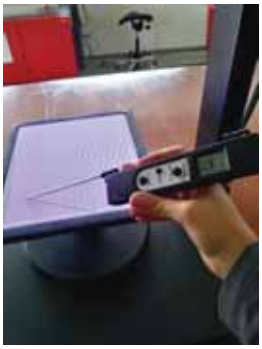

After giving al the parameters, the calibration instructions will appear, these need to be followed, when the instruction is completely followed, it will show the visual legend "optimum position".

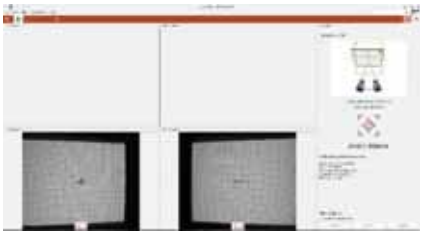

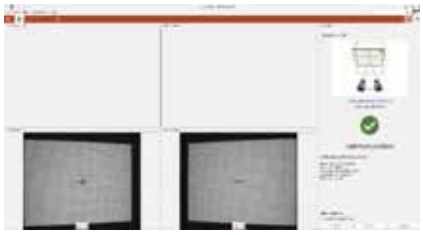

Once all the calibration is done, the software will show the following window. Then going again to the menu, the digitalize option will appear available.

The following is the screen of the digitalize option, here is where the real scanning will occur. In the horizontal menu there are several tools that will help to have a good piece scanning.

The first button is to create a new shoot, the second is the cut out point button, the third is the button transform by reference points, the fourth is polygonise and recalculate, and the fifth is the export stl button.

Since the piece couldn´t be completely scanned on one measurement, two measurements were taken, the noise was eliminated with the cut out point tool and then matched to creating the final piece.

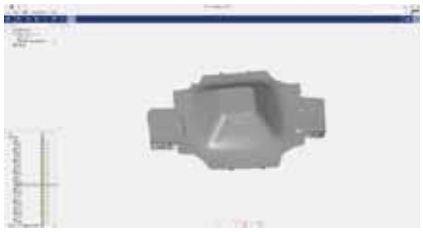

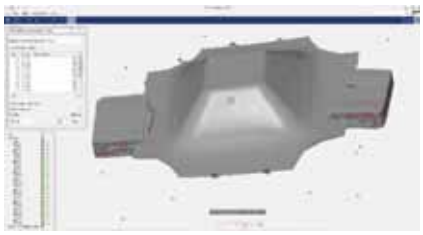

But until this point the piece is only a cloud of points, so we need to transform it into a stl piece, so the polygonise tool is used, we used the standard option, and then exported as a stl file.

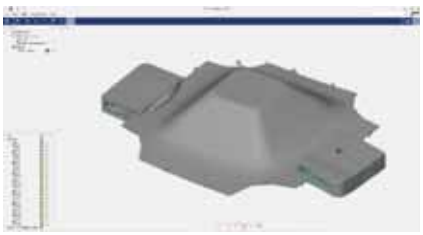

A.2 Inspection (GOM Inspect)

After the scanning process, the inspection of the scanned piece was needed, and the sequence of inspection will be explained next. The following is the initial window of the software Gom Inspect. Here six options are presented: New Project, Open Project, Sample Data, Project Templates, Recently Used Projects, Gom Community. The menu button is located at the top left side of the screen, on the menu it can be found the options: Mesh Fixing, Inspection, and Report.

After opening a new project, the first step is to import the stl file, it can be found on file > import and then searched.

The file can be imported as a mesh and as a CAD. Mesh files are the ones to be analyzed they are presented in grey color, while the CAD files are the ones to be compared to, these ones are presented in blue color.

When a mesh is imported, the mesh can present some mistakes, so tools to solve them can be obtained on the horizontal menu, for hole closing there are 2 options, automatic and

interactive, for very small holes, the automatic is recommended, while very big holes or with a complex shape are recommended .

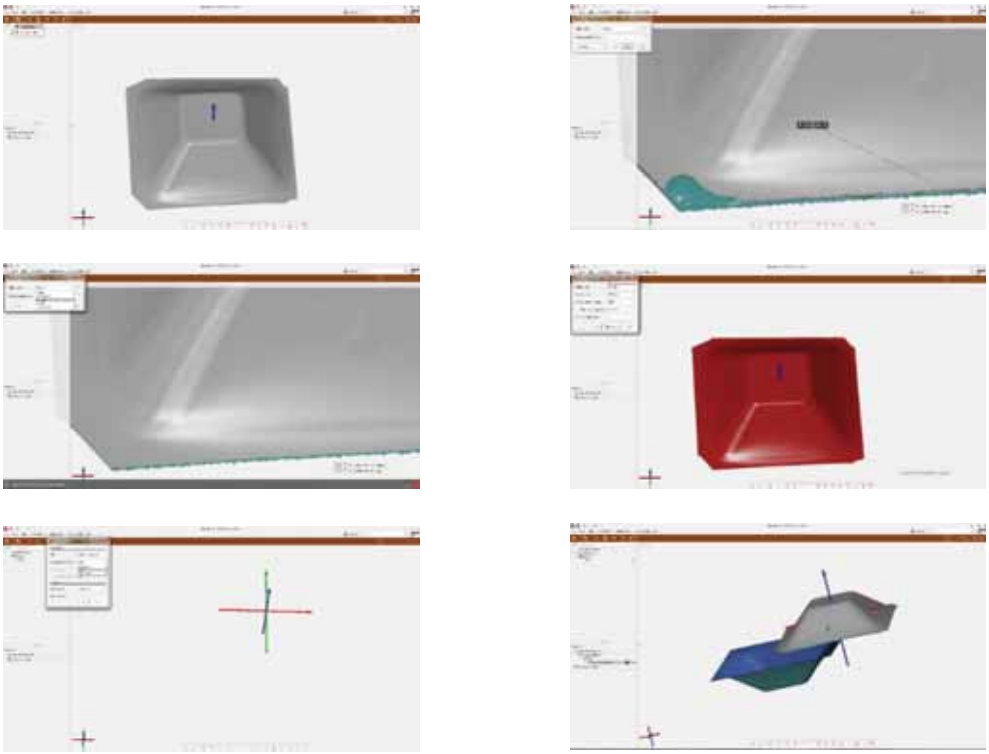

After the CAD was imported, it could be seen that the CAD had no thickness, so an offset was created to get a thickness, in our case, it was the ideal thickness. It is very important to understand from now on, that the word “nominal” refers to the imported CAD, and the word “actual” refers to the imported scanned mesh.

After the CAD thickness is created, an alignment is needed, but in some cases like this, the alignment can be difficult since one of the pieces is turn around or cannot be aligned automatically for some other reason.

In cases like these, a prealignment may be useful, so in the horizontal menu > Operations > Single element transformation, here different alignments that can be applied are listed, what is important of “single element transform” alignments is that they are not registered in the inspection tree at the left side. This means that every modification will be taken as if that was the original position of the CAD. The advantage of this is that a better or more specific alignment can be performed.

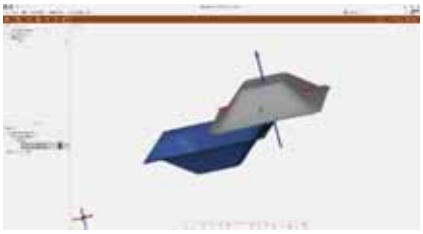

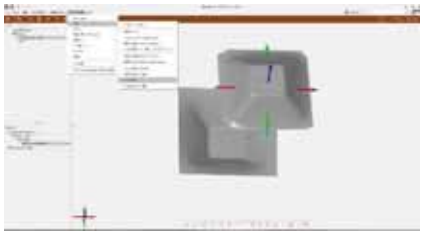

In our case the alignment by coordinate elements tool was used, so the coordinate system could be placed exactly at the middle of the three axis and in the next piece could be used the same standard. To use this tool several step are needed, but the result is very precise.

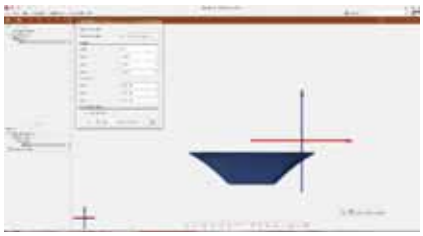

To modify the position of a piece on an easy way, the tool set matrix on the single point transformation location can be used. This tool is really easy to use, but it isn´t very precise unless the exact modifications needed are known, in this tool two key parameters are taken in count to place the piece in the correct position. Translation, which means a lineal movement in the direction of any axis; Rotation is the parameters where specified degrees turn the piece taking the axis as reference to turn the piece. In this case a 180° turn on the "X" axis.

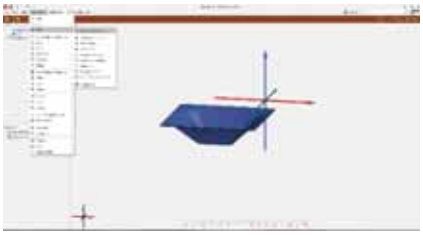

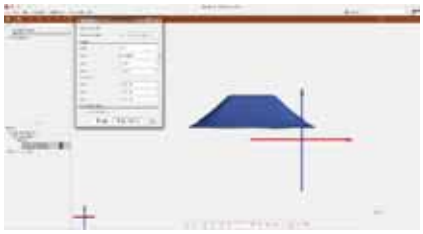

Talking back about the coordinate elements tool, first the nominal pyramid needs to have the three main planes (X, Y and Z) so the intersection between the three can be taken as the origin. To create a plane on the exact middle, first planes were applied on the walls of the pyramid. The path for this planes is construct > planes > auto planes (nominal). Here with ctrl and click you start to select each wall and give ok on the bottom (the software make an automatic selection of the surface to create the plane, if it isn't good enough, another point can be selected). Then the planes on the middle of the piece need to be created. For this purpose, the tool symmetric planes also located in planes is useful, here two pre made planes are the elements asked. There is a small square on the lower part saying "from the actual angle", this needs to be unselected to create a plane in the middle even if the planes aren´t parallel, if this isn´t done the plane will be created where both planes get intersected. Once the plane is created clicking "create" will be needed.

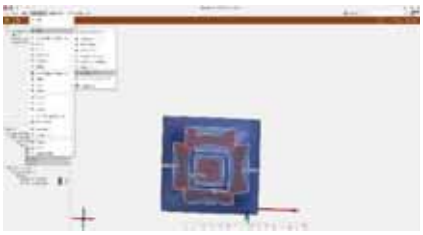
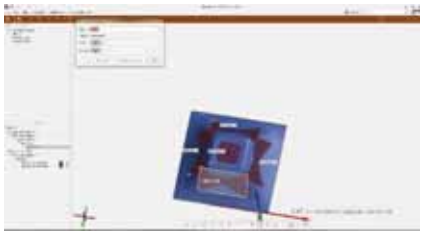



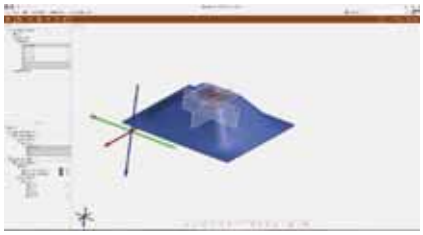

The same procedure is required for the actual parte (scanned), but for this case the tool nominal planes won´t be suitable. For the plane creation the tool fitting plane also located in planes is suggested.

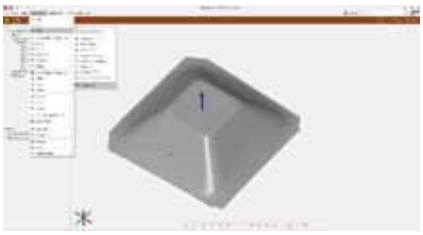

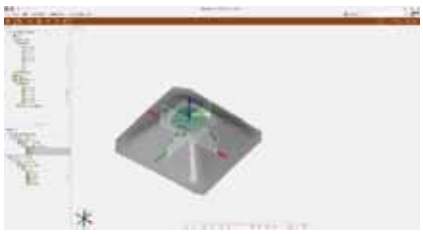

After all the plane creation the tool alignment by coordinate elements can finally be used. The function of this tool is really easy, you give two planes the same position or reference, for example let´s take “X” as the reference, in this point there are 3 “x” planes on the system, the first one is the software´s defined “x” plane, the second is the CAD (nominal) one we created, and the third one is the scanned (actual) plane we also created, so when this tool is used, the actual gets the same characteristic as the target, so we could make nominal “x” axis to take the same position as the system´s one and then make the actual axis to take the nominal´s reference. This tool have 6 main parameters divided in 3 elements to locate the coordinate system, each element can be used for any axis, but the information needs to be consistent between the actual and target or the piece can be changed into an unwanted position, at the right side it is asked if it is wanted to get aligned in a positive or negative position. A very specific task that needs to be done is to select the piece, so it can move and show how the final alignment will stay. Click on “apply and close” once the alignment has the right position.

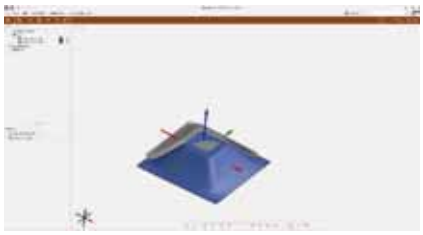

Once the coordinate system is on the right position, the alignment between the pieces is needed, so they can get inspected later. For this intention, on the menu at the right side, the easy access "+" can be found, there we find the initial alignments, in our case the "prealignment" tool was used to create the union between both pieces. For a better alignment in complex parts, the searching time can be adjusted for a longer time, but in our case the part got the same results on any case, so the normal searching time was used. It might come the case like ours, were a specific alignment is needed, for us the toolpath string needed to be on the same position for both pieces, so the optional menu "additional help point" is used. Here a point on the nominal piece needs to be selected, as well as another point on the actual piece, it doesn´t have to be on the exact place, but a close position might achieve better results. This step was needed because the pieces could get aligned into different positions with a slight difference on the result, for us also the presence of the toolpath string could affect later results.

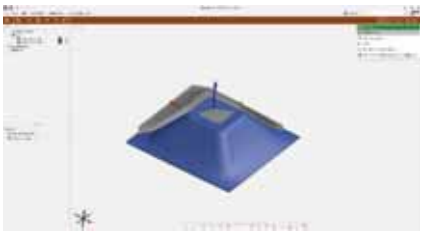

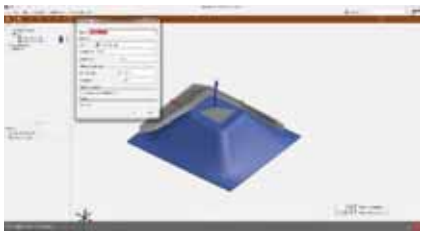

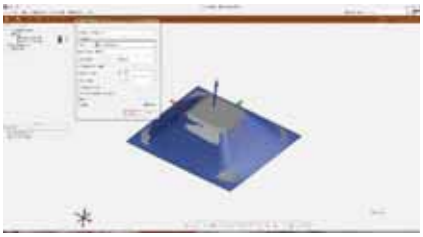

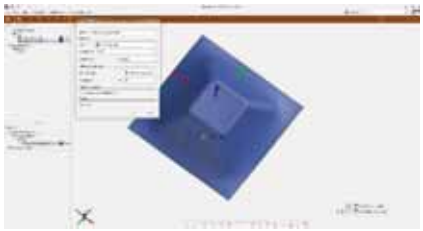

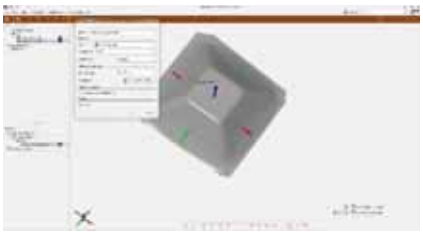
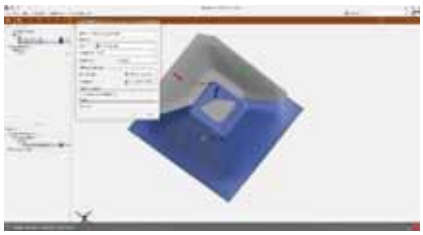
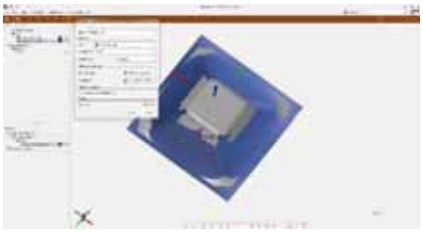
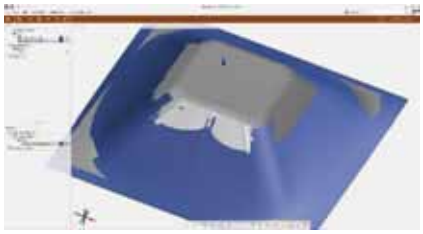

At this point where the pieces are aligned, the inspection can be performed, for this, on the menu at the left side the option “inspection” can be selected. On the appearing options the “surface comparison” is the first one, we select this tool to show us how alike the shapes between our pieces are. Two alternatives are shown, to make the comparison over the nominal piece or to make it over the actual, we decided to use the “surface comparison on actual”, but in our case it would get almost a null difference. The tool is very easy to use, since the analysis is taken automatically, only the maximum distance accepted is asked, and it can be changed if needed. To see the result, the nominal piece can be hidden. On the right side the color legend appears, here the areas with colors close to red means that the piece is far one from the other on a positive way (to the outside), when the areas present a green color it means that the pieces match and they are similar on those areas, and when bluish colors are showed the meaning is that the piece is far from the other on a negative way (to the inside). Talking back about the legend, the automatic values present the highest and the lowest value on the piece, but it can be changed and get the same value for both sides.

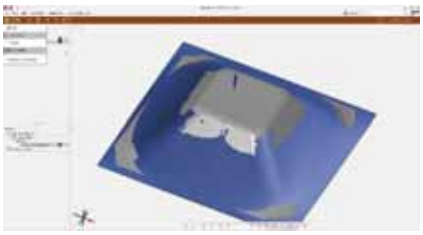
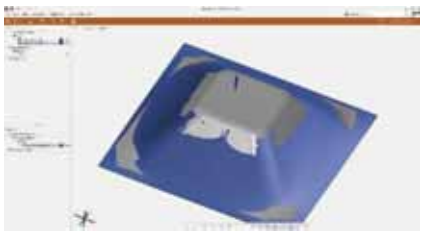
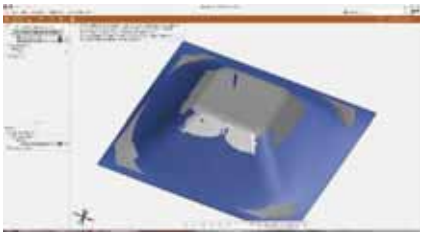
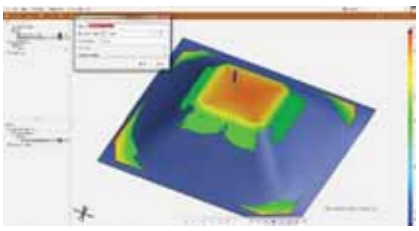
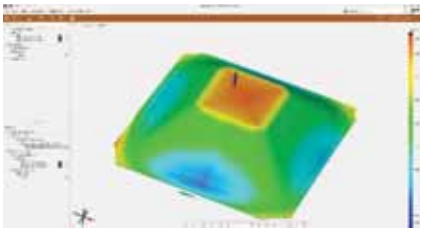
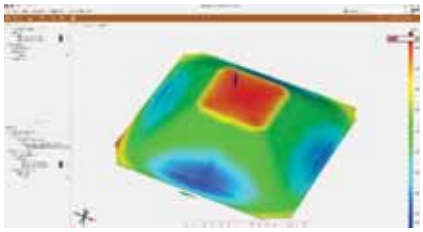

On the case of needing specific values on a certain area, on the menu, the lens picture is shown, here several tools are presented, it is suggested to keep it there so extra inspections or information can be obtained. There on the check access the deviation labels tool can be found, it is also accessible on the menu. With this tool, the deviation on an exact position is displayed. To select Ctrl+Click is needed. The colors on the labels are consistent with their value on the legend.

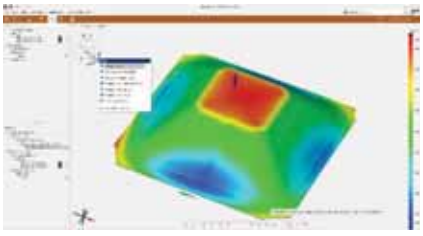
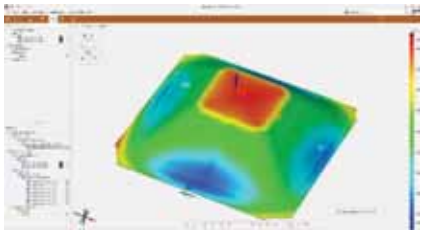

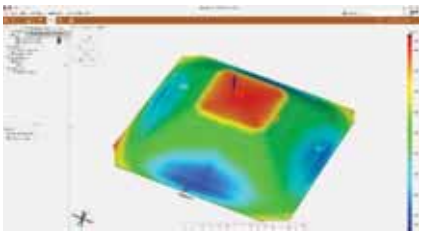

The next tool used is the “inspection on section” the same as the last tool it can be applied on actual or on nominal. For this tool, a certain position to create the section is needed, it can be a created plane with a certain angle or a position or the coordinated axis can also be handled. After creating this, the piece is cut, analyzed, and displayed on the plane. Also on this inspection a legend is shown and labels can be obtained.

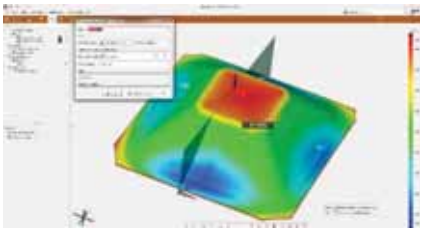

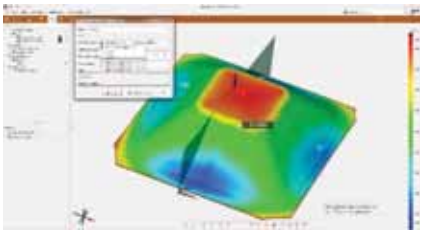

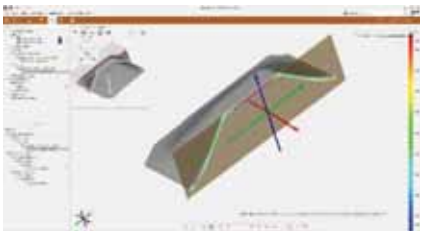

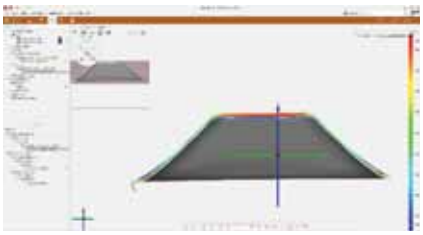

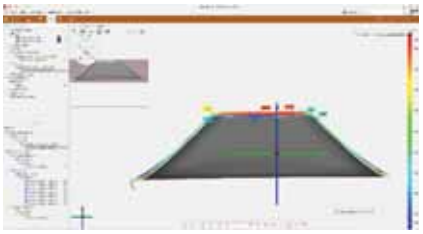

The las step to evaluate the geometry is to ensure the pieces angle. For this, two planes need to be created on the walls of the pyramid. To obtain the angle go to Construct > Angle > 2 directions angle. With this tool the created planes are selected and the real angle is calculated.

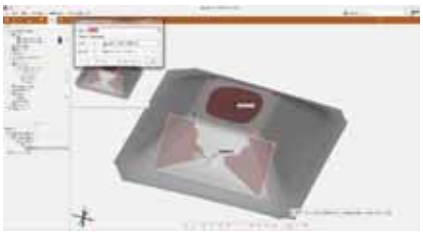

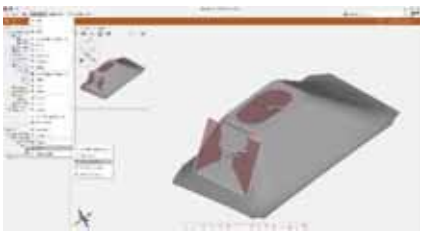

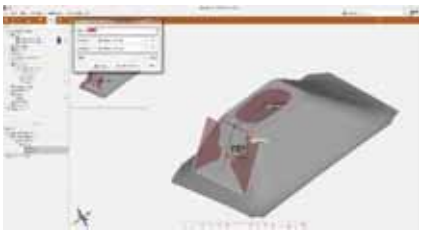

Up to this part, the geometrical analysis is finished, so the thickness evaluation will be described, this steps can be done after the alignment if the geometrical inspection isn´t needed.

For the thickness inspection, first some points need to be created, to do so, the tool “surface points” located on Construct > Point > Surface point. Once the parameters are open, the position needs to be selected the keys Ctrl+Click are useful for this. After this, on the lens tool on check the access copy as nominal element is found, this helps to locate a point on the same position as the one presented on the actual piece, so both thickness can be evaluated. In our case to know the exact position of the point was vital, son on the lens tool on check the three positions were selected. When both points are created, on Inspection > Analyze surfaces > Material thickness on inspection point is the tool that will be used. Here the created point is selected and the thickness is calculated. Several points can be obtained, also the points can be placed exactly on the axis so the position there would be cero.

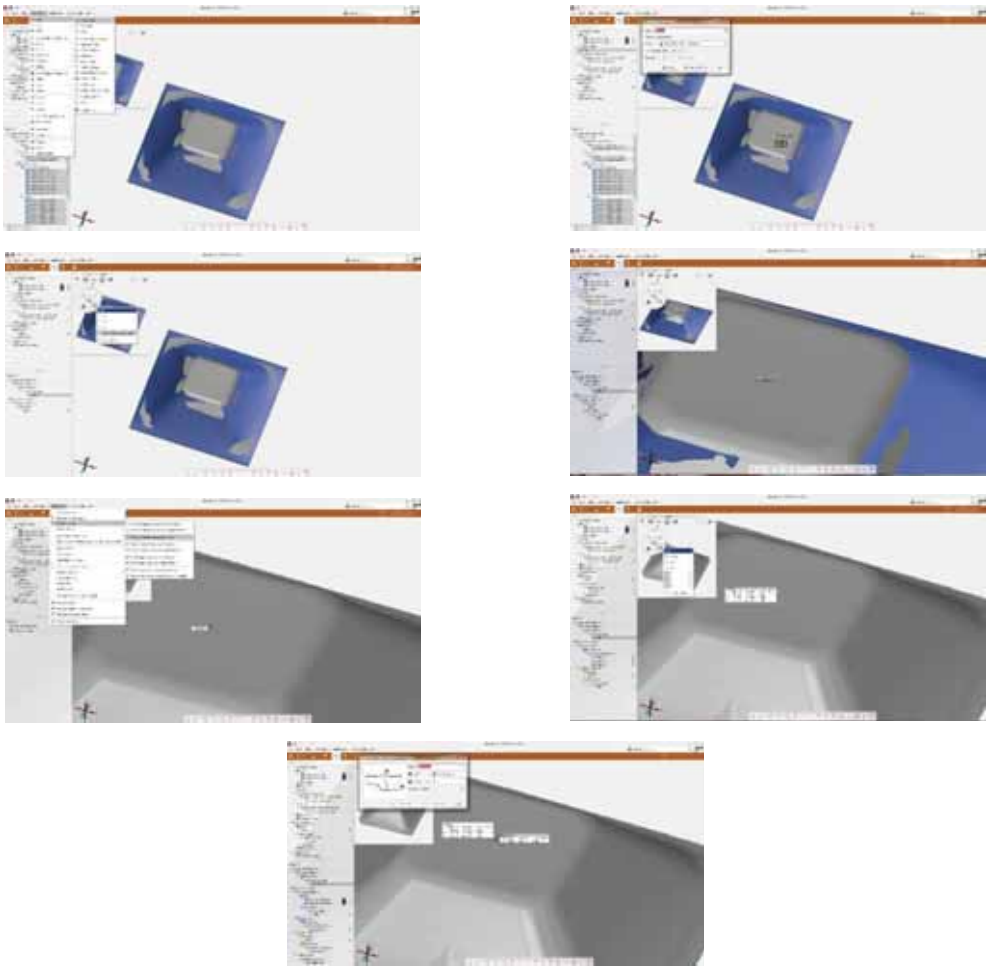

Once this is done, the steps for the thickness inspection is finished. On the menu it can be accessed to the report area, where images, tables, and data can be acquired. There are several sheet formats, and the possibility to adjust any image to the desired position, or the information on the tables. This report as the data spreadsheet can get exported for further analysis.

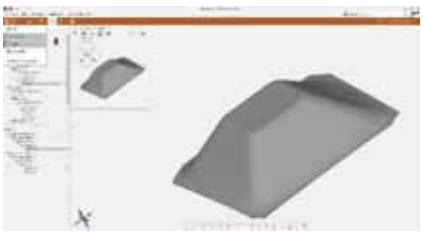
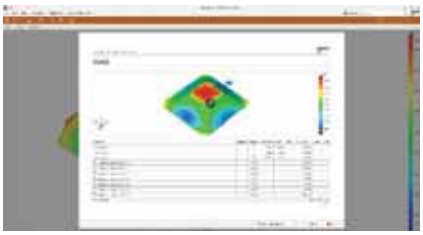
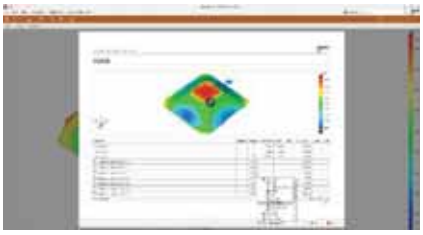


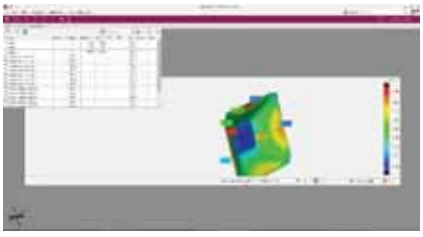
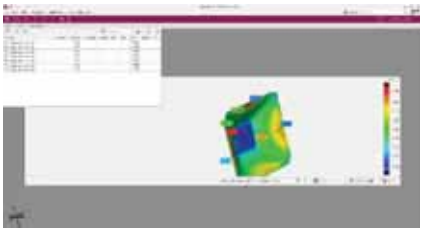
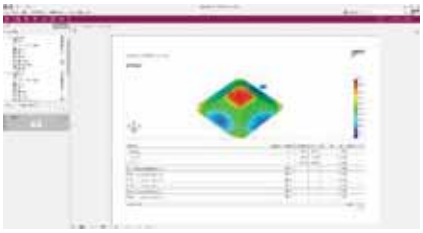

APPENDIX B

B.1 Stamping drawings.

- Bill of materials.

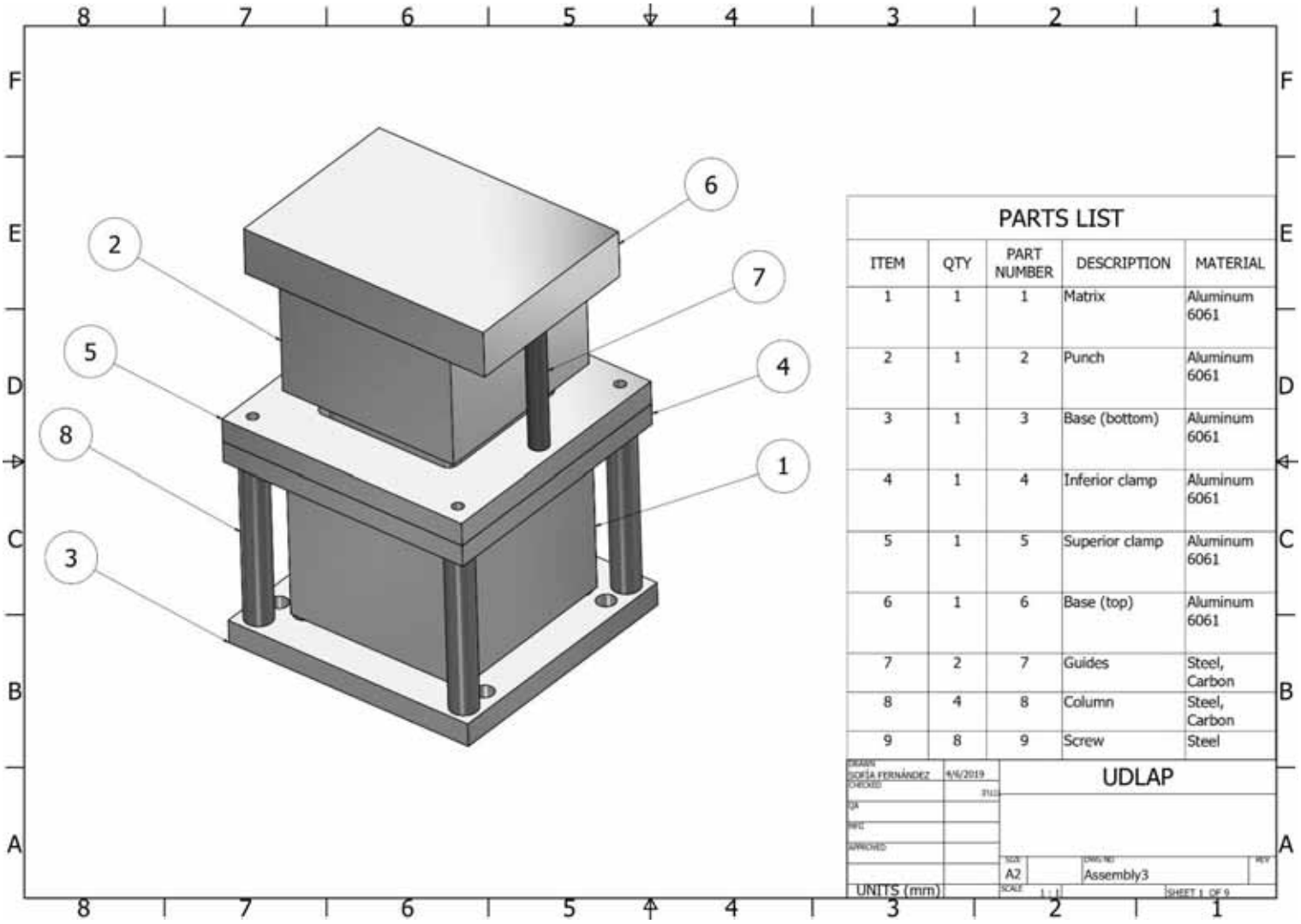

PARTS LIST

ITEM	QTY	PART NUMBER	DESCRIPTION	MATERIAL
1	1	1	Matrix	Aluminum 6061
2	1	2	Punch	Aluminum 6061
3	1	3	Base (bottom)	Aluminum 6061
4	1	4	Inferior clamp	Aluminum 6061
5	1	5	Superior clamp	Aluminum 6061
6	1	6	Base (top)	Aluminum 6061
7	2	7	Guides	Steel, Carbon
8	4	8	Column	Steel, Carbon
9	8	9	Screw	Steel

DRAWN SOFÍA FERNÁNDEZ 4/6/2019
CHECKED
QA
MFG
APPROVED
UNITS (mm)
UDLAP
SIZE A2
DWG NO Assembly3
REV
SCALE 1 : 1
SHEET 1 OF 9

- Matrix

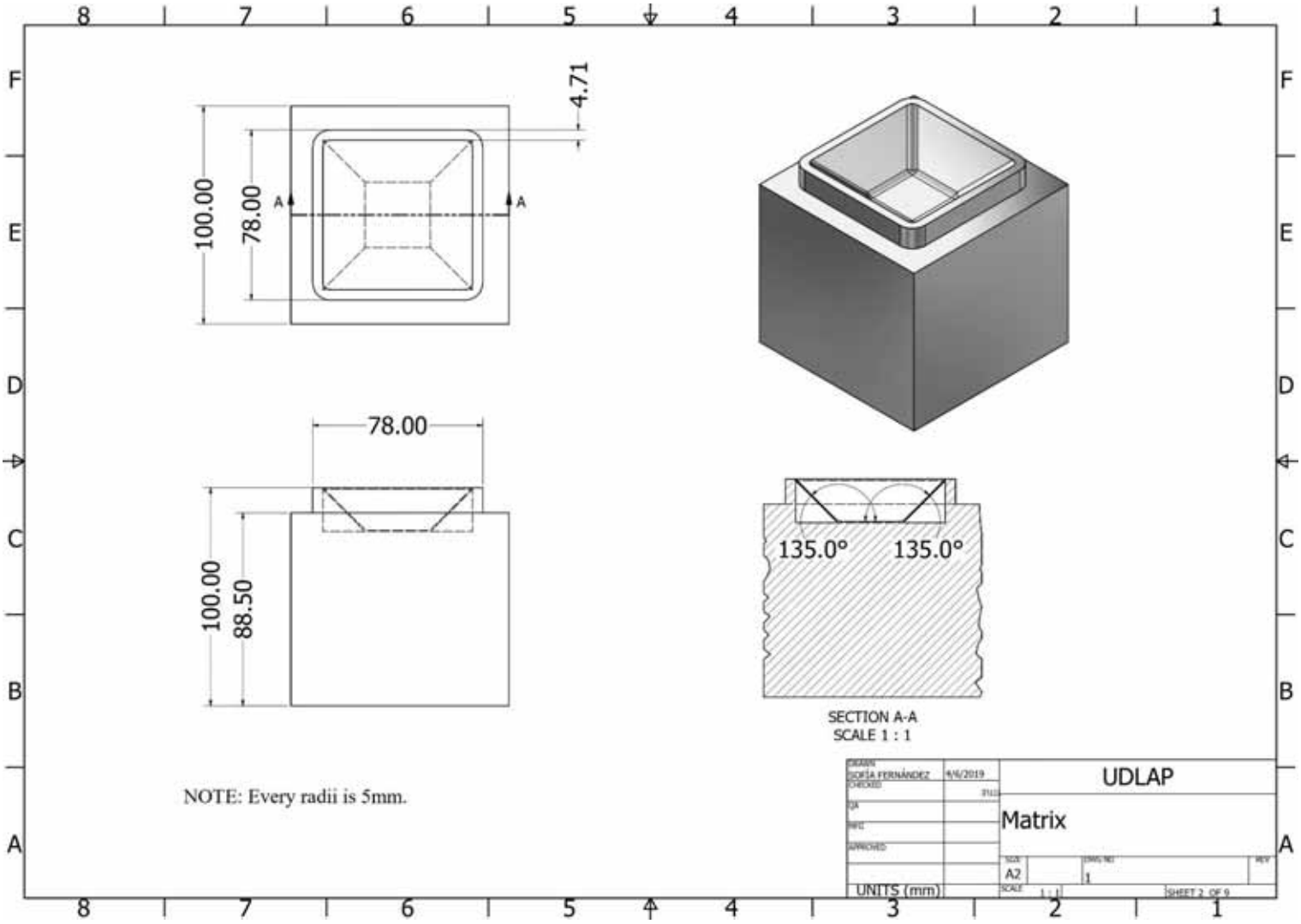
4.71
100.00
78.00
A
A
78.00
100.00
88.50
135.0°
135.0°
SECTION A-A
SCALE 1 : 1
NOTE: Every radii is 5mm.
SOFÍA FERNÁNDEZ
9/6/2019
UDLAP
Matrix
A2
1
UNITS (mm)
SHEET 2 OF 9

- Punch

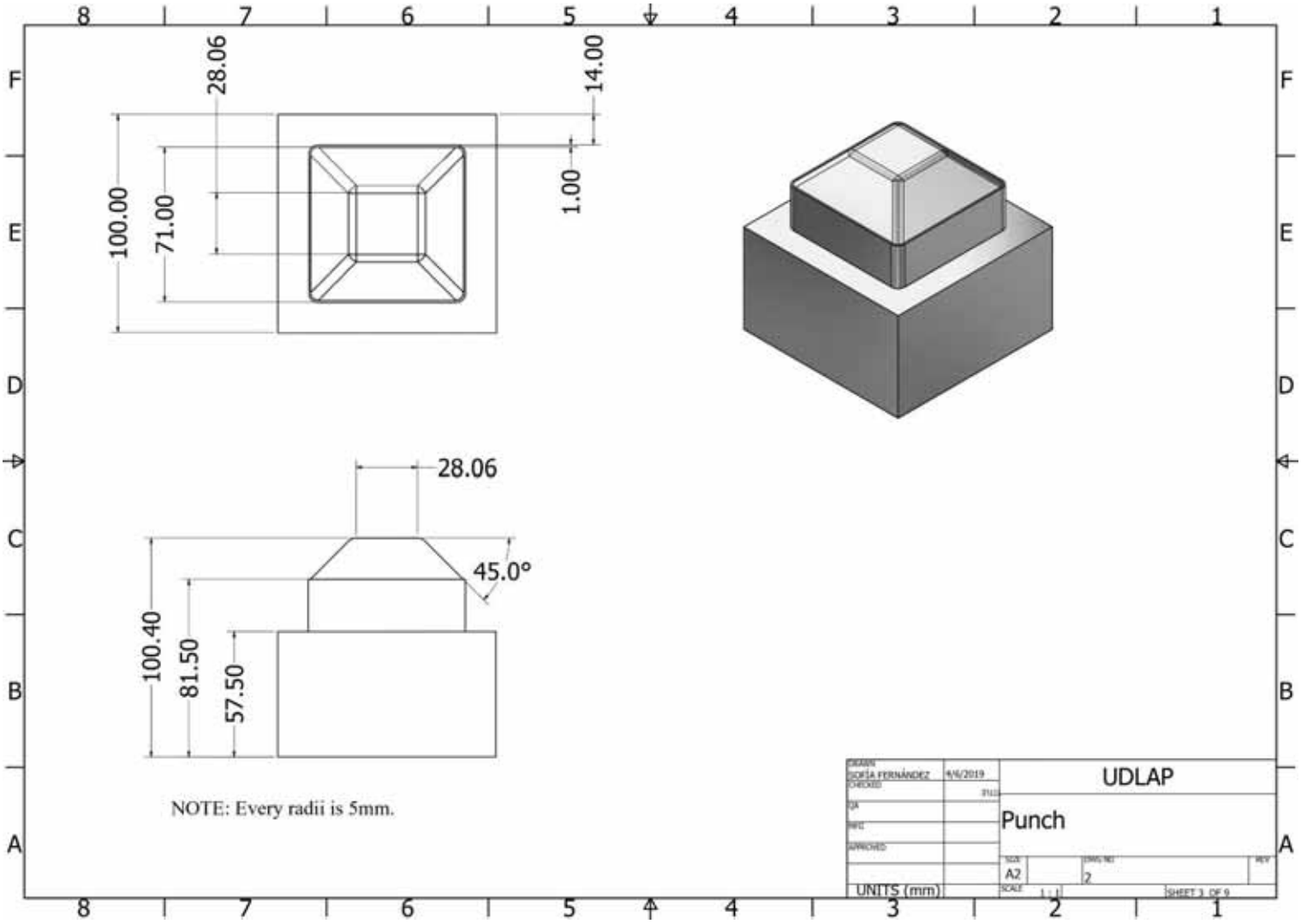
28.06
14.00
100.00
71.00
1.00
28.06
45.0°
100.40
81.50
57.50
NOTE: Every radii is 5mm.
UDLAP
Punch
A2
UNITS (mm)

- Bottom base (press set)

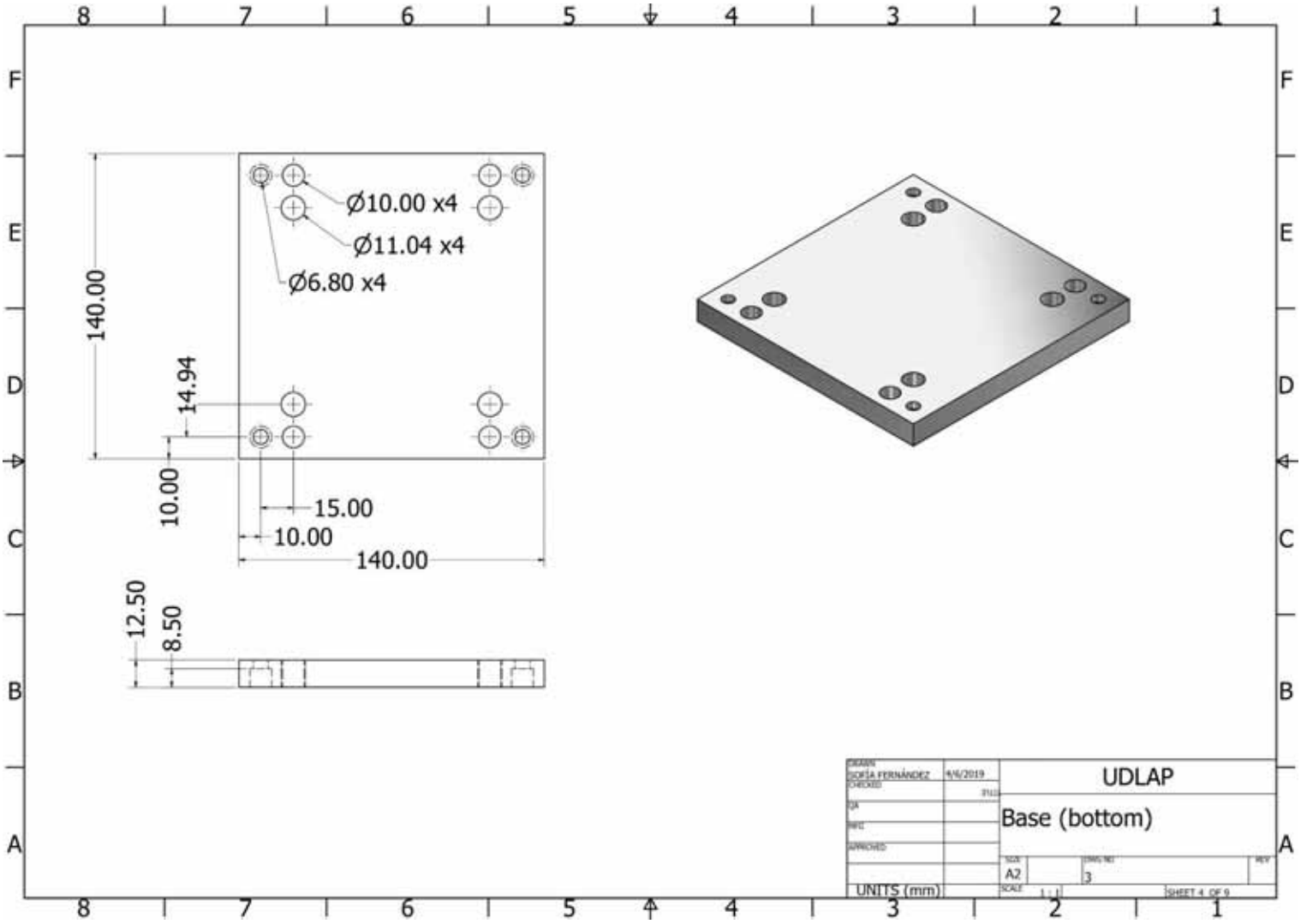

- Inferior clamp (press set)

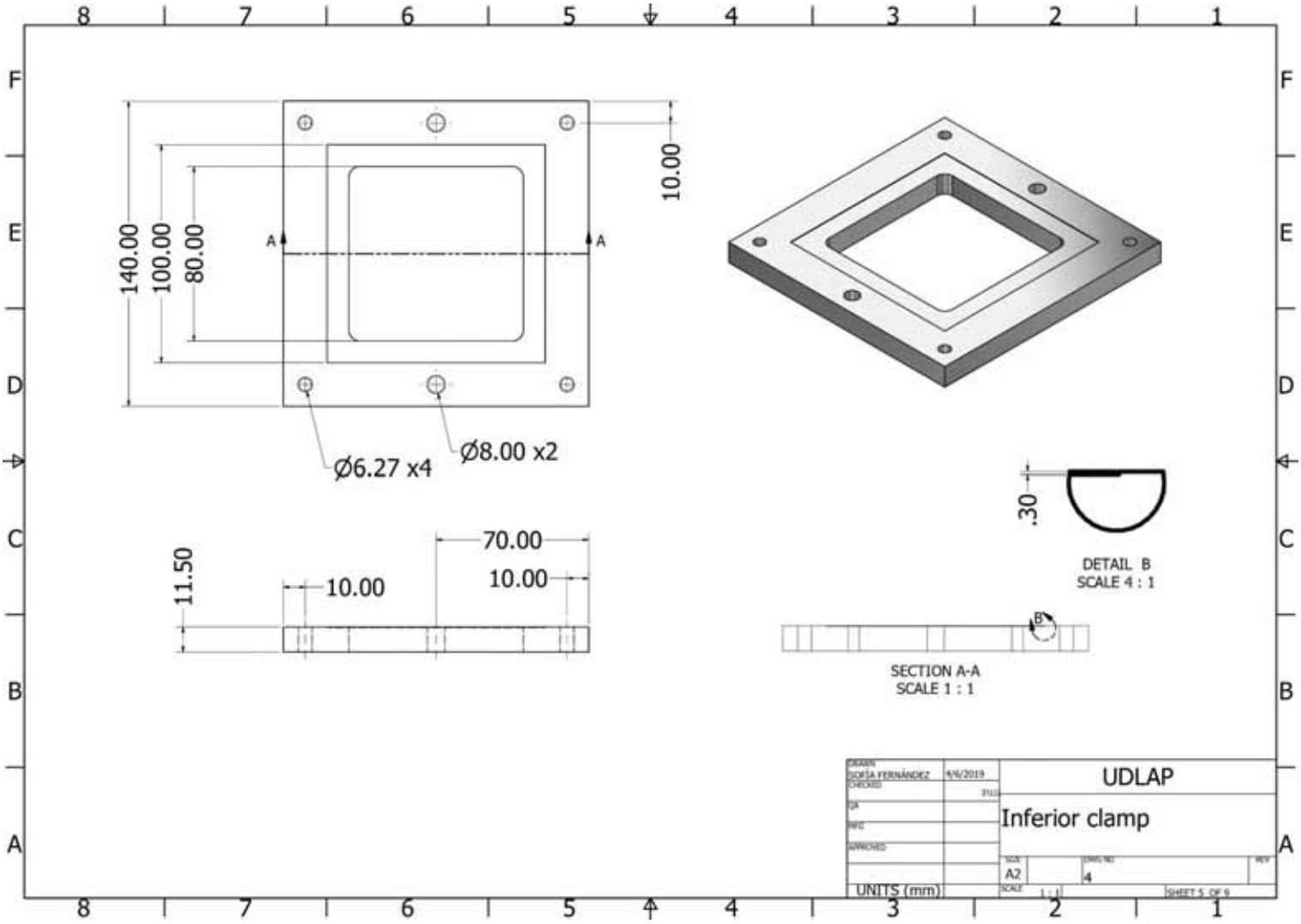

- Superior Clamp (press set)

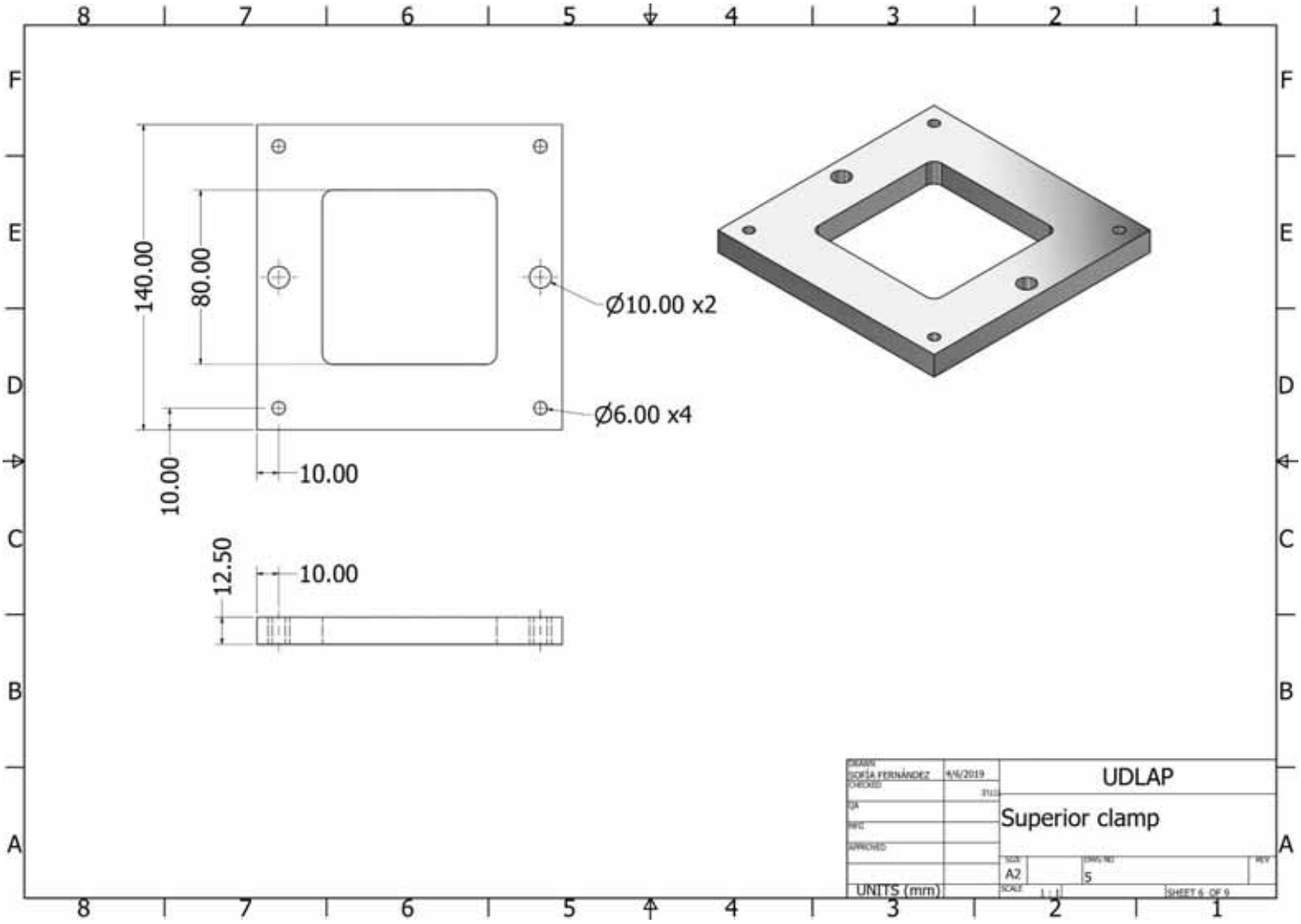

- Top base

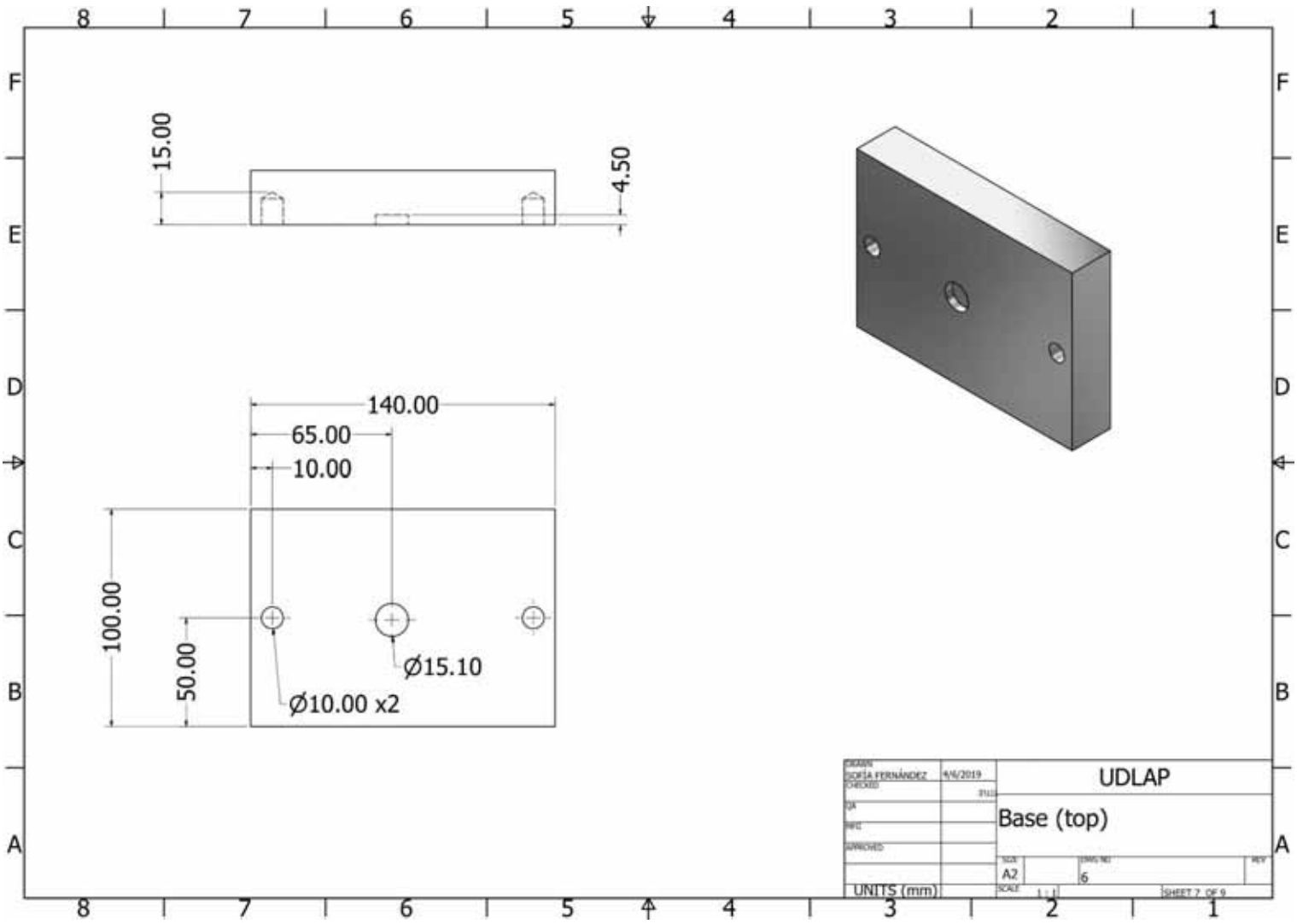
15.00
4.50
140.00
65.00
10.00
100.00
50.00
Ø15.10
Ø10.00 x2
UDLAP
Base (top)
UNITS (mm)
A2
6
SHEET 7 OF 9

- Guides

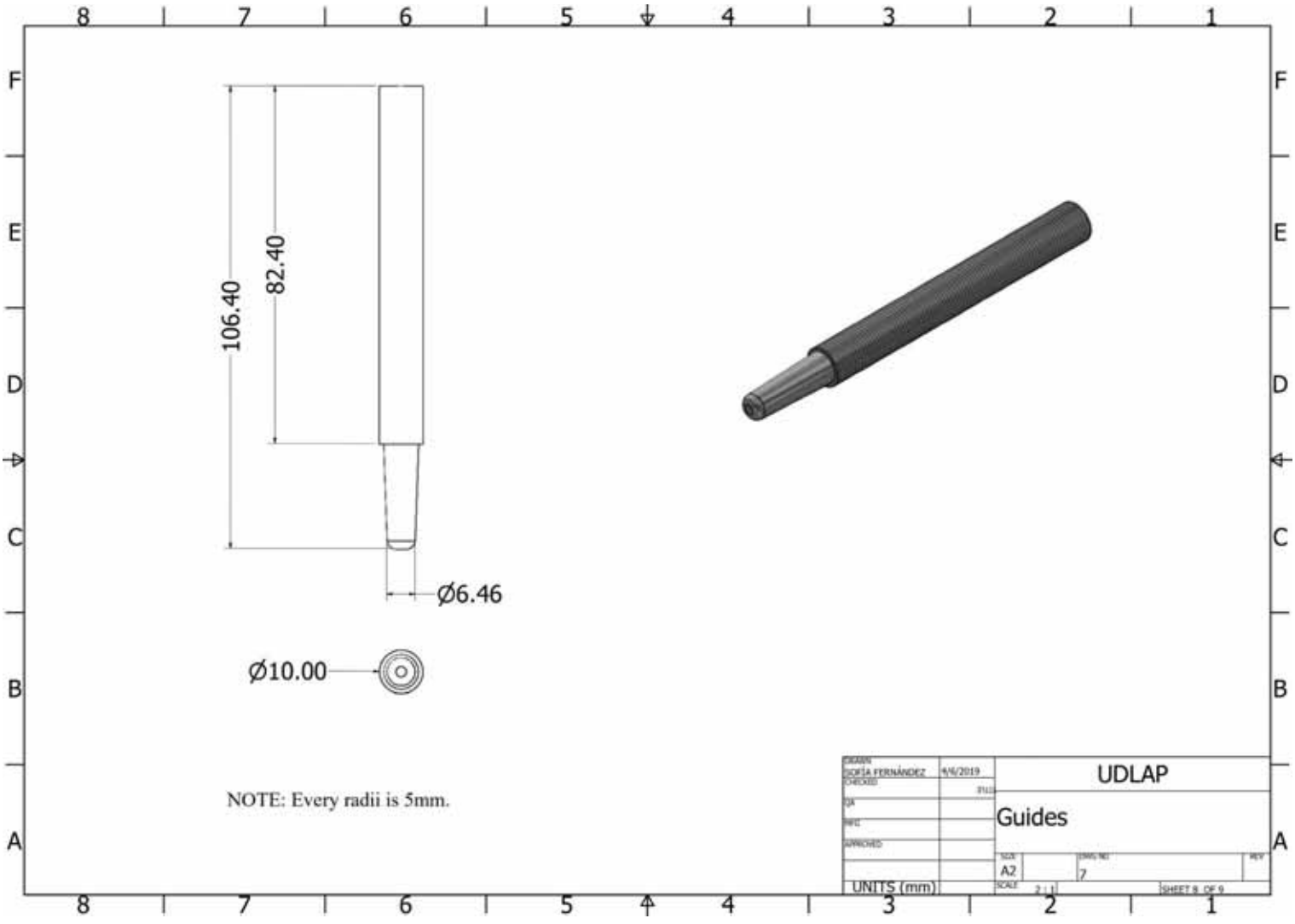
106.40
82.40
Ø6.46
Ø10.00
NOTE: Every radii is 5mm.
UDLAP
Guides
A2
UNITS (mm)

- Columns

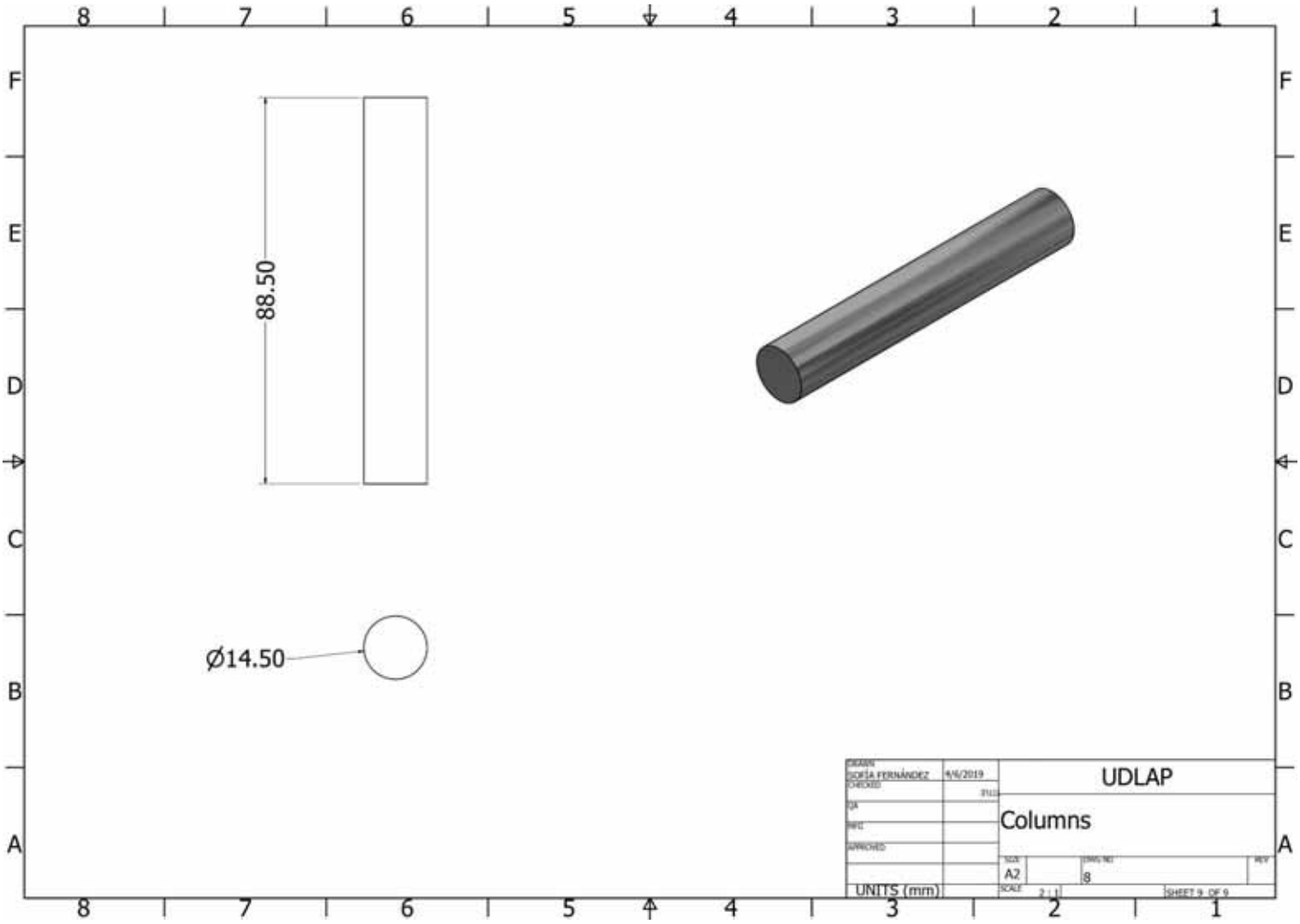
88.50
Ø14.50
UDLAP
Columns
SOFÍA FERNÁNDEZ
9/6/2019
UNITS (mm)
A2
8
SHEET 9 OF 9

B.2 SPIF drawings.

- Inferior clamping plate (SPIF set)

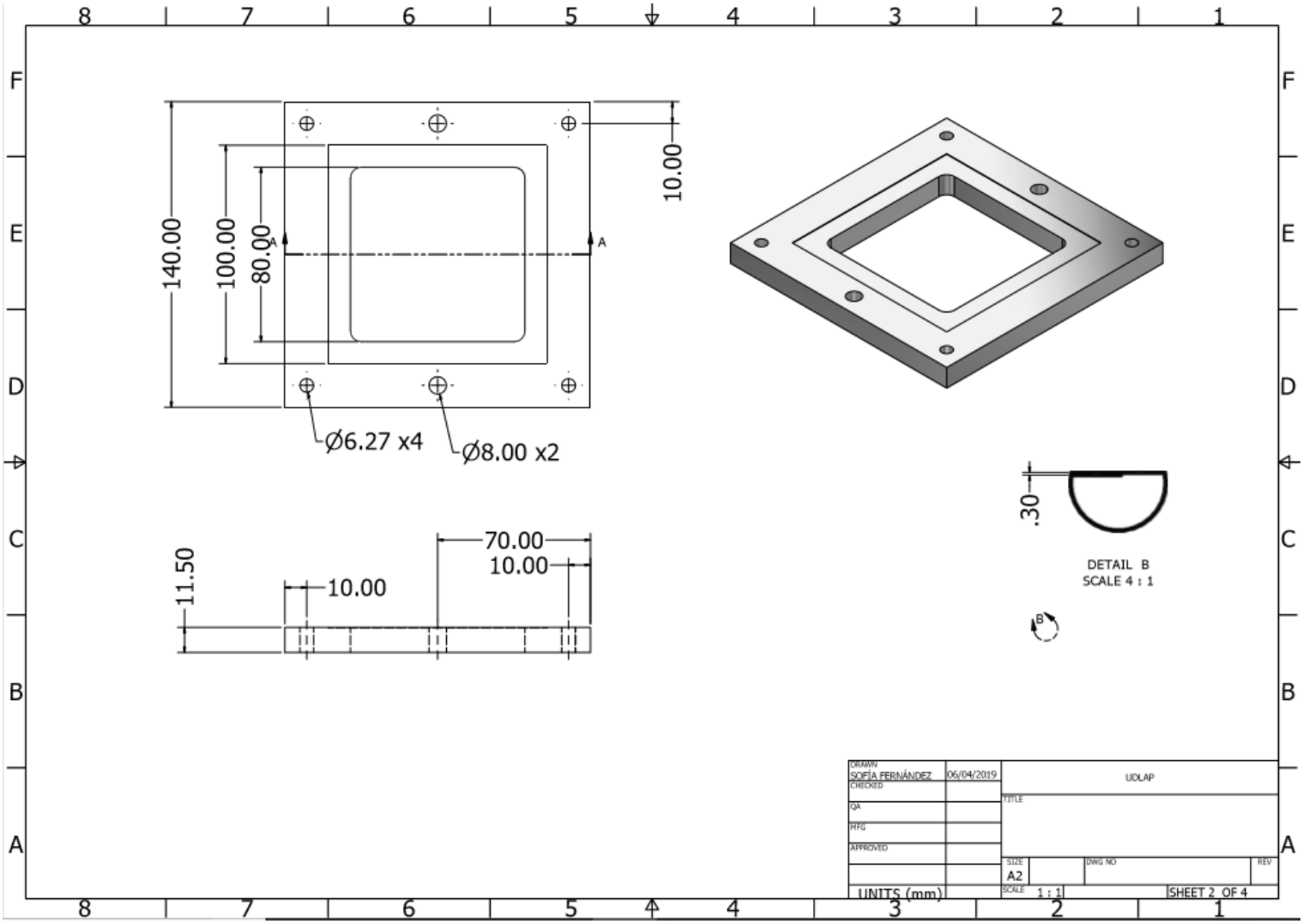

- Superior clamping plate

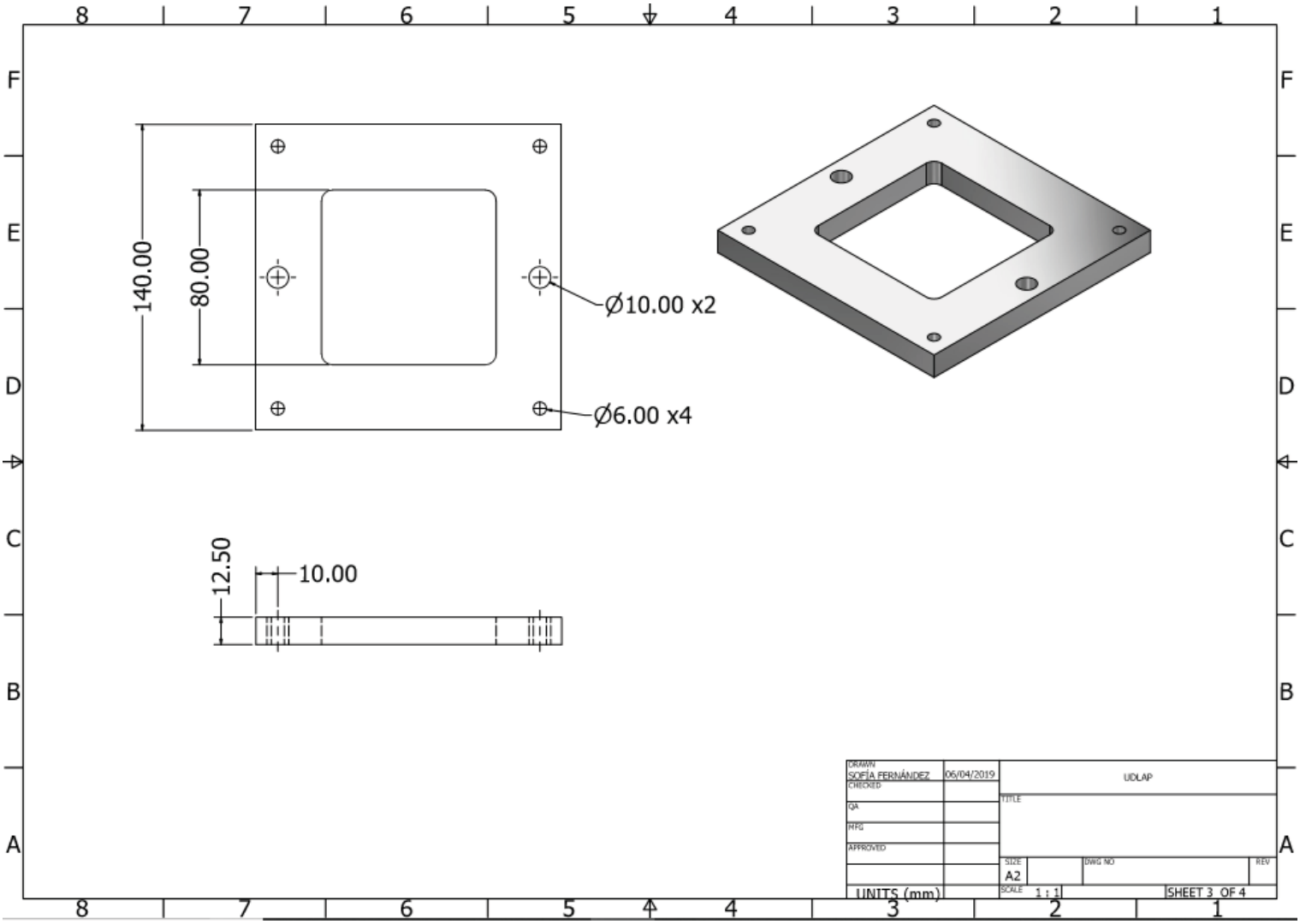

- Bottom base

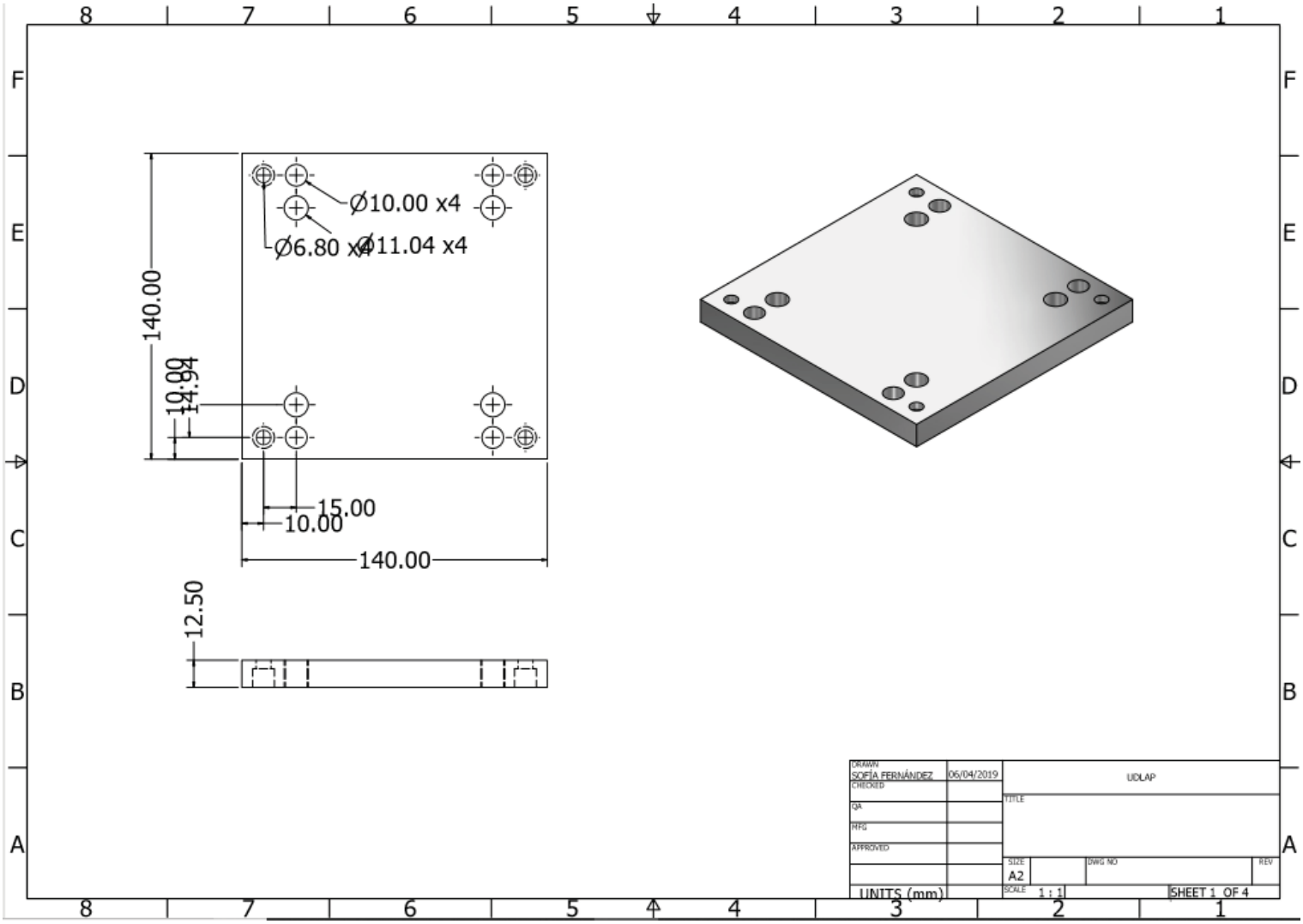
Ø10.00 x4
Ø6.80 x4
Ø11.04 x4
140.00
10.00
14.94
15.00
10.00
140.00
12.50
DRAWN
SOFÍA FERNÁNDEZ
06/04/2019
CHECKED
QA
MFG
APPROVED
UNITS (mm)
UDLAP
TITLE
SIZE
A2
DWG NO
REV
SCALE
1 : 1
SHEET 1 OF 4

- Columns

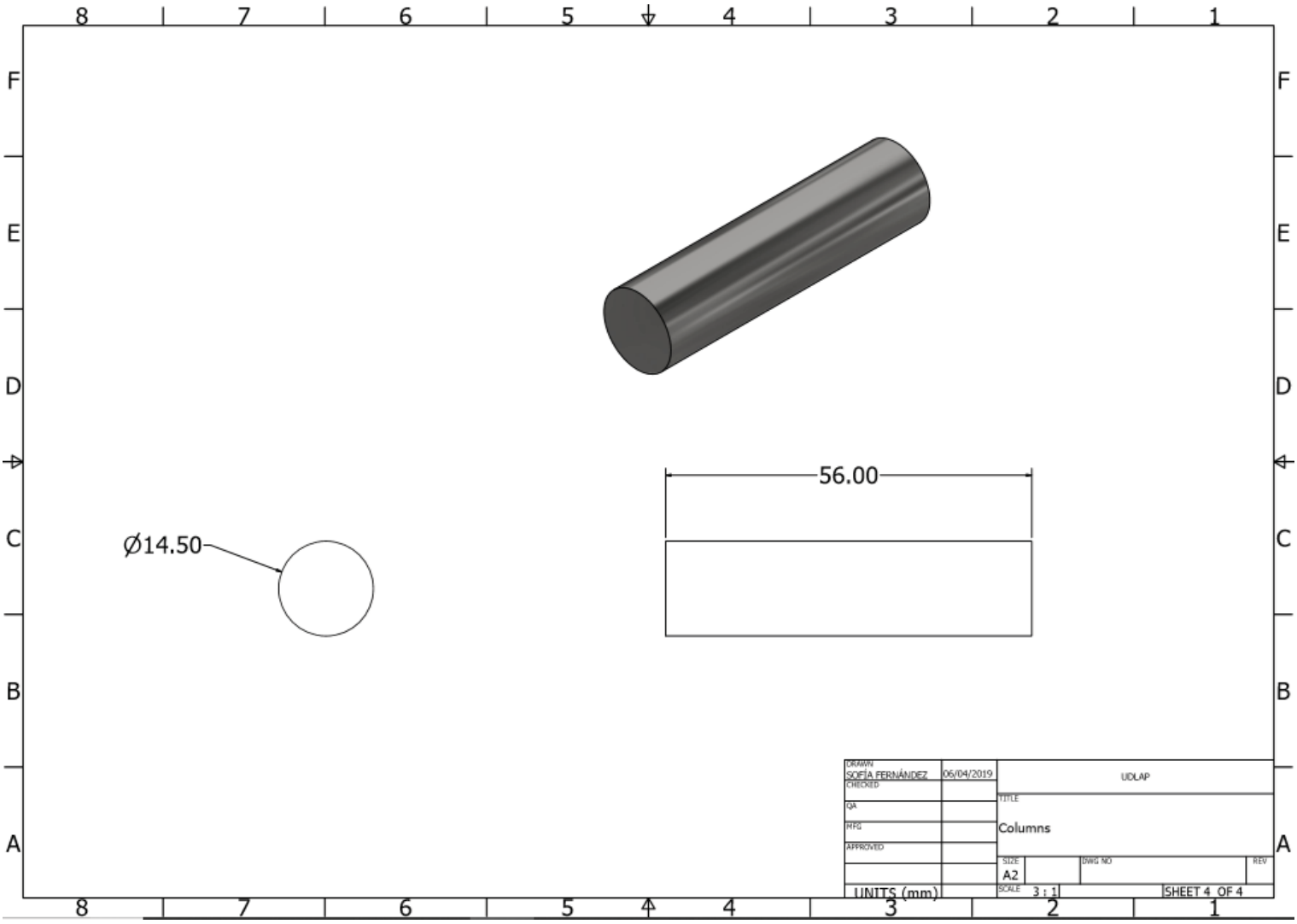
8
7
6
5
4
3
2
1
F
E
D
C
B
A
56.00
Ø14.50
DRAWN
SOFÍA FERNÁNDEZ
06/04/2019
CHECKED
QA
MFG
APPROVED
UNITS (mm)
UDLAP
TITLE
Columns
SIZE
A2
DWG NO
REV
SCALE
3 : 1
SHEET 4 OF 4

B.3 Three dimension printing drawings.

- Sheet support for SPIF

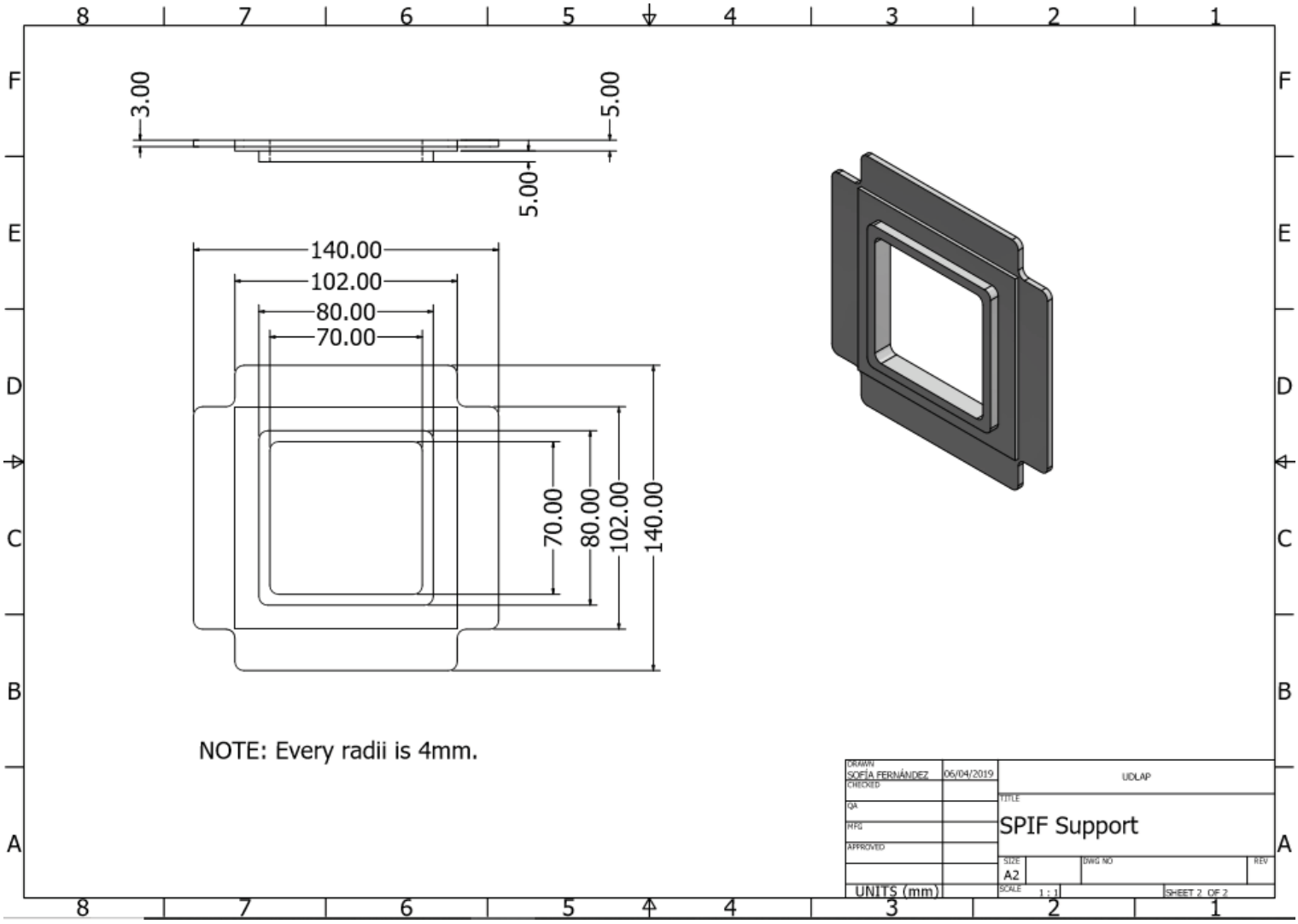

- Middle marker.

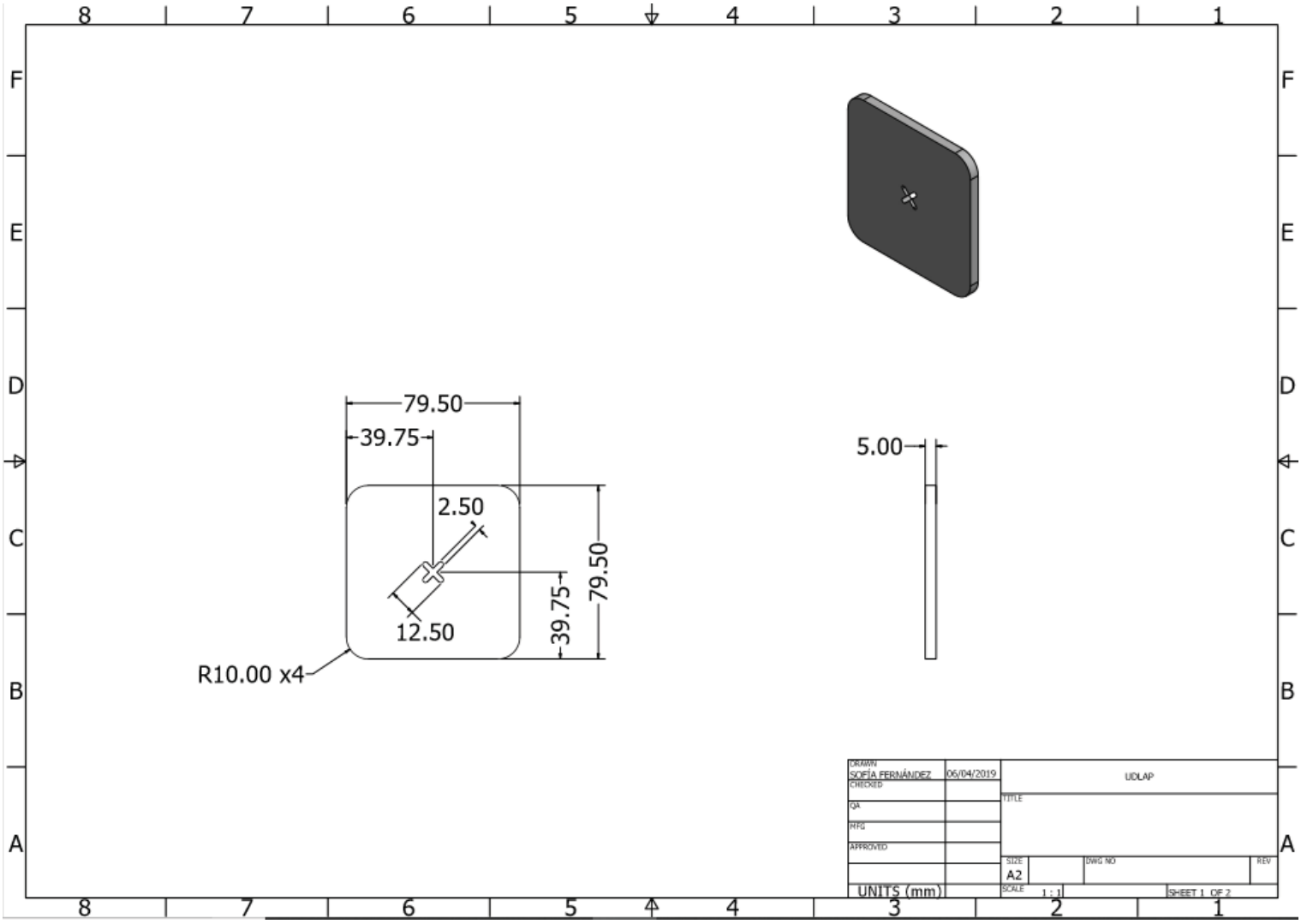

BIBLIOGRAPHY

[1] Al-Ghamdi, K. A., Hussain, G., & Butt, S. I. (2014). Force variations with defects and a force-based strategy to control defects in SPIF. Materials and Manufacturing Processes, 29(10), 1197-1204.

[2] Ambrogio, G., Costantino, I., De Napoli, L., Filice, L., Fratini, L., & Muzzupappa, M. (2004). Influence of some relevant process parameters on the dimensional accuracy in incremental forming: a numerical and experimental investigation. *Journal of Materials Processing Technology*, *153*, 501-507.

[3] Ambrogio, G., Cozza, V., Filice, L., & Micari, F. (2007). An analytical model for improving precision in single point incremental forming. Journal of Materials Processing Technology, 191(1-3), 92-95.

[4] Bagudanch, I., Perez-Santiago, R., Garica-Romeu, M. L., & Rodríguez, C. (2011). Forming force in SPIF of variable wall angle components: FEM modeling and experimental results. In *Proceedings of 10th International Conference of Technology of Plasticity* (pp. 541-546).

[5] Bambach, M., Araghi, B. T., & Hirt, G. (2009). Strategies to improve the geometric accuracy in asymmetric single point incremental forming. *Production Engineering*, *3*(2), 145-156.

[6] Bambach, M. (2010). A geometrical model of the kinematics of incremental sheet forming for the prediction of membrane strains and sheet thickness. *Journal of Materials Processing Technology*, *210*(12), 1562-1573.

[7] Behera, A. K., Vanhove, H., Lauwers, B., & Duflou, J. R. (2011). Accuracy improvement in single point incremental forming through systematic study of feature interactions. In *Key Engineering Materials* (Vol. 473, pp. 881-888). Trans Tech Publications.

[8] Belmont Gálvez, A. J. (2018). Comparison of two sheet metal forming processes: Conventional Stamping vs. Incremental Sheet Forming. Universidad de las Américas Puebla. Retrieved from https://search-ebscohost-

com.udlap.idm.oclc.org/login.aspx?direct=true&db=ir00003a&AN=irfudla.lim.belmont.galvez.aj&lang=es&site=eds-live

[9] Bibee, J. (2009). Understanding Optical Measurement. *Quality Digest*. https://www.qualitydigest.com/magazine/2009/apr/article/understanding-optical-measurement.html

[10] Buffa, G., Ingarao, G., Fratini, L., & Micari, F. (2011). Shape Distortion and Thickness Distribution during SPIF Processes: Experimental and Numerical Analysis. In Key Engineering Materials (Vol. 473, pp. 913-918). Trans Tech Publications.

[11] Centeno, G., Martínez-Donaire, A., Bagudanch, I., Morales-Palma, D., Garcia-Romeu, M., & Vallellano, C. (2017). Revisiting formability and failure of AISI304 sheets in spif: Experimental approach and numerical validation. Metals, 7(12), 531.

[12] Cooper, D. R., Rossie, K. E., & Gutowski, T. G. (2017). The energy requirements and environmental impacts of sheet metal forming: An analysis of five forming processes. Journal of Materials Processing Technology, 244, 116-135.

[13] Dejardin, S., Thibaud, S., & Gelin, J. C. (2008). Finite element analysis and experimental investigations for improving precision in single point incremental sheet forming process. International Journal of Material Forming, 1(1), 121-124.

[14] Dejardin, S., Thibaud, S., Gelin, J. C., & Michel, G. (2010). Experimental investigations and numerical analysis for improving knowledge of incremental sheet forming process for sheet metal parts. *Journal of Materials Processing Technology*, *210*(2), 363-369.

[15] Duflou, J. R., Lauwers, B., & Verbert, J. (2007). Study on the achievable accuracy in single point incremental forming. In Advanced methods in material forming (pp. 251-262). Springer, Berlin, Heidelberg.

[16] Filice, L., Fratini, L., & Micari, F. (2002). Analysis of material formability in incremental forming. CIRP Annals, 51(1), 199-202.

[17] Garcia-Romeu, M. L., Ciurana, J., & Ferrer, I. (2007). Springback determination of sheet metals in an air bending process based on an experimental work. Journal of Materials Processing Technology, 191(1-3), 174-177.

[18] Groover, M. P. (2007). Fundamentals of modern manufacturing: materials processes, and systems. John Wiley & Sons.

[19] Groover, M. P., Aguilar, J. E. A., Lopez, U. F., & Palafox, F. J. S. (2014). Introducción a los procesos de manufactura. McGraw Hill Education.

[20] Garechana, G., Río-Belver, R., Bildosola, I., & Cilleruelo-Carrasco, E. (2019). A method for the detection and characterization of technology fronts: Analysis of the dynamics of technological change in 3D printing technology. *PLoS ONE*, *14*(01), 1–27. https://doi-org.udlap.idm.oclc.org/10.1371/journal.pone.0210441

[21] Hagan, E., & Jeswiet, J. (2003). A review of conventional and modern single-point sheet metal forming methods. Proceedings of the Institution of Mechanical Engineers, Part B: Journal of Engineering Manufacture, 217(2), 213-225.

[22] Ham, M., & Jeswiet, J. (2008). Dimensional accuracy of single point incremental forming. International journal of material forming, 1(1), 1171-1174.

[23] Hu, J., Marciniak, Z., & Duncan, J. (Eds.). (2002). Mechanics of sheet metal forming. Elsevier.

[24] Hussain, G., & Gao, L. (2007). A novel method to test the thinning limits of sheet metals in negative incremental forming. International Journal of Machine Tools and Manufacture, 47(3-4), 419-435.

[25] Hussain, G., Gao, L., Hayat, N., & Ziran, X. (2009). A new formability indicator in single point incremental forming. Journal of Materials Processing Technology, 209(9), 4237-4242.

[26] Jeswiet, J., Duflou, J. R., & Szekeres, A. (2005). Forces in single point and two point incremental forming. In Advanced Materials Research (Vol. 6, pp. 449-456). Trans Tech Publications.

[27] Jeswiet, J., Hagan, E., & Szekeres, A. (2002). Forming parameters for incremental forming of aluminium alloy sheet metal. Proceedings of the Institution of Mechanical Engineers, Part B: Journal of Engineering Manufacture, 216(10), 1367-1371.

[28] Le, K. D., Nguyen, T. H., Nguyen, T. B., Le, T. S., Nguyen, H. B., & Nguyen, T. N. (2015). Recommendation of a Measure for Enhancing the Precision of Dimensions

of Foil Products in Single Point Incremental Forming Technology. In Key Engineering Materials (Vol. 656, pp. 479-483). Trans Tech Publications.

[29] Long, Y., Pan, J., Zhang, Q., & Hao, Y. (2017). 3D printing technology and its impact on Chinese manufacturing. *International Journal of Production Research*, *55*(5), 1488–1497. https://doi-org.udlap.idm.oclc.org/10.1080/00207543.2017.1280196

[30] McAnulty, T., Jeswiet, J., & Doolan, M. (2017). Formability in single point incremental forming: A comparative analysis of the state of the art. CIRP Journal of Manufacturing Science and Technology, 16, 43-54.

[31] Mendricky, R. (2016). Determination of Measurement Accuracy of Optical 3D Scanners. *MM Science Journal*, 1565–1572. https://doi-org.udlap.idm.oclc.org/10.17973/MMSJ.2016_12_2016183

[32] Mohammadi, A., Qin, L., Vanhove, H., Seefeldt, M., Van Bael, A., & Duflou, J. R. (2016). Single point incremental forming of an aged AL-cu-mg alloy: influence of pre-heat treatment and warm forming. Journal of Materials Engineering and Performance, 25(6), 2478-2488.

[33] Nguyen, T. H., Le, K. D., Nguyen, N. P., Nguyen, H. B., Nguyen, T. N., & Vo, T. Y. (2017). The Effect of Heating to the Formability of Titanium Sheet by SPIF Technology. In *Key Engineering Materials* (Vol. 749, pp. 171-177). Trans Tech Publications.

[34] Park, J. J., & Kim, Y. H. (2003). Fundamental studies on the incremental sheet metal forming technique. *Journal of Materials Processing Technology*, *140*(1-3), 447-453.

[35] Perez-Santiago, R., Fiorentino, A., Marzi, R., & Rodriguez, C. A. (2011, May). Advances in simulation of two point incremental forming. In AIP Conference Proceedings (Vol. 1353, No. 1, pp. 183-188). AIP.

[36] Perez-Santiago, R., Garcia-Romeu, M., & Bagudanch, I. (2011, September). Fabrication of a Biopsy Micro-Forceps Prototype with Incremental Sheet Forming. In Innovative Developments in Virtual and Physical Prototyping: Proceedings of the 5th International Conference on Advanced Research in Virtual and Rapid Prototyping, Leiria, Portugal, 28 September-1 October, 2011 (p. 429). CRC Press.

[37] Perez-Santiago, R., Bagudanch, I.; & García-Romeu, M., Hendrichs, N. J. (2012, Septiembre) Fuerzas de Formado en Piezas Fabricadas por Conformado Incremental de Chapa: Memorias del XVIII Congreso Internacional Anual de la SOMIM, Salamanca, Guanajuato, México, 19 al 21 de septiembre, 2012 (p. 820). SOMIM.

[38] Reljić, I., & Dunđer, I. (2019). Application of Photogrammetry in 3D Scanning of Physical Objects. *TEM Journal*, *8*(1), 94–101. https://doi-org.udlap.idm.oclc.org/10.18421/TEM81-13

[39] Rodriguez-Alabanda, O., Narvaez, M., Guerrero-Vaca, G., & Romero, P. (2018). Manufacturing of non-stick molds from pre-painted aluminum sheets via single point incremental forming. Applied Sciences, 8(6), 1002.

[40] Singh, D. K. (2008). Fundamentals of manufacturing engineering. CRC Press.

[41] Tanner, J. P. (1990). *Manufacturing Engineering: An Introduction to the Basic Functions, Revised and expanded* (Vol. 36). CRC Press.

[42] Van Bael, A., Eyckens, P., He, S., Bouffioux, C., Henrard, C., Habraken, A. M., & Van Houtte, P. (2007, April). Forming Limit Predictions for Single-Point Incremental Sheet Metal Forming. In AIP Conference Proceedings (Vol. 907, No. 1, pp. 309-314). AIP.

[43] Young, D., Jeswiet, J., 2004. Wall thickness variations in single-point incremental forming. J. Eng. Manufact. Part B 218,1453-1459.

[44] Zhang, W. (2010). Intelligent energy field manufacturing: interdisciplinary process innovations. CRC Press.

[45] Quiroz Vazquez, E. J. (2018). *Study on formability and aisotropy effects on Single Point Incremental Forming of Stainless Steel AISI - 304*. Universidad de las Américas Puebla.

[46]